

DYNAMITED

FINAL REPORT

	Name and Function	Date	Signature
Prepared by	<u>DYNAMITED Project Team:</u> M. BÖSWALD (DLR) E. CAVRO (INTESPACE) A. GIRARD (INTESPACE) S. IUGOVICH (ASTRIUM) S. LABORDE (ASTRIUM) M. LINK (UNIVERSITY OF KÄSSEL)		
Verified by	S. LABORDE DYNAMITED Project Manager J.-B. VERGNIAUD Head of Mechanical Analysis and Test section		
Approved by	A. CAPITAINE Head of Mechanical and Thermal Analysis and Test department – ASG23		
Authorized by	S. LABORDE DYNAMITED Project Manager		
Application authorized by			

Document type	Nb WBS	Keywords

SUMMARY

Dynamic tests have a great importance in order to design spacecraft structure as launchers generate a severe vibratory environment. It is thus required to have a deep knowledge of the spacecraft dynamic behaviour. Many previous studies have led to improve test efficiency and quality and also the post-processing of the measured data. However some significant difficulties encountered in dynamic test (either modal or base sine) remained insufficiently treated and is one of the native reasons of this study: to overwhelm them and improve dynamic testing effectiveness.


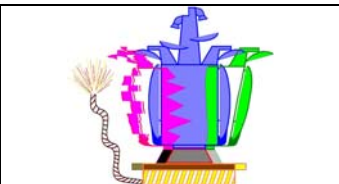
The ESA funded “DYNAMITED” study (standing for DYNAMics: AssessMent and Improvement of TEst Data) has been performed by a consortium of European industries and university (INTESPACE, University of Kassel and DLR), led by EADS ASTRIUM Satellites. This team took benefits from all heritages of previous major studies in the field of dynamic testing.

The main family domains tackled are:

- **Non-linearities:** Structures have always more or less non-linear behaviour which affect the measurements and may alter the test data exploitation if not taken into account in a proper way.
- **Interface parasitic motion:** test fixture softness may disturb the dynamic behaviour of the tested specimen as incorrect clamped boundary conditions are assumed whereas dynamic coupling of shaker and tested specimen should be taken into account.
- **Uncertainties:** test data always contain the results of basic uncertainties sources such as test parameters or test instrumentation. This induces by essence unknown scatter that should be taken into account for a better test exploitation.
- **Mathematical model validation:** the main objective of FEM validation by test is disturbed by numerous phenomena such as those previously mentioned. These problems have to be fixed to get a more robust and reliable method for FEM validation.
- **Test and measurement quality:** raw dynamic test measurements are time-recorded on acquisition machine. Treatment is thus necessary and it is important to have a proper knowledge of their effect on the exploited data. Moreover these data should respect some basic criteria derived from theory that should be verified in order to have a proper test quality assessment.

The DYNAMITED study allowed providing very fruitful improvements in a wide variety of mechanical testing domains. The state of the art allowed highlighting the actual test process, methodologies, tools and uncertainties.

The pre-test activities investigated new approaches based on uncertainty derivation to uncertainty on modal parameters which revealed interesting results. These data could then be derived as stochastic

		Ref : MTF.AIDT.TN.2168 Issue : 1 Rev. : 1 Date : 03/03/2010 Page : iii
---	---	--

notching profile which is of great importance in test preparation to save precious time in test in terms of efficiency, robustness and confidence. New base load recovery techniques were discussed and implemented in tools. The sine sweep rate effect have been fully discussed and two methods were proposed to estimate the maximum sweep rate wrt some predefined accuracies on modal parameters and to correct the modal parameters for a given sweep rate. Finally an original method and tool were proposed for sensor positioning in order to improve some sensors location wrt some mode of interest to maximize the distinguishability with and observability status.

The post test studies have also investigated a wide variety of domains. First a new fast modal extraction and correlation methodology has been proposed. This allows providing a quick correlation between FEM and test as well as to follow the specimen behavior evolution between two different tests. A second major milestone has also been achieved thanks to a sharper synthesis of the parasitic motion and an approach to remove its effect to recover the perfectly guided specimen behavior. Unless it is limited to numerical problems linked to test data quality, these methods are very ambitious and are a first step for a further realization by slight different approaches. Moreover, some methods to elaborate reduced experimental model were proposed. The study summarized the basic verification to do in order to assess the measurement quality. Finally an important effort has been done to propose a complete catalogue of powerful and applicable methods to detect, characterize and quantify non linear phenomenon. This has been extended by a method and a tool to interpolate and/or extrapolate the non linear behaviour to other not passed levels.

The most promising and useful methods in test have been implemented in 14 new tools in DynaWorks environment and one as an ISSPA extension to ensure an efficient industrial use of all the developments.

Based on the development and fruitful technical discussions, a new consideration of the best practice in test has been recorded, leading to propose a new process to improve test preparation and test assessment and exploitation.

The methodologies, tools and guidelines developed in the frame of this study have been deployed on the SWARM STM qualification test at a real scale to demonstrate their efficiency, robustness and reliability. The methods allow saving about 4 hours per test thank to the enhanced processes and tools.

Document controlled by Sébastien LABORDE
--

DOCUMENT CHANGE LOG

Issue/ Revision	Date	Modification Nb	Modified pages	Observations
1/0	31/12/09			Original document

PAGE ISSUE RECORD

Issue of this document comprises the following pages at the issue shown

Page	Issue/ Rev.	Page	Issue/ Rev.	Page	Issue/ Rev.	Page	Issue/ Rev.	Page	Issue/ Rev.	Page	Issue/ Rev.
All	1/0										

TABLE OF CONTENTS

1	INTRODUCTION	8
2	DOCUMENTATION	9
2.1	APPLICABLE DOCUMENTATION	9
2.2	REFERENCE DOCUMENTATION	9
3	ACRONYMS	10
4	STUDY OVERVIEW	10
5	ENHANCEMENTS IN VIBRATION TESTING	12
5.1	INTRODUCTION	12
5.2	CURRENT PROCESSES FOR DYNAMIC TESTING	12
5.2.1	<i>Modal test</i>	12
5.2.2	<i>Base sine test</i>	13
5.3	METHODS FOR TEST EXPLOITATION	14
5.3.1	<i>DYNAWORKS macros</i>	14
5.3.2	<i>IMES tools</i>	15
5.3.3	<i>PROTO tools</i>	15
5.4	REVIEW OF LAUNCHERS DYNAMIC SPECIFICATION	16
5.5	ALTERNATIVE TESTING METHODS	17
5.6	DYNAWORKS® FUNCTIONALITIES	17
5.7	TEST UNCERTAINTIES	18
5.8	CONCLUSIONS	19
6	PRE TEST METHODOLOGIES	20
6.1	INTRODUCTION	20
6.2	DERIVATION OF TEST UNCERTAINTIES TO UNCERTAINTY ON MODAL PARAMETERS	21
6.2.1	<i>Introduction</i>	21
6.2.2	<i>Methodology</i>	21
6.2.3	<i>Taking into account test uncertainties in FEM</i>	22
6.2.4	<i>Application on telecom spacecraft</i>	24
6.2.5	<i>Comparison with test data</i>	29
6.2.6	<i>Stochastic notching prediction</i>	29
6.3	BASE LOAD MEASUREMENT	33
6.3.1	<i>Introduction</i>	33
6.3.2	<i>Force Measurement Device</i>	33
6.3.3	<i>Mass operator</i>	35
6.3.4	<i>Coil Current</i>	36
6.3.5	<i>Mass operator building strategy</i>	37

6.4	SINE SWEEP RATE	40
6.4.1	<i>Sine sweep rate effect on modal parameters</i>	40
6.4.2	<i>Sine sweep rate selection</i>	42
6.5	SENSOR LOCATION	42
7	DURING TEST AND POST TEST METHODOLOGIES	44
7.1	INTRODUCTION	44
7.2	NEW CORRELATION CRITERIA BASED ON FRF	45
7.2.1	<i>Sensor global and local peak extraction</i>	45
7.2.2	<i>Mode extraction</i>	46
7.2.3	<i>Mode building</i>	47
7.2.4	<i>Test correlation</i>	47
7.3	TEST DATA QUALITY ASPECTS.....	48
7.3.1	<i>Parasitic motion</i>	48
7.3.2	<i>Motion of the specimen without parasitic motion</i>	51
7.3.3	<i>Static and residual terms for modal identification</i>	56
7.3.4	<i>Elaboration of reduced experimental model</i>	57
7.3.5	<i>Measurement quality</i>	58
7.4	NON LINEAR ASPECTS	62
7.4.1	<i>Detection, characterisation and quantification of non-linearities in dynamic tests</i>	62
7.4.2	<i>An approach to non-linear experimental modal analysis</i>	76
8	IMPLEMENTATION IN TOOLS	79
8.1	PRE TEST TOOLS	79
8.1.1	<i>Coil current determination</i>	79
8.1.2	<i>Estimation of suitable sine sweep rate for test preparation on piloting aspects</i>	80
8.1.3	<i>Sensor positioning for mode observability</i>	81
8.1.4	<i>Sign correlation matrix</i>	81
8.1.5	<i>Mass operator tool</i>	82
8.2	POST TEST TOOLS	83
8.2.1	<i>Estimation of sine sweep rate effects</i>	83
8.2.2	<i>Fast modal extraction and correlation</i>	84
8.2.3	<i>Static terms, residual modes and sensor orientation</i>	85
8.2.4	<i>Parasitic motion</i>	86
8.2.5	<i>Motion of the specimen without parasitic motion</i>	87
8.2.6	<i>ISSPA</i>	87
9	GUIDELINES	89
9.1	PRE TEST GUIDELINES	89
9.1.1	<i>Instrumentation guidelines</i>	89
9.1.2	<i>Test preparation guidelines</i>	90
9.2	POST TEST GUIDELINES	91

9.2.1	<i>Step 0: Tools preparation guidelines</i>	91
9.2.2	<i>Step 1: Test data assessment guidelines</i>	92
9.2.3	<i>Step 2: Test data and transfer function exploitation guidelines</i>	92
9.2.4	<i>Step 3: Test extrapolation to higher level guidelines</i>	93
9.2.5	<i>Step 4: Run sheet consolidation guidelines</i>	94
9.2.6	<i>Step 5: Modal extraction & correction and non linear exploitation guidelines</i>	94
10	REAL LIFE APPLICATION CASE	96
11	ATV TEST DATA	97
12	CONCLUSIONS	98
12.1	STUDY CONCLUSIONS.....	98
12.2	THE STEP BEYOND DYNAMITED	99
13	ANNEXES: NEW TEST PROCESS	101

1 INTRODUCTION

Structural dynamics is an important topic in order to design spacecraft structure as launchers generate a severe vibratory environment. It is thus required to have a deep knowledge of the spacecraft dynamic behaviour. This is usually done by a combination of analysis by Finite Element Model and dynamic testing, either modal or base sine tests. The aim of these tests is both spacecraft qualifying vs dynamic qualification environment and characterisation of its dynamic behaviour to correlate Finite Element Model which is used for Coupled Launcher Analysis.

As a consequence of the dynamic tests importance, many previous studies have led to improve test efficiency and quality and also the post-processing of the measured data. However some significant difficulties encountered in dynamic test (either modal or base sine) remained insufficiently treated and is one of the native reasons of this study: to overwhelm them and improve dynamic testing effectiveness.

The ESA funded “DYNAMITED” study (standing for DYNAMics: AssessMent and Improvement of TEst Data) has been performed by a consortium of European industries and university (INTESPACE, University of Kassel and DLR), led by EADS ASTRIUM Satellites. This team took benefits from all heritages of previous major studies in the field of dynamic testing (“Real-Time Modal Vibration Identification”: RTMVI, “Enhancements of Dynamic Identification for Spacecraft”: EDIS and a CNES R&T study “Modal Identification on Sine-base Excitation”: IMES). The main family domains tackled are:

- **Non-linearities:** Structures have always more or less non-linear behaviour which affect the measurements and may alter the test data exploitation if not taken into account in a proper way.
- **Interface parasitic motion:** test fixture softness may disturb the dynamic behaviour of the tested specimen as incorrect clamped boundary conditions are assumed whereas dynamic coupling of shaker and tested specimen should be taken into account.
- **Uncertainties:** test data always contain the results of basic uncertainties sources such as test parameters or test instrumentation. This induces by essence unknown scatter that should be taken into account for a better test exploitation.
- **Mathematical model validation:** the main objective of FEM validation by test is disturbed by numerous phenomena such as those previously mentioned. These problems have to be fixed to get a more robust and reliable method for FEM validation.
- **Test and measurement quality:** raw dynamic test measurements are time-recorded on acquisition machine. Treatment is thus necessary and it is important to have a proper knowledge of their effect on the exploited data. Moreover these data should respect some basic criteria derived from theory that should be verified in order to have a proper test quality assessment.

The main tasks of this study have been therefore to define methodologies and processes to tackle the different subjects and to develop related tools usable in an industrial context. To reach a deeper assessment these tools have been developed in DynaWorks environment to make them available during every test campaign, or as an extension of ISSPA to take benefits of the experimental modal analysis tool basis. All the developments have been finally tested during the SWARM STM dynamic test campaign.

2 DOCUMENTATION

2.1 APPLICABLE DOCUMENTATION

AD 1 Assessment and Improvement of Dynamic Test Data
In answer to ESA ITT AO/1-5095/06/NL/IA
Reference: 2124.PR.JBB.06.8519.ASTR – July 2006

AD 2 Assessment and Improvement of Dynamic Test Data
ESA contract n°20307/06/NL/IA

2.2 REFERENCE DOCUMENTATION

RD 1 RTMVI Final Report

Reference: MTE 959.NT.YML.6908.01 – 28/10/01 – Issue 0, Revision 3

RD 2 Identification modale sur essais sinus – Rapport final

Reference: DO05.016 DCT/ag – 29/04/05 – Issue 1, Revision 0

RD 3 Enhancement of Dynamic Identification for S/C – Final Report

Reference: DO05.016 DCT/ag – 29/04/05 – Issue 1, Revision 0

RD 4 ISSPA 02 User's Guide

Kassel Universität – Rev Jan, 19th 2004

RD 5 DYNAMITED – WP2000 – Enhancements in Vibration Testing

Reference: AOE23.AIDT.TN.0338 – 29/03/07 – Issue 1, Revision 0

RD 6 DYNAMITED – TN2 – Test methodology

Reference: MTF.AIDT.TN.0656 – 31/03/09 – Issue 2, Revision 0

RD 7 DYNAMITED – TN3 – Implementation of methodologies in tools

Reference: MTF.AIDT.TP.1201 – 18/11/09 – Issue 2, Revision 0

RD 8 DYNAMITED – TN4 – Test procedures

Reference: MTF.AIDT.TP.1203 – 18/11/09 – Issue 2, Revision 0

RD 9 DYNAMITED – TN5 – Application report of the methodologies and tools on the SWARM sine tests

Reference: MTF.AIDT.TP.1987 – 30/09/09 – Issue 1, Revision 0

RD 10 DYNAMITED – TN6 – Application case on the ATV perturbed sine test data

Reference: MTF.AIDT.TP.2174 – 01/02/10 – Issue 1, Revision 0

RD 11 DYNAMITED – TN7 – Software tool user’s manual

Reference: MTF.AIDT.TP.2093 – 18/11/09 – Issue 1, Revision 1

3 ACRONYMS

CLA	Coupled Load Analysis	MAC	Modal Assurance Criterion
CoG	Centre of gravity	MASSOP	MASS OPERator
Dof	Degree of Freedom	MDOF	Multi Degree Of Freedom
DYNAMITED	DYNAmics: AssessMent and Improvement of TEst Data	MVS	Moyen de Vibration Système
ESA	European Space Agency	RTMVI	Real Time Modal Vibration Identification
ESTEC	ESA Space Research and Technology Centre	QSL	Quasi Static Loads
FEM	Finite Element Model	S/C	Spacecraft
FMD	Force Measurement Device	SDOF	Single Degree Of Freedom
FRF	Frequency Response Function	STM	Structural Test Model
IMES	Identification Modale sur Essai Sinus	wrt	with respect to

4 STUDY OVERVIEW

The study has been managed in four times:

- In a first time the study provided a wide range state of the art in mechanical testing in order to have a global overview of the existing methods and give a 1st basis for the possible enhancement ways.

The state of the art allowed giving an overview of the current processes for dynamic testing (modal or base sine excitation), the methods most generally used by ASTRIUM for test exploitation (test process and macros tools, IMES tools, PROTO tools and DYNWORKS software), a wide overview of the launcher variety and dynamic specifications and finally after review of alternative testing methods, a detailed analysis of the test uncertainties have been studied and quantified to serve as entry of the 2nd step.

- In a second time the study concentrated on the test preparation improvement. It interested to methodologies, tools and general best practices to avoid or minimise troubles and provide a shaper valuable analysis to save time. The best methodologies have been implemented in tools in DYNWORKS software environment and best practice guidelines have been written.

The study interested to derive the identified and quantified test uncertainties to uncertainty on

modal parameters by FEM analysis and correlation with test data cloud. These uncertainties effects have been used to build stochastic notching profile which revealed to be of great interest in test preparation to save precious time in test in terms of efficiency, robustness and confidence. A complete study is provided to improve base load measurement techniques. The sine sweep rate effect and prediction has been fully detailed as well as a powerful method to improve sensor positioning on the specimen wrt mode distinguishability and observability.

- In a third time the same approach has been led to improve test assessment and exploitation during and after the test. The aims are to provide a better assessment of the raw test data, to improve additional parameters extraction for FRF completion and provide additional methods to help identify, characterize and quantify the malfunctions or undesired phenomena in order to know their precise nature and better deal with them. The best methodologies have been implemented in tools in DYNWORKS software environment and in an extension of ISSPA and best practice guidelines have been written.

The study interested to a new correlation criteria based on FRF to provide a fast modal extraction and correlation in test (between test and FEM or to follow specimen behaviour evolution between two tests). The test data quality aspects have been widely discussed to provide different method to detect and synthesise parasitic motion and its effect on the specimen, as well as an original method to remove it to recover the perfectly guided specimen response. Additional static and residual terms could also have been extracted to complete the FRF database. Some methods were proposed to elaborate reduced experimental models and other to checks measurement quality thanks to basic properties. Finally an important effort has been made to provide a complete set of method to detect, characterize and quantify non linearities in the mechanical behaviour. This has been extended to a method and tool to interpolate and/or extrapolate the non linear behaviour to other not passed levels.

- Finally the last step of the study aimed to demonstrate the development powerful, utility and relevant advantage in a real test context: it has been apply on the real scale test campaign: the SWARM STM qualification tests at IABG in June/July 2009.

5 ENHANCEMENTS IN VIBRATION TESTING

5.1 INTRODUCTION

The first study step consists in providing a detailed description of the actual processes generally used in space industry to manage dynamic tests, focusing on:

- INTESPACE process to deal with acquisition and treatment of test data.
- ASTRIUM processes for both base sine test and modal tests.

A wide description of DynaWorks software is provided as a complete tool to deal with dynamic testing.

A bibliographical research synthesis has been made in order to have a global view of test requirements all over the world as well as for launchers dynamic specifications and the way to deal with them. Alternative testing methods are also shortly presented.

A specific study has been tackled to provide a detailed list of all uncertainties source that may be encountered in dynamic test. The objective is to provide inputs to the stochastic work package.

5.2 CURRENT PROCESSES FOR DYNAMIC TESTING

5.2.1 Modal test

The modal survey tests are used to characterize precisely the modal behaviour of a structure. Based on a wide experience an efficient test process split in 4 steps is applied by ASTRIUM:

1. **Test configuration.** This concerns the proper test configuration installation which can be split in 5 points:
 - Specimen boundary conditions: this aims to correctly take into account the boundary conditions representative of the real used configuration (free-free, clamped, ...)
 - Test instrumentation: it is important to have appropriate test instrumentation location, sensor allowing a correct measurement range and connection to the specimen
 - Test facilities: an adequate acquisition chain and test piloting hardware is necessary.
 - Type of excitation: the excitation is generally realized with an electro dynamic shaker in free-free interface conditions whose power must be adapted to the structure robustness and mode amplification.
 - Test configuration checks: it is necessary to apply basic checks to verify correct test implementation and measurement chain continuity.
2. **Quick modal identification:** this aims to quickly identify mode location by short rough test to verify the correct measurement parameter to avoid overloading.
3. **Excitation and reciprocity check:** this important check aims to verify the reciprocity principle.
4. **Complete acquisition and linearity characterisation:** the test can be achieved taking into account different input level allowing verifying linearity behaviour (frequency and amplitude).

5.2.2 Base sine test

The mechanical tests are a critical point in the spacecraft development. To deal as efficiently and fast as possible with such complex tests a dedicated powerful process is applied by ASTRIUM. It is both based on a complete preparation phase before the test as well as on a robust and secure global process for managing the dynamic tests. This allows saving time in the test data treatment.

This process is split in four main parts shortly explained hereafter and completely detailed in the RD 5:

1. **Test data measurement pre-treatment:** This aims to:
 - take into account all the test parameters (test variables, max band per frequency band ranges, previous run sheet definition) to parameter tools variables.
 - apply basic measurement check on raw data (correct measurement of pilot sensors, global/fundamental comparison, ...)
 - Calculate transfer function for prediction process analysis with the pilot inaccuracy and complete the transfer function base with the additional sensors (bi sensors, lateral and resultants sensors, QSL and mass operator) and create an image of the mode location thanks to the max band per frequency bands applied on transfer functions.
2. **Test data measurement exploitation:** this aims to exploit the raw test data in parallel from the previous step 2. The objective is to:
 - Complete the raw test data by the post processed achieved levels (bi sensors, lateral and resultants sensors, QSL and mass operator).
 - Status about the achieved levels to compare with CLA objectives.
 - Perform the spacecraft health status by comparing the response levels with the limitation database and correlating the behaviour with the FEM and with the previous run by raw test data comparison or transfer functions comparison.
3. **Notch spectrum determination or Pre/Post low level comparison:** This aims at:
 - Comparing low level responses in case of low levels or for the last run of an axis or
 - Preparing the next level run in case of a prediction to an upper level by:
 - Finding notching profile based on limitation database
 - Finding the critical reduced set of sensor for notching strategy building
 - Build the notching strategy with a reduced set of sensors (input level shape and notch criteria). This iterative steps aims to get a final notch profile lower or equal to the one obtained from limitation database.
4. **Run sheet preparation and verification:** this final part aims to verify the run sheet, calculate the abort margins on the notching sensors, to define the abort sensor and criteria. This difficult step is done thanks to the pilot inaccuracy. A maximum value per frequency range is calculated on the notched responses to verify the expected CLA coverage.

5.3 METHODS FOR TEST EXPLOITATION

The methods for test exploitation are based on three tools:

1. DynaWorks macros tools developed in the Dynaworks environment.
2. IMES study heritage and developments
3. Proto developed in MATLAB environment

5.3.1 DYNWORKS macros

ASTRIUM has developed integrated in DynaWorks® a complete and powerful environment which helps to manage quickly and efficiently all types of mechanical tests allowing automatic treatment of large amount of data. This environment developed in user functions and macros supports directly the process presented in §5.2.

The main tools lines are shown here. For a complete description, refer to RD 5.

The tool is split in 4 parts (as shown in Figure 5-1):

1. **CONFIGURATION:** This part allows loading data parameters and variables necessary for the macros.
2. **UTILITY:** This part brings together some useful utilities dealing with database management and additional data calculation.
3. **CURVES TREATMENT:** This part brings together some useful utilities dealing with data post processing.
4. **PREDICTION:** This part brings together some useful utilities dealing with prediction to upper level.

=====> CONFIGURATION
Load macros data
=====> UTILITY
Clean registers
Test creation
Curve creation
Write Registers
Additional Sensors
Load List
=====> CURVES TREATMENT
Display Responses
Display Program Responses
Plot Curves
Curves Maximum Value
Curves Maximum Value per frequency range
Sine -> Random
gRMS calculation
=====> PREDICITON
Pilot and transfer functions calculation
Prediction
Sensors Response
Calculation of the Q factor evolution between two tests

Figure 5-1: ASTRIUM tool

5.3.2 IMES tools

The IMES study (CNES funding) aimed to improve the modal identification method previously developed in RTMVI which allowed:

- developing a modal identification method based on shaker sine test,
- validate the feasibility of this method using a prototype software and a test example,
- Identify necessary improvements.

The works in this study consist in improving some RTMVI method points and validate these improvements and prepare industrialization. This work deals with the two following points:

- Improve measurement methodology for a better results measurement exploitability. This has been done by a better instrumentation and systematic control particularly at low frequency:
 1. Definition of quality measurement quantitative indicator to evaluate error sources (as non linearity's, noise, parasitic motion)
 2. Definition of an adapted test methodology: type of sensor, their mounting, frequency data treatment. Measured transfer function control (low frequency, locally and reciprocity) and sensor treatment.
 3. Low frequency data exploitation in relationship with FEM for coherence check between sensor measurement and geometry, between measured forces and masses. Coherence verification between static and modal data.
- Improve analysis technical to reduce calculation times and/or increase precision.

The complete study results are available in RD 2. The DYNAMITED study aims to take heritage of this to integrate the results and developed tools in DynaWorks® as an industrial tool.

5.3.3 PROTO tools

Proto-dynamic is a software developed in MATLAB environment by INTESPACE and LMARC.

Proto-dynamic is a combination of MATLAB uncompiled functions providing tools for advanced structure analysis. This platform allows treating NASTRAN data as well as experimental data.

The main functionalities are:

- FEM correlation update
- Modal identification from FRF
- Mode shape comparison: MAC ...
- FEM response calculation
- Modal strain energy calculation
- Mode sensitivity wrt a physical parameter calculation

5.4 REVIEW OF LAUNCHERS DYNAMIC SPECIFICATION

A complete review of launchers dynamic specifications has been done to have a complete overview of the mechanical specification variety. The detailed analysis is given in RD 5.

The main conclusions are that above the two launchers categories studied:

1. Classic launchers (generally used for commercial launches)
2. Exotic launchers: new launchers or specific launch (military, high capacity)

A wide variety of mechanical specifications are applicable to the spacecraft, as shown hereafter:

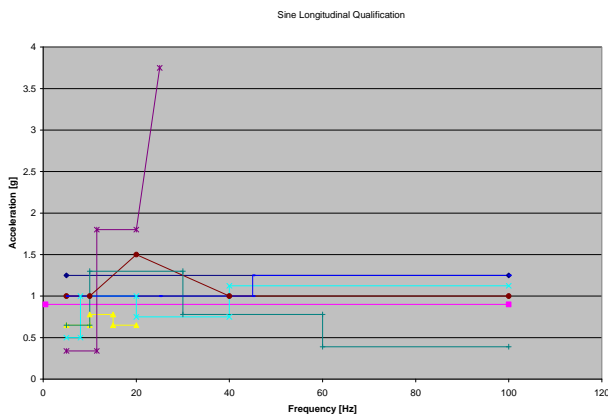


Figure 5-2 : comparison of sine longitudinal specification for classic launchers

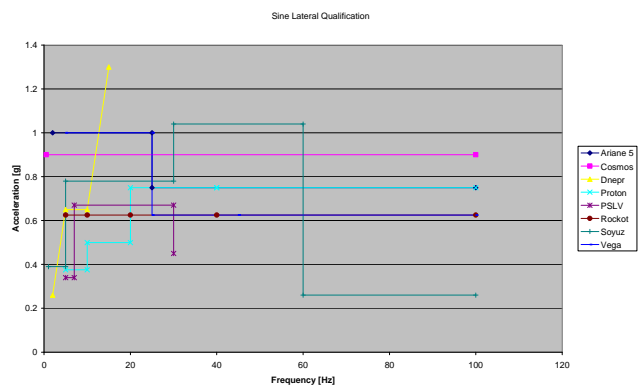


Figure 5-3 : comparison of sine lateral specification for classic launchers

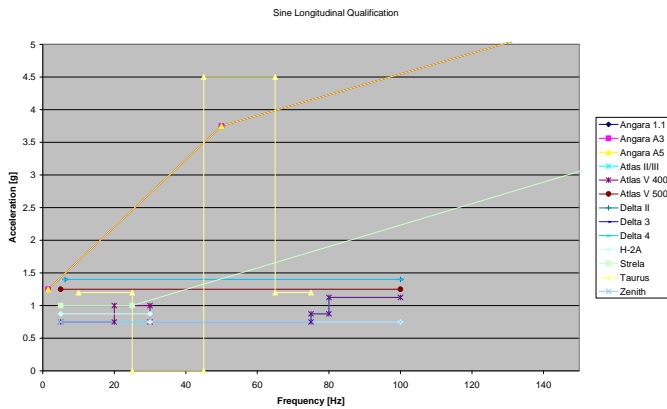


Figure 5-4 : comparison of sine longitudinal specification for exotic launchers

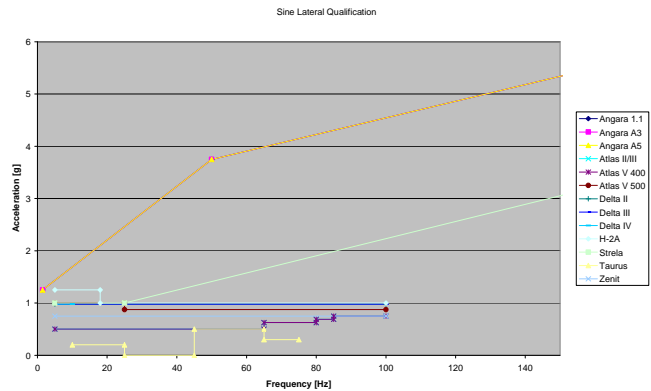


Figure 5-5 : comparison of sine lateral specification for exotic launchers

		Ref : MTF.AIDT.TN.2168 Issue : 1 Rev. : 1 Date : 03/03/2010 Page : 17
--	--	---

5.5 ALTERNATIVE TESTING METHODS

The classical testing methods consist to apply to the specimen the specified environments whose levels intensity are progressively injected to achieve the specified qualification level and avoid failure in test:

- **Sine and random:** The specimen is generally clamped at his base on the adaptor connected to the shaker table with a base sine excitation.
- **Acoustic:** the specimen is generally put in a reverberation room and clamped at his base on a table.

Alternative testing methods are used generally in particular cases:

1. If the specimen is **recurrent** from another fully tested model. Lower levels could be injected not on all the axis to verify the correct modal behaviour wrt a STM or PFM model and save test time duration.
2. **Equipments.** For large equipments, random excitation could be replaced by direct acoustic test whereas for small equipments the qualification could be achieved by random excitation.

Other alternative testing methods are:

3. Transient excitation. This type of excitation is very close to the real environment but this way of qualification is not used mainly due to the two following reasons: the launcher time history signal is confidential and subject to important variability risk and the actual qualification method is dimensioning allowing covering the launcher environment uncertainty.
4. Multi-axis excitation presents a lot of configuration advantages and a type of excitation close to the real excitation on launcher but it is not used due to the specification provided by the launcher authorities and the complexity of piloting such tests. Moreover such installations are very rare.

5.6 DYNAWORKS® FUNCTIONALITIES

The DynaWorks® software is a powerful tool to process and analyze dynamic tests data, and to compare these results to analytical ones. It may be used for test exploitation such as analytical phase, and correlation.

The main DynaWorks® functionalities very useful to analyze dynamic test data are the following:

- Simple and quick availability of analytical results in a DynaWorks® database with different importing way supporting all common formats.
- Process the measured data via the available functions library to create harmonic, global responses and transfer functions.
- Extract modal parameters and shapes via available identification tools thanks to 2 DynaWorks® modules implemented: ISSPA method and RTMVI method.
- Analyze the results and compare to analysis.

These functionalities are completely detailed in the RD 5 and DynaWorks user's manual.

5.7 TEST UNCERTAINTIES

The measurement uncertainty in vibration testing is a combination of several types of elementary uncertainties which can be grouped as follows:

- **Specimen/interface transducer** uncertainties related first to the transducer's location and orientation, then to the way the transducer is connected to the specimen.
- **Acquisition chain uncertainties** related to the transducer, to the conditioner and the digitalizer.
- **Post-processing** depending on the type of the test (sine or random), uncertainties related the post-processing of raw data.

For each case, a list of uncertainties is provided and quantified (taking into account the AFNOR recommendations) even if some of them are in fact negligible.

Each elementary uncertainty is reduced to 1 standard deviation (1σ) according to the COFRAC recommendations:

- for results obtained from statistics: assuming a Gaussian distribution for which the maximum uncertainty is about 3 times the standard deviation (3σ), this 3σ value has to be divided by 2,
- for manufacturer specifications: assuming a rectangular distribution the specified value has to be divided by 1.7.

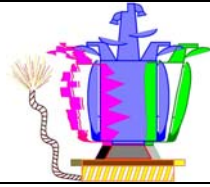
Intermediate uncertainties at 1σ result from various elementary uncertainties at 1σ combined quadratically, except if systematic error (direct sum), following the COFRAC accreditation organization.

A global value at 1σ is then derived from intermediate uncertainties at 1σ combined quadratically. A coverage factor of 2 is finally applied to provide a global uncertainty at 2σ corresponding to a confidence level of 95.5 %, as presented in Table 5-1.

Uncertainty type	Piezoelectric acc. + ENDEVCO	Piezoelectric acc. + DIFA	Acc. with integrated electronics + PCB	Strain gages
Specimen/transducer interface	2.1 %	2.1 %	2.1 %	7.1 %
Transducer	4.0 %	4.0 %	2.9 %	0.5 %
Conditioner	1.9 %	1.5 %	0.8 %	1.5 %
Digitalization	0.047 %	0.047 %	0.047 %	0.047 %
Sine sweep	0.1 %	0.1 %	0.1 %	0.1 %
Uncertainty at 2σ	9.8 %	9.5 %	7.3 %	14.5 %

Table 5-1: Global uncertainties at 2σ

Uncertainty on frequency at 2σ : 0.2 %.



5.8 CONCLUSIONS

An overview of mechanical testing has been addressed concerning the system aspects related to the current processes for dynamic testing, the methods for test exploitation, a complete review of launchers dynamic specification and alternative testing. Likewise, the testing aspects have been addressed related to the current tool for dynamic testing with a complete description of DynaWorks® test functionalities and a quantification of test uncertainties.

This state of the art allowed revealing the enhancements to be wished in vibration testing to improve the quality and representativity of test data. These actions can be split in pre test and post activities.

In pre-test activities, the following topics have to be studied:

- Take into account the test uncertainties in test pre parathion to derive their effect on modal parameters,
- Derive the stochastic notching prediction,
- Improve base load measurement techniques,
- Take into account the sine sweep rate effect,
- Improve the instrumentation thank to a better positioning of the sensors.

For post-test activities, the following topics have to be studied:

- Propose a new correlation criteria based on FRF,
- Improve the test data assessment and quality by a better characterisation of the parasitic motion, determine its effect on the specimen and propose a method to recover the perfectly guided specimen behaviour,
- Improve the test data assessment and quality by completing the FRF data base with static and residual terms,
- Propose new methods to build with experimental models without having resort to a finite element model,
- Remind the basic principles to verify to check measurement quality,
- Propose techniques to identify, classify and characterize non linearities
- Propose techniques to deal with non linear behaviour to predict not passed levels.

Theses approaches are presented in the following paragraphs.

6 PRE TEST METHODOLOGIES

6.1 INTRODUCTION

The pre test methodologies focus on all activities that can be achieved before the dynamic test in order to anticipate possible difficulties, to secure its progress and to have the best inputs with respect to the test objectives. Different methodologies have been developed to meet the multiple study objectives.

The methodologies studied concerns the following themes:

- **Uncertainties** have been tackled on two aspects: on one hand, test uncertainties and on the other hand prediction uncertainties.

Test uncertainties may have various origins but all of them induce dispersion on measurement. The aim is therefore to give an *a priori* assessment of test uncertainties in order to build a standardised cloud for test data and therefore to match the EDIS philosophy. Using the different uncertainties identified in the state of the art, evaluation of their impact are made on all output parameters of interest of a dynamic test. Either analytical or Finite Element methods are used to derive these impacts. For instance, the impacts of uncertainties concerning sensors orientation and location have been evaluated using stochastic FEM calculations. Finally an assessment of incertitude on outputs is provided for each source of uncertainty. Method for combining the incertitude sources has also been studied using standard stochastic methods.

FEM used for test prediction are always approximated. This model uncertainty knowledge is derived before the test to build a stochastic notching profile: such approach goes beyond the modal approach directly to the sine response, which is effectively measured during test. Doing so facilitate the negotiation with launcher authorities during the test if a notching profile envelope is agreed before the test. Building such notching profiles require stochastic calculations and adequate post-processing with evaluated FEM uncertainty as input.

- **Base load measurement** is of high importance in base sine test and should always be measured or at least evaluated. The aim is of this part is to make an assessment on the precision of the various methods dedicated to base load evaluation, basically coil current and mass operator. Optimisation techniques are compared to direct static reduction of the FEM.
- **Sine sweep rate** is an important parameter for base sine tests, as it is linked to piloting stability and has an influence on test data. Two different aspects have been studied here: the estimation of the sine sweep rate effect on the FRF peaks (frequencies, levels, width) and the calculation of the suitable sweep rate in order to not exceed on specific mode minimum modal parameters precision.
- **Sensor location** is of primary importance for test results since it defines the specimen dynamic behaviour by providing components of the deformed shapes. It is thus worthwhile to improve it the sensor location with respect to general criteria of mode observability. The measured components must allow making distinction between the shapes with a good observability. An optimisation methodology for sensor location according to the orthogonality criteria (Modal Assurance Criteria or MAC) has been built using a mathematical model providing relevant data.

6.2 DERIVATION OF TEST UNCERTAINTIES TO UNCERTAINTY ON MODAL PARAMETERS

6.2.1 Introduction

The objective of this study is to compute using a stochastic approach a cloud representing the global error on test results due to the identified test uncertainty parameters. The way to do this is to use a standard finite element model and to derive on it all these test uncertainties using NASTRAN finite element solver.

The objective is not to study correlation between FEM model results and real test data but to determine the dispersion that may be expected on test data due to test uncertainties. As the main objective is the improvement of test prediction using finite element approach, taking into account these uncertainties into the FEM may anticipate such dispersion in test results. The final expected result is that predicted sine responses envelop shall include sensor response measured during vibration test.

6.2.2 Methodology

The NASTRAN output corresponding to test result is sine response (amplitude versus frequency curve) on restitution grids, corresponding to test transducers. The main difficulty, using this kind of output, is to generate a cloud defined by points with amplitude versus frequency curves as input.

To fit with the EDIS philosophy (RD 3), a modal approach is used. Modes have to be identified on sine responses (maximum pick on a frequency range) and have to be treated separately. The final objective is to get a cloud representing one mode on amplitude versus frequency diagram for each degree of freedom.

The following example shows the principle of the computation of the global stochastic cloud studying a plate submitted to Z sine excitation. A Monte-Carlo analysis using all test uncertainty parameters has been executed with 60 shots. As Q-factor is identical for all shots, the gap on amplitude represents the variation of the identified modal shape. The 60 Z responses of one of the grid of the model are given in Figure 6-1:

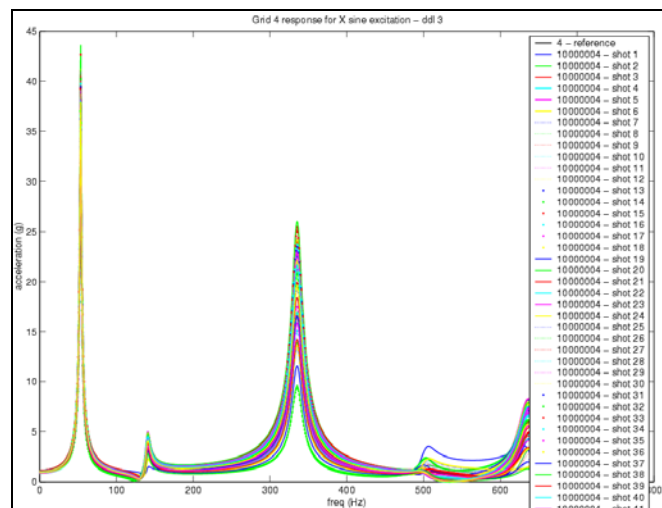
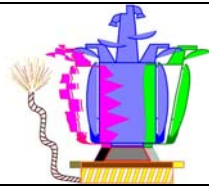


Figure 6-1 : Stochastic sine response example



Focusing on the amplitude and the frequency of the first mode, the stochastic cloud is achieved calculating the maximum peak in the frequency range of interest. If no peak is identified then the maximum value is used (i.e. value at lower or upper frequency). The maximum value is associated to its frequency. The Figure 6-2 shows the response of the grid 4 (Z response) for the first mode:

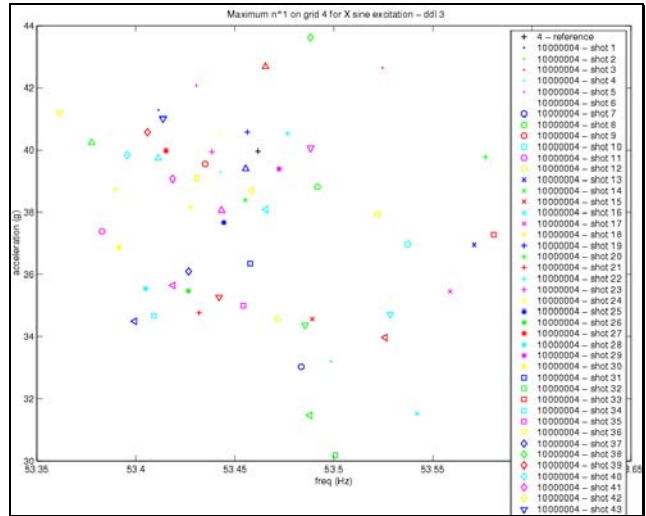


Figure 6-2 : Amplitude/frequency cloud for mode 1 at grid 4

This cloud is normalized thanks to amplitude and frequency reference values (from the nominal case). Finally, all degrees of freedom (of all grids) normalized clouds achieved from the same mode study are superposed to get a single cloud representing the mode of interest. The Figure 6-3 shows the association of 2 grid clouds:

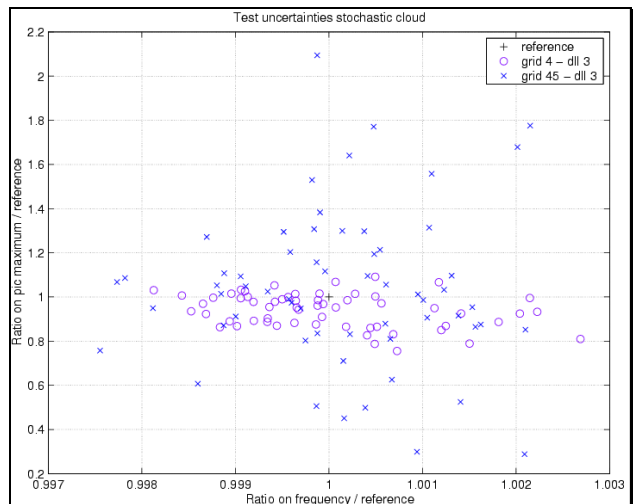


Figure 6-3 : Normalized amplitude/frequency cloud for mode 1 at grid 4

All amplitude and frequency values are divided by the reference so mode clouds should be superposed to get the whole cloud that represents the analysis. It is thus easier to compare FEM prediction to test data.

The associated hypothesis to this method is that all grids may be used to identify one mode which is only true for global modes.

6.2.3 Taking into account test uncertainties in FEM

All the test uncertainty parameters generally met have been classified in Table 6-1 with respect to the kind of output they modify in a FEM analysis. To illustrate, it is simple to estimate for example that frequency extraction is not sensitive to sensor orientation while MAC analysis is.

Test uncertainty	FEM analysis type sensibility				
	Frequency extraction	MAC analysis	Effective masses calculation	Sine Analysis	Notched profiles
Sensor orientation		X		X	X
Sensor location		X		X	X
Specimen/transducer's interface "accelerometers"		X		X	X
Specimen/transducer's interface "Strain gauges"				X	X
reaction Force thanks to coil current intensity			X	X	X
Acquisition chain: "piezoelectric accelerometers"		X		X	X
Acquisition chain: "accelerometers with intergrated electronics"		X		X	X
Conditioner		X		X	X
Post-processing: Acquisition from sine sweep (frequency estimation)	X	X	X	X	X
Digitalisation	X	X	X	X	X

Table 6-1: FEM analysis type sensibility to test uncertainty parameters

Sine analysis approach is mainly of concern in this study as it corresponds directly to test measurement and thus is impacted by all the listed test uncertainty parameters.

The different uncertainties taken into account are listed here below and are assumed to have a Gaussian repartition:

- **Sensor location**

This test uncertainty is the most difficult to take into account in a NASTRAN finite element model as it shall not modify the mathematical validity of the model, thus moving restitution grids is not allowed. Two solutions (described in RD 6) are proposed to solve this problem: the MPC and the tangent plane methods.

- **Sensor orientation**

Sensors may be incorrectly oriented during the sine vibration test and thus impact directly the responses. This is mainly due to difficulties to access to sensor location during the S/L instrumentation. The principle here (described in RD 6) consists in modifying sine responses using Eulerian angles to take into account this error on FEM results.

- **Other uncertainties**

Other uncertainties are directly applied to FEM sine responses:

- transducers signal error (frequency or temperature dependent, linearity...) and specimen/transducer interface error (mass, quality of connection, cable effect...),
- acquisition chain uncertainties: the conditioner or digitalisation system error,
- uncertainties from post-processing: sine sweep rate (frequency estimation).

- **Neutral fibre specific influence**

FEM are an idealisation of the reality which induces an additional uncertainty on the calculated FRF wrt the one measured in test due to shell thickness in one hand and transducer interface mounting system in the other hand. The principle here (described in RD 6) consists in offsetting the restitution point from the neutral fibre.

All of these test uncertainty parameters apply to sine responses amplitude except the sine sweep rate which applies to frequency. Some uncertainties apply independently to each dof (sensor location, orientation...) while others are applied to all of them (sine sweep rate).

As a first simplification all these uncertainties are merged in two kinds of parameters that apply to each restitution dof which means that all acquisition tracks are considered as independent:

- Parameters relative to amplitude which correspond to the sum of transducer and acquisition chain errors (5% at 1σ),
- Parameters relative to frequency which correspond to sine sweep rate error (0.1% at 1σ).

The number of parameters is thus 2 times the number of restitution dofs.

6.2.4 Application on telecom spacecraft

The uncertainties have been applied on a representative typical telecom spacecraft based on a classical Eurostar 3000 platform in test configuration tested on INTESPACE test facilities. The spacecraft FEM is composed of 700 000 dof and 175 000 elements.

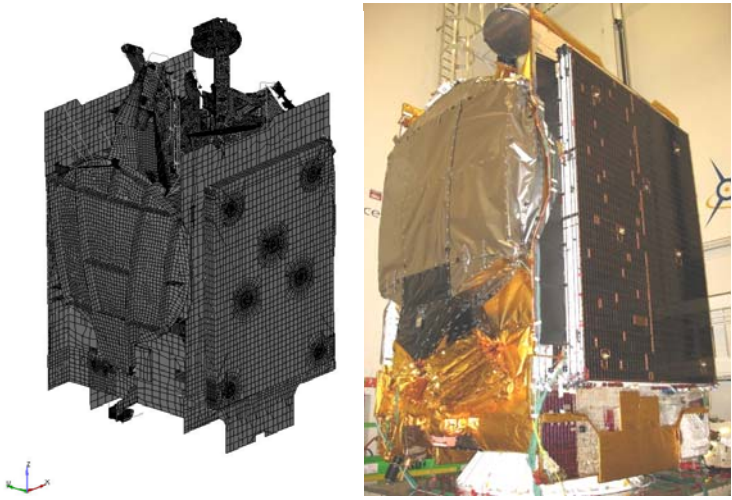


Figure 6-4: Telecom spacecraft application case

To study the impact of test uncertainty parameters, it is necessary to focus on main modes on the three excitation axes. Three modes of interest per axis are selected (see Figure 6-5) using the reference effective mass criterion first and notchings observed during sine vibration test. For each stochastic shot, these modes will be identified on all restitution grid responses leading to stochastic clouds.

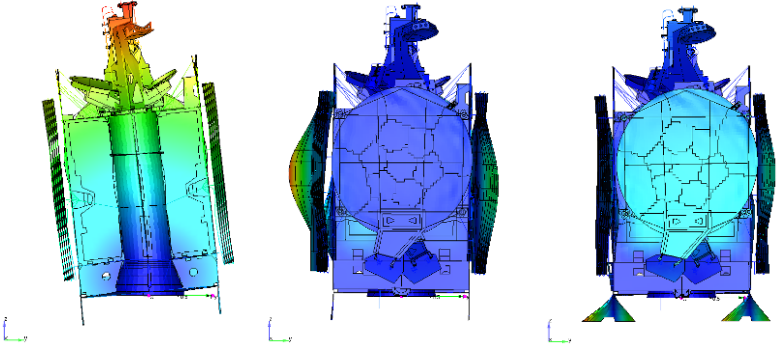


Figure 6-5: Y modes - first lateral mode, solar arrays mode and coupled S/C mode

This method allows building dispersion clouds (Figure 6-6) for each uncertainty type from which are derived: error probability density diagram (Figure 6-7) (that gives complementary dispersion information on the stochastic cloud) and probability diagrams (Figure 6-8). The probability diagram is computed from Equation 1.

$$\text{Equation 1 } P(f \leq f_0; \gamma \leq \gamma_0) = \iint_{\substack{f \leq f_0 \\ \gamma \leq \gamma_0}} p(f, \gamma) df d\gamma$$

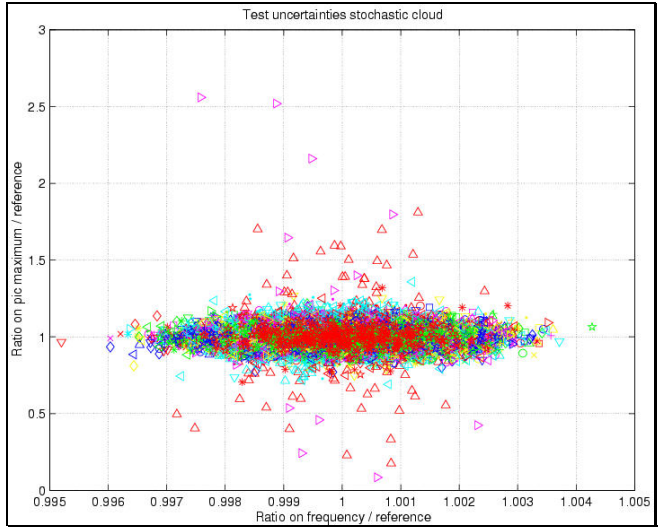


Figure 6-6: Dispersion cloud example for sine X mode n°1

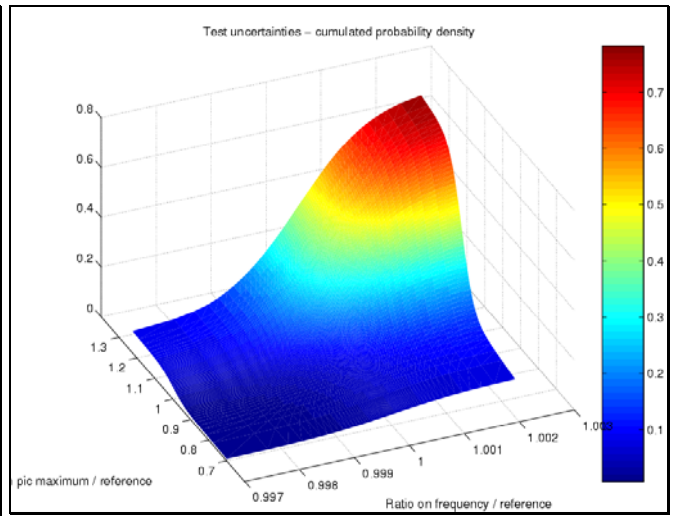
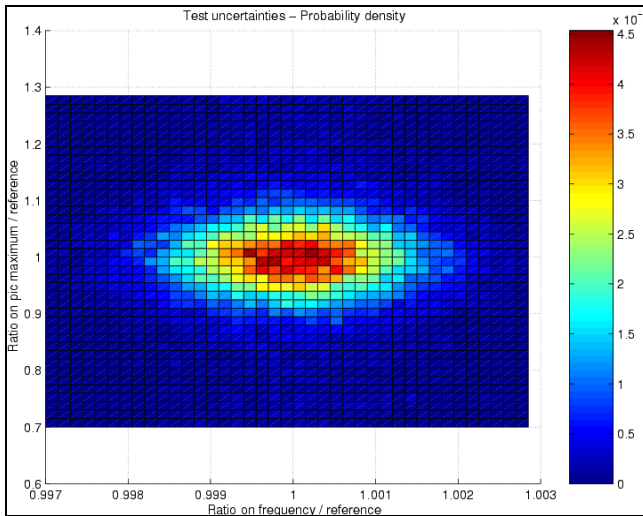
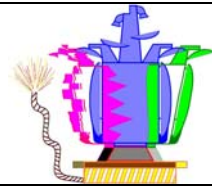


Figure 6-7: Probability density for sine X mode n°1 Figure 6-8: Probability diagram for sine X mode n°1

The detailed application is provided in RD 6. The Monte-Carlo stochastic analysis sequence includes super elements generation, modal and sine analysis for the different uncertainties (Table 6-1). This represents a huge amount of calculations (2124 parameters and 120 shots).



However, the main results of this study are given here below for each uncertainty type:

- **Sensor location and orientation error**

The probability to have an error due to sensor location and orientation lower than 10% is between 95 and 98% depending on the mode. More globally, the probability to have an error on amplitude due to sensor location lower than 2% is 66% which would consist in a $\sim 2\%$ error at 1σ assuming Gaussian repartition.

The second main result is that this error is not as mode dependent as expected. The third result is that frequency is not dependent on sensor location error.

Thus to improve test preparation, sensors that give large dispersion on results due to error on their location shall be identified.

- **Other uncertainties parameters**

The error on sine responses is mode dependent. The first X and Y lateral modes are more sensitive than the other to test uncertainty parameters. In fact, the lateral modes have about the same frequency (15.9Hz in X direction, 16.0Hz in Y direction), so the orientation of the sensor may add non negligible transverse response. The sensor orientation parameter seems to be the origin of the large dispersion in the two lateral modes.

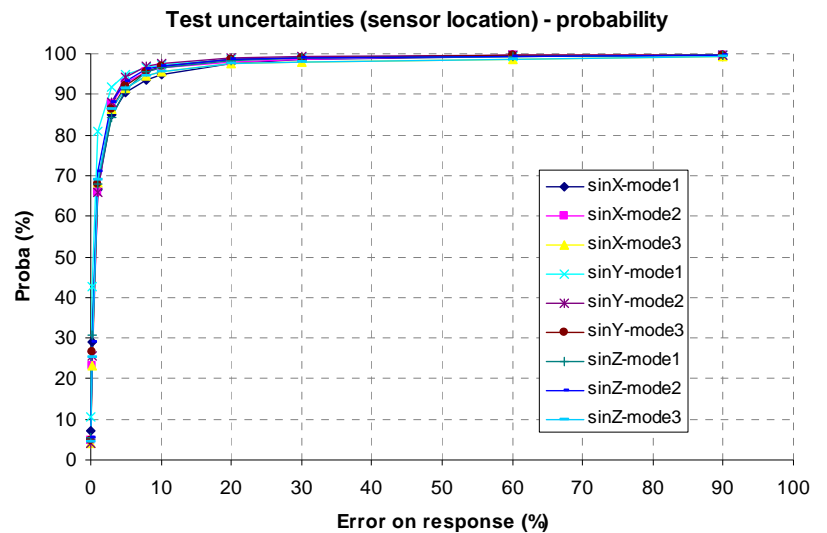


Figure 6-9: Probability error due to sensor location and orientation

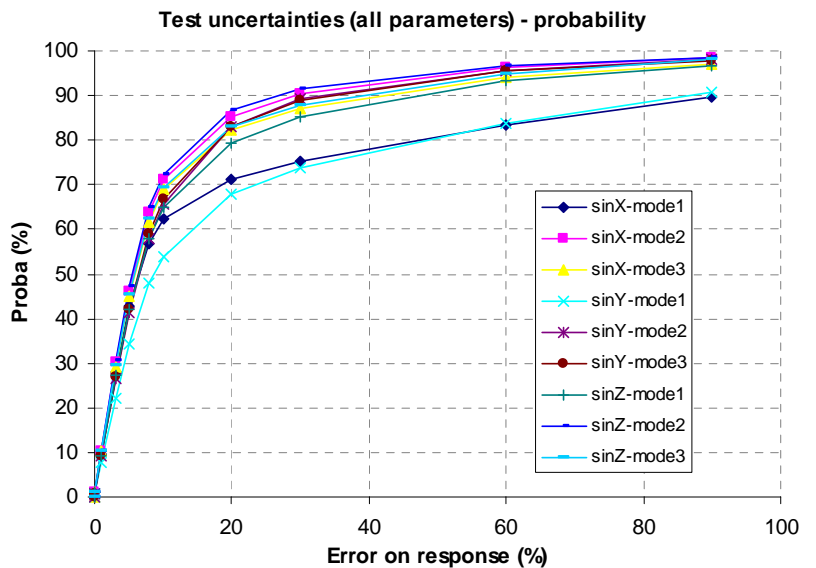


Figure 6-10: Error due to all uncertainty parameters

The diagram shows a significant dispersion on acceleration responses:

- Except for first lateral modes, the probability to have less than 20% of error on the amplitude is 80%,
- On first lateral modes, the probability to have less than 20% of error on amplitude is equal to 65%.

However even if error on acceleration on first lateral modes may be considered as significant, it is mainly due to transverse response that leads to negligible acceleration compared to the axial response.

If transverse responses are suppressed on first lateral modes, the result is better as the probability to have an error less than 20% becomes 90% (versus 65% without filtering transverse responses).

As main conclusion, the probability to have an error on amplitude due to all test uncertainty parameters lower than 10% is 66% which would consists in 10% at 1σ assuming Gaussian repartition.

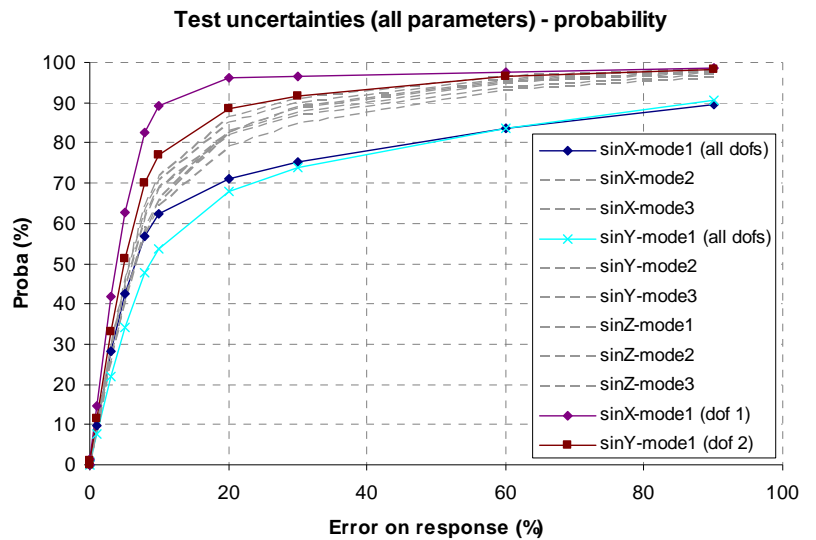


Figure 6-11: Error due to all uncertainty parameters (first mode focus)

- **Neutral fibre specific influence**

The most stable modes are first lateral modes as they are less sensitive to transverse grid location.

The probability to have an error on sine response (amplitude) due to transverse location lower than 5% is 66% which would consist in 5% at 1σ assuming Gaussian repartition. In particular for first lateral modes, this error is lower: $\sim 3\%$ at 1σ . Thus the errors in transverse sensor location in a S/C finite element model are not critical for sine test prediction.

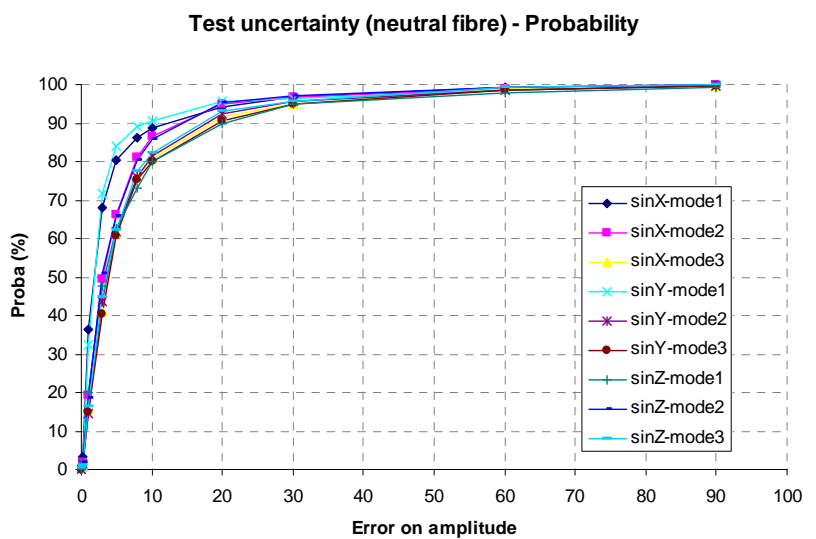

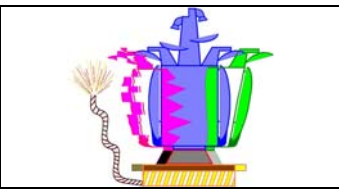


Figure 6-12: Probability error due to neutral fibre

However the impact of the transverse sensor location on result (5% at 1σ for 2cm of location error) is at least

		Ref : MTF.AIDT.TN.2168 Issue : 1 Rev. : 1 Date : 03/03/2010 Page : 28
--	--	---

equivalent or more significant than in-plane sensor location (2% at 1σ for 1 cm of location error).

6.2.5 Comparison with test data

To demonstrate the approach interest and efficiency, the next step consists in building a test stochastic cloud and verify that it is included in the one obtained by analysis from the whole identified test scatters.

To avoid structure fatigue and damage, it is not possible in test to play many times runs on a spacecraft, thus the stochastic cloud is built from the pre-and post low level runs.

As test data are not filtered, dispersion on frequency may appear larger. More than 90% of points are included in all test uncertainty parameters cloud.

The test repeatability comparison with test uncertainty parameters impact on analysis result is quite satisfying. On global modes, as considered here, repeatability gives always a lower dispersion than studied sources of error. Furthermore, variation on both amplitude and frequency responses are consistent. Only first Y lateral mode gives non satisfying results because of the non repeatability of test data.

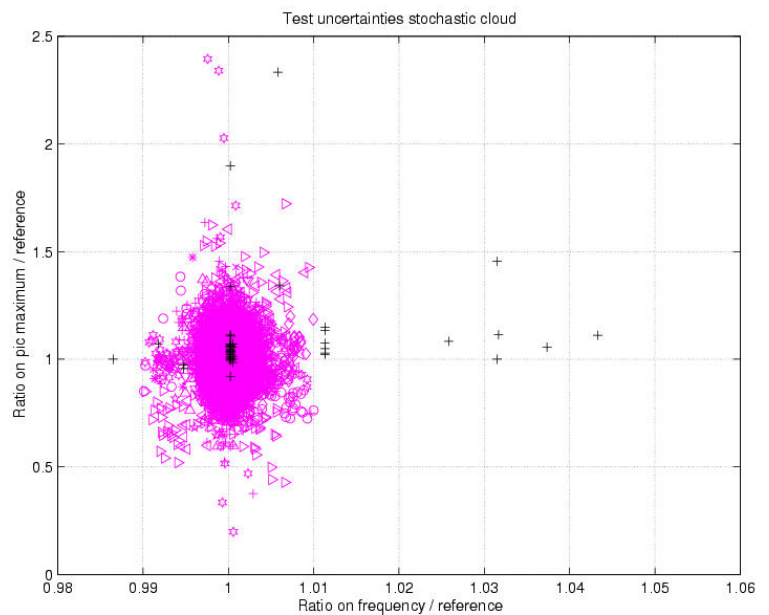


Figure 6-13: Test / uncertainty study comparison for sine Z mode 2

6.2.6 Stochastic notching prediction

Spacecraft mechanical tests aim at qualifying structures with respect to a launcher flight environment and to provide data to validate the FEM representativeness. An input spectrum is specified by the launcher authority to cover the flight events. If no flight event is expected on some narrow frequency bands, this spectrum can be “notched” to avoid structure over testing on particular modes.

These tests are prepared thanks to FEM analysis. The structure FEM is composed of different sub-systems models provided by the sub contractors. All these models have different accuracy in modelling the true hardware behaviour which leads to dispersion on the global results and thus on the predicted final notched spectrum. Moreover discrepancies and errors due to test uncertainty parameters, damping and cross coupling may also significantly affect the notched profile.

After introducing the different kind of uncertainties in the FEM sine responses, the outputs are notched input spectrums allowing characterizing the FEM prediction robustness and the sensitivity to the different parameters.

Customer and launcher authority agree before the test on the “reference” model final notched spectrum but which may be largely affected by different parameters on particular frequencies. This approach helps to anticipate problems (large dispersion on critical sensors) and facilitate iterations with the launcher authorities by providing probability of different input spectrum due to different discrepancies and errors.

6.2.6.1 Methodology

To get a good understanding of each error source effect, the stochastic analysis is split in four parts:

- **Study 1:** Study on subsystem modal and mass parameters: first natural frequencies (on clamped conditions modal analysis = 10%) and rigid mass (2%) of each subsystem.
- **Study 2:** Test uncertainty parameters effect (previously presented) are added to “study 1” parameters, the global error due to these uncertainties is equal to ~10% (at 1σ).
- **Study 3:** Cross-coupling effects are added to “study 2” parameters, each transverse excitation is expected to be null as average value with 5% (at 1σ) of the nominal excitation. All transverse excitations are added (including phases component) to nominal excitation.
- **Study 4:** Damping estimation error will be added to “study 3” parameters. Damping is a permanent source of uncertainty as it is difficult to measure and is often non-linear with respect to the input level and is frequency and subsystem dependent. Thus the error made on damping will be considered as a global error of only 10% on sine responses.

A Gaussian repartition is assumed for all the parameters.

This sequence is linear and inverting studies would have outcome to the same final result.

6.2.6.2 Application

The method has been applied on the previous spacecraft with a sequence of 120 shots.

The different output in Figure 6-14 and Figure 6-15, provides the parameters influences. The reference curve is added on each figure (in black).

Figure 6-15 presents the **study 1**, **study 2**, **study 3** and **study 4** envelop. Figure 6-16 provides information on the robustness and conservativeness of the reference results.

First lateral modes are fully decoupled to subsystem modes as no modification on frequency or amplitude is observed on the notchings at 15.91Hz (X excitation) and 16.0Hz (Y excitation).

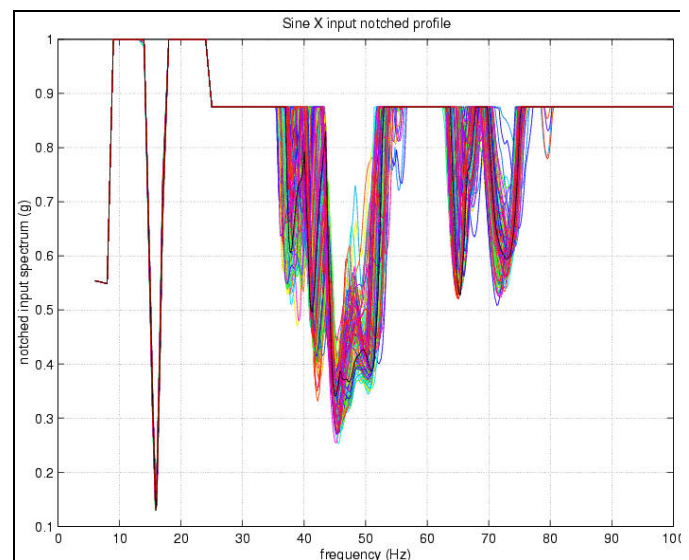


Figure 6-14: Sine X – all notched profiles (study 1)

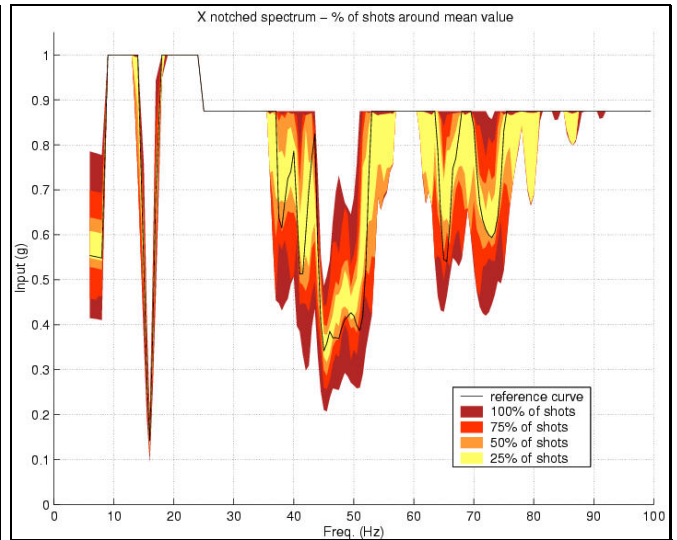
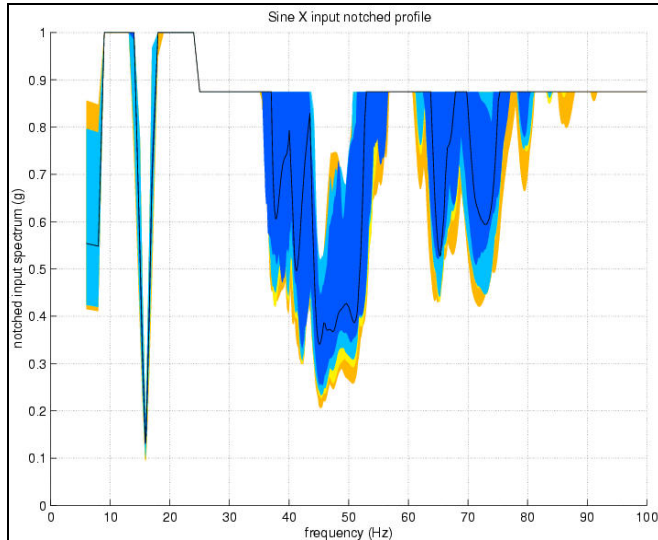
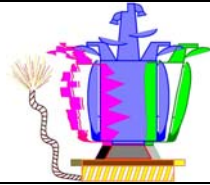


Figure 6-15 : Sine X – notched profile envelope (study 1+2+3+4)

Figure 6-16 : Sine X – % of shot around the average values

The following point may be highlighted:

- Due to uncertainty on subsystem dynamic behaviour some notchings may appear (for example at 55 and 80Hz) or may be deeper (for example at 45Hz). This may be critical for the test prediction phase when the manual notching philosophy will be decided. The impact of subsystem modal parameters is quite important in the 35-80Hz frequency range as subsystems reference case first frequencies are located around 50-60Hz.
- All uncertainties parameters may impact sine response with 10% of error at 1σ . This impact on sine response leads to new notched profiles. It is important to notice that test uncertainty error is applied on sine response and not directly on notched profiles because it allows new notching apparition.
- The cross-coupling effect may impact sine response and thus notched profiles. Cross-coupling error is applied adding transverse sine responses, taking into account phase shift, to nominal sine response to compute new notched profiles. No major modifications appear on X and Y notched profiles. Adding transverse response leads to an amplification of the nominal response and thus a deeper notching.
- Damping may also impact the sine response and thus notched profiles. Damping is really complicated to estimate in a S/C FEM as modal damping is generally used and applies to all the structure. Thus the goal is just to illustrate what a damping estimation error of 10% may lead on notched profiles.

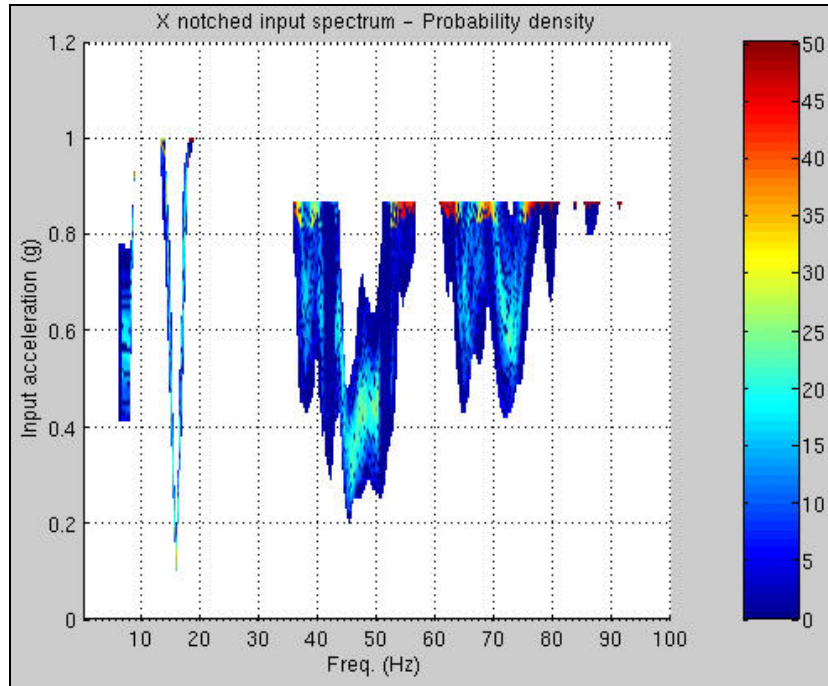


Figure 6-17 : Sine X – notched profile envelope (probability density)

All these diagrams have shown various ways to display notched profile envelopes: simple envelop, density probability and percentage around average value.

It should be noted that the notchings at 62 Hz and 80 Hz are not predicted by the reference FEM. Since reasonable assumptions on the uncertain parameters have been used, the predicted additional notchings appear to be realistic.

Some notchings have shown to be robust with respect to the subsystem modal parameters. Other notchings are strongly dependent on the kind of assumed errors. The deepest notchings are normally robust.

The cross-coupling excitation shows that the first lateral mode may generate a notching during a longitudinal vibration test even if cross-coupling effect is not very high (5% of transverse excitation assumed here). A particular attention must be paid in case the excitation is produced by more than one shaker.

All these informations are critical as they inform on probability of occurrence and robustness of predicted notchings. This is important to compute this kind of diagram prior to test vibration campaign as they represent a good support to negotiation with launcher authority.

6.3 BASE LOAD MEASUREMENT

6.3.1 Introduction

One of the main objectives of the base sine excitation test is to cover the base force and moment predicted by the coupled load analysis. But it is also an important measure to determine effective mass. It is consequently of high importance to access the base loads and associated frequency during the sine tests.

An assessment on the precision of the different existing methods dedicated to the base load (force and moment) evaluation is made:

- The Force Measurement Device is the best solution to measure directly the complete base forces and moments but such device is not available in every test facility centre.
- The mass operator which uses a linear combination of a set of sensors intelligently spread over the S/C associated to mass coefficient and level of arm.
- Finally, using the coil current injected during the test to recover global force used on the mode. By removing the shaker moving parts, the S/C base force can be recovered. Nevertheless it is not possible to recover the base moment.

To improve the base load mass operator determination, an optimization technique is proposed and compared to the direct static reduction of the FEM.

6.3.2 Force Measurement Device

The force measurement device is a general term naming a device able to measure, between two interface planes, the complete load torsor. Its general generic design is composed of two rigid interfaces separated by load cells.

Thus the force measurement devices can exist for different specimen type and interface.

As an example, the ESTEC 1194 FMD is shown in Figure 6-18.



Figure 6-18 : View of the ESTEC FMD

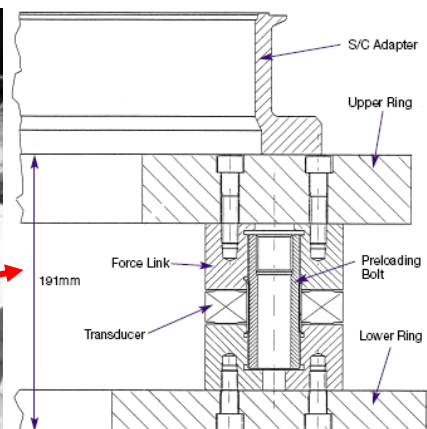


Figure 6-19 : Force link cut out

The main FMD characteristics are the following:

- Frequency measurement range: up to 100 Hz at high level, up to ~300 Hz at low level
- Measurement range: up to 800 kN axially, up to 200 kN laterally
- Moment measurement range: up to 260 kN.m in bending, up to 130 kN.m in torsion
- Axial/bending stiffness: 9.55×10^9 N/m / 2.73×10^9 N.m/rad
- Overall mass / height: 494 kg / 40 cm

This device provides a complete torsor recovery (6 components), as shown hereafter:

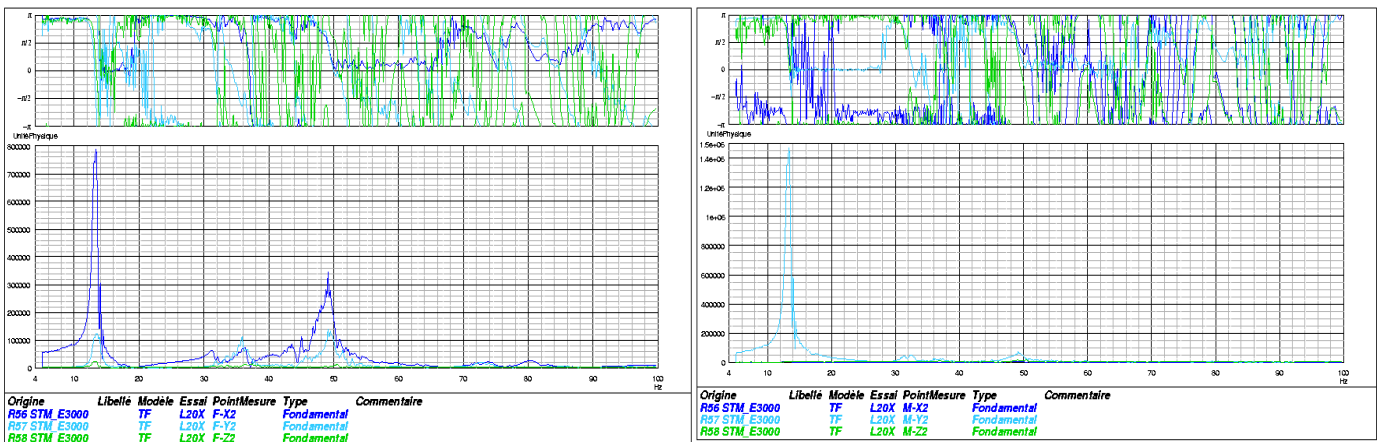


Figure 6-20: Force base load (MX, MY and MZ)

Figure 6-21: Moment base loads load (MX, MY and MZ)

The FMD is the best way to determine the base loads as it:

- Provides the direct measurement of the **complete** interface loads with high accuracy which can be used for direct automatic notching.
- Validates immediately the qualification level achieved on main mode, whatever the FEM quality and thus provides useful data for the FEM correlation
- Presents a high stiffness generating a limited frequency shift, a good linearity and low cross talk. The spacecraft mode stiffness higher, the error higher.
- The integration in the test set-up is transparent and can be adapted to every interface diameter thanks to the modular concept.

However some particular points have to be noticed wrt to its use:

- In general an extra load spreader is required between the slip table and the FMD, which increases the over turning moment on the slip table due to the additional FMD mass and a higher CoG.
- It requires a special device which is not always available and calls for time and money.
- It generates a low frequency shift on the most important mode dependant of the effective inertia involved on the mode.



6.3.3 Mass operator

In the case where it is not possible to use in the test set-up a Force Measurement Device, the other alternative way to determine the base loads is to build a **Mass Operator**.

The mass operator principle is to assume that the base load force in the excitation direction and moment are proportional to the spacecraft local sub-system part mass and lever arm (from the S/C interface plane) and their associated internal acceleration.

Thus it is necessary to determine an intelligent set of sensor representative of the mass spread over the spacecraft height that match with the base loads (force and moment) response shape as shown on the Figure 6-22.

The mass operator can define the base load force in the excitation direction and moment around the in-plane crossed direction but can't provide the two others base forces and moments components (as the FMD does).

Each sensor will be associated to a mass and lever arm (only in the case of moment calculation) coefficients and the following relationship can be built:

Equation 2
$$F(\omega) = \sum_{i=1}^{nbsensors} m_i \times \gamma_i(\omega)$$

Equation 3
$$M(\omega) = \sum_{i=1}^{nbsensors} m_i \times h_i \times \gamma_i(\omega)$$

- with F the spacecraft base force in the excitation direction,
- M the spacecraft base moment in the interface plane around the crossed excitation axis due to a lateral excitation,
- m_i mass associated to sensor i,
- γ_i acceleration associated to sensor i and
- h_i lever arm associated to sensor i.

The mass operator building consists to define a set of sensors and to determine the associated masses to have the better possible approached value of the base load force and moment. The lever arm is intrinsically given by the sensor height from the spacecraft interface plane.

The mass operator building process strategy is completely detailed in the RD 6.

The method accuracy is directly linked to the sensor accuracy and to the FEM reliability to represent reality. Nevertheless its efficiency and reliability has been demonstrated by comparison with the ESA FMD.

To get more confidence into the mass operator results, it is recommended to correlate the calculated levels on the mode with the base force extracted from the coil current. If the mass operator is not within $\pm 20\%$ of the coil current value, this is a warning message upon the mass operator validity.

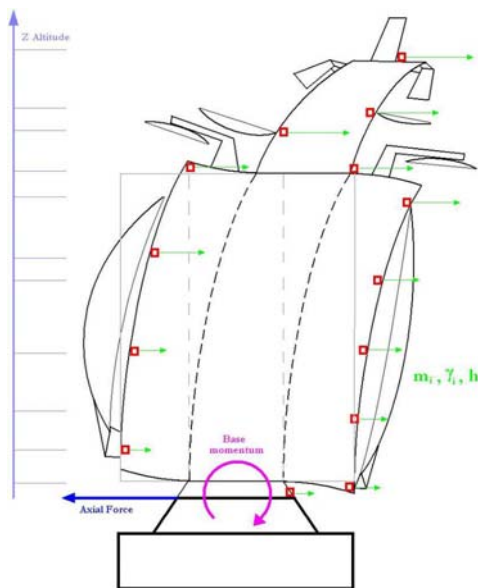
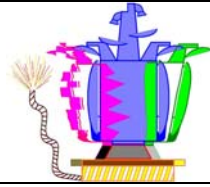


Figure 6-22 : Mass Operator base load and moment principle



6.3.4 Coil Current

The interface force in the nominal direction of motion at the specimen base can be deduced by removing the contribution of the shaker moving part. This standard test result provides only one force component, which is sufficient for order of magnitude correlation with more accurate techniques.

The base load force from the coil current is calculated thanks to the coils intensity conversion coefficient. This coefficient is determined by the proof tests realized by the test facility centre before the sine tests to calibrate and demonstrate the shaker capability to pilot correctly the runs. Such test provides acceleration pilot measurements on the shaker table as well as the measured coils current. As no shaker mode can be expected on the spacecraft first mode frequency bandwidth, this also provides a frequency dependant correlation factor between Force and Ampere current in the coils.

Equation 4
$$F_{\text{coils current}} = F_{\text{coils}}^{\text{to move}} + F_{\text{shaker table}}^{\text{to move}} + F_{\text{adaptor}}^{\text{to move}} + F_{\text{harness}}^{\text{to move}}$$

Equation 5
$$F_{\text{coils current}} = \text{Coefficient} \times \sum_{i=1}^{\text{number of coils}} I_{\text{coil } i} = (m_{\text{coils}} + m_{\text{shaker table}} + m_{\text{adaptor}} + m_{\text{harness}}) \times \bar{\gamma}_{\text{base}}$$

This coefficient is shown on the Figure 6-23. It has been calculated based on test results realized on the INTESPACE MVS lateral shaker and are different for other tests facility centres.

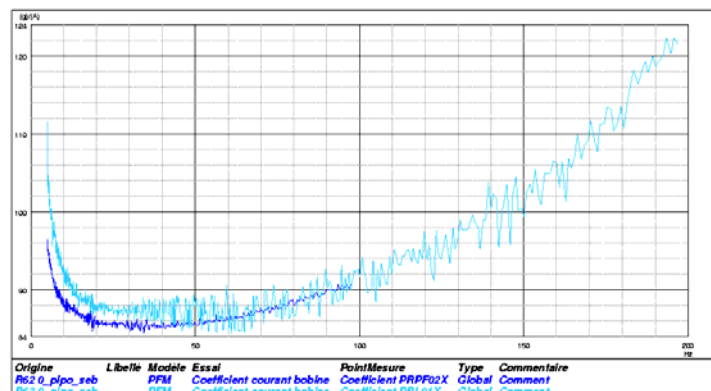
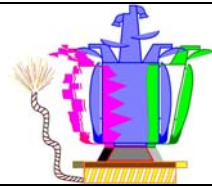


Figure 6-23: X axis shaker coefficient for low level (0.1 g input) and high level (1 g input)

It can be noted on the Figure 6-23 that this highly non-linear coefficient is function of:

- The shaker itself: the moving part slides along bearing guides which generates viscous friction.
- The frequency and the input level.
- The mass on the shaker table: it slightly modifies the coil impedance.

The coil current coefficient value will be chosen around the correlation mode frequency of interest and on the level input as close as possible to the test conditions.



To recover during test the load force in the excitation direction at the spacecraft base, it is necessary to convert the coils intensity into force and remove the contribution of the rigid shaker moving parts (Coils mobile parts, Shaker table mobile part, Spacecraft adaptor, Harness on the spacecraft).

The base force load is consequently given by:

Equation 6
$$F_{S/C\ base} = Coefficient \times \sum_{i=1}^{number\ of\ coils} I_{coil\ i} - (m_{coils} + m_{shaker\ table} + m_{adaptor} + m_{harness}) \times \bar{\gamma}_{base}$$

The coil current force calculation is not very accurate due to acceleration measurement error (about 9.8% at 2σ) and low Ampere-metre resolution (less than 5% at high frequency but about 20% at low frequency) whose discrepancy increases inversely wrt the mode effective mass (as demonstrated in RD 6). However, it provides the order of magnitude value at low frequency (corresponding to the main spacecraft mode) to give confidence in the mass operator calculation results obtained by other techniques.

6.3.5 Mass operator building strategy

6.3.5.1 Optimization techniques

Following the mass operator philosophy, it is possible to improve and automate the mass coefficient determination. The main idea to determine the mass operator sensors and coefficients, for a given set of sensors, is based on an optimization under constraints of the masses to associate to the sensors with least squared method criterion.

The constraints to fulfil are of different types:

- The total spacecraft mass must be spread over the sensors in the excitation axis

Equation 7
$$M_{total\ S/C} = \sum_{i=1}^{number\ sensors\ excitation\ axis} m_i$$

- The total spacecraft inertia must be spread over the sensors wrt the associated masses and lever arm (height from interface plane) in the excitation axis

Equation 8
$$M_{total\ S/C} \times z_{CoG} = \sum_{i=1}^{number\ sensors\ excitation\ axis} m_i \cdot h_i$$

Where h_i is the sensor i lever arm (or height) wrt the considered axis.

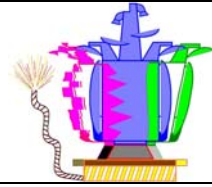
- Mass ranges associated to the sensors to respect mass physical repartition over the spacecraft

Equation 9
$$m_i^{inf} \leq m_i \leq m_i^{sup}$$

 (default values are at least: $m_i^{inf} = 0$ and $m_i^{sup} = M_{total\ S/C}$)

- Mass equality on couples of sensors (to take into account spacecraft symmetry properties)

Equation 10
$$m_k = m_l$$



- Base load force (and moment for lateral excitation axis) on one or several peaks determined:
 - Exactly

Equation 11

$$\left\{ \begin{array}{l} F(\omega_{peak}) = \sum_{i=1}^{number\ sensors} m_i \times \gamma_i(\omega_{peak}) \\ M(\omega_{peak}) = \sum_{i=1}^{number\ sensors} m_i \times h_i \times \gamma_i(\omega_{peak}) \end{array} \right.$$

- Or Approached with a given percentage of peak value: α_{peak}

Equation 12

$$\left\{ \begin{array}{l} \left| \frac{F(\omega_{peak}) - \sum_{i=1}^{number\ sensors} m_i \times \gamma_i(\omega_{peak})}{F(\omega_{peak})} \right| \leq \alpha_{peak} \\ \left| \frac{M(\omega_{peak}) - \sum_{i=1}^{number\ sensors} m_i \times h_i \times \gamma_i(\omega_{peak})}{M(\omega_{peak})} \right| \leq \alpha_{peak} \end{array} \right.$$

The optimization principle consists to minimize the differences between:

- on one side base load Force $F(\omega)$ and its mass operator approximation $\sum_{i=1}^{number\ sensors\ excitation\ axis} m_i \times \gamma_i(\omega)$,
- and on the other side the base load moment $M(\omega)$ and its mass operator approximation $\sum_{i=1}^{number\ sensors\ excitation\ axis} m_i \times h_i \times \gamma_i(\omega)$.

Thus a cost function can be built; which can be balanced by the base load force or moment modulus (linearly or quadratically) to impose an optimization mainly on the base load transfer function peaks. A balance factor “p” can be defined to 0 (no balance), 1 (linear balance) and 2 (quadratic balance).

The optimization is realised on the transfer function imaginary part to take into account the sensor phase.

Finally, the cost function can be written:

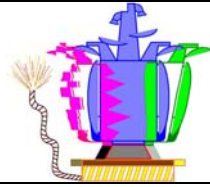
Equation 13

$$H_1 = \sum_{i=1}^N \left[\left(\sum_{i=1}^{number\ sensors\ excitation\ axis} m_i \cdot \text{Im}(\gamma_i(\omega_i)) - \text{Im}(F(\omega_i)) \right)^2 \right] \times |F(\omega_i)|^p + \sum_{i=1}^N \left[\left(\frac{\sum_{i=1}^{number\ sensors} m_i \cdot h_i \cdot \text{Im}(\gamma_i(\omega_i)) - \text{Im}(M(\omega_i))}{z_{CoG}} \right)^2 \right] \times \left| \frac{M(\omega_i)}{z_{CoG}} \right|^p$$

Remarks:

- The Equation 13 second member relative to the moment calculation is normalized by the CoG height of the studied system to have homogenous left and right terms
- In the particular case of a longitudinal excitation, moment is not considered and the H_1 criterion is reduced to its first member.

This equation can easily be minimized in MATLAB (see RD 6 for more details).



6.3.5.2 Static FEM reduction

Another original way to build a Mass Operator relies on static reduction of the model on the chosen set of sensors.

The idea is based on the fact that a static condensation of the FEM on the mass operator sensors (instrumented dof) would associate to each of these points the local FEM mass properties.

The GUYAN static reduction principle is to build a simplified model in terms of mass and stiffness with which internal accelerations can be determined as responses to a forced excitation at the spacecraft basis.

The start point are the physical model and the fundamental equations: $K \cdot q = F$ and $M \cdot \ddot{q} = F$.

Once the FEM is condensed on the instrumentation, we recover the interface base loads by multiplying the condensed mass matrix on the set of instrumented sensors by the rigid body motion vector and the acceleration on the instrumented sensors:

Equation 14
$$\Phi_{Rigid}^T \cdot M_{condensed} \cdot \gamma_{sensors}(\omega) = F_{base}(\omega)$$

The static FEM reduction leads to the following main conclusions:

- The condensation on the complete S/C instrumentation leads to very good loads recovery on the whole frequency range (not only on the peaks). In fact the larger the number of sensor is, the better the base loads recovery is.
- The base loads recovery is generally better in lateral axis than for longitudinal axis.
- Reducing the condensation set of sensors leads to debase the recovery quality. The degradation is more important in longitudinal force recovery than in lateral (force and bending moment) recovery.
- Keeping all the sensors for the base loads recovery improves the recovery robustness even if it calls for wide measured data verification during the test.

To recover the global loads applied a sub-system (and then the quasi static load), it is easy to condense statically only its mass on the whole spacecraft instrumentation (the stiffness matrix will remain the same). Even if it is not possible to recover precisely the loads on each foot of the sub-system for hyper-staticity reasons (the local loads are linked to the sub-system local stiffness), this is a good method to recover QSL in test.

Of course, this method leads to good results only if instrumentation close to the sub-system is sufficient.

6.4 SINE SWEEP RATE

With a base driven sine sweep, the measured FRFs are mainly the dynamic transmissibilities or masses $X_{ir}(\omega)$ between the rigid base (subscript r) and the accelerometers or reaction forces (subscript i).

So, identification of mode k may be reduced to natural frequencies $\omega_k = 2\pi f_k$, modal damping values ζ_k and modal effective parameters $\tilde{X}_{ir,k}$ (normalized modal components).

In practice, if the mode, behaving like a single degree of freedom oscillator, provides a well isolated peak, the identification process on FRF is schematically the following:

- f_k is directly related to the frequency of the peak,
- ζ_k is directly related to the peak width (sharpness),
- $\tilde{X}_{ir,k}$ is directly related to the amplitude of the peak A_k by the approximate relation:

Equation 15
$$\tilde{X}_{ir,k} \approx 2 \zeta_k A_k$$

The peak corresponding to mode k can be represented by the 3 parameters $(f, A, \zeta)_k$. The sweep rate V must be very low to provide a quasi stationary motion and, in practice, it has 3 effects:

- a variation (sign of V) of the frequency of the peak : Δf
- a decrease of the peak amplitude : ΔA
- an increase of the peak width (with loss of symmetry) : $\Delta \zeta$

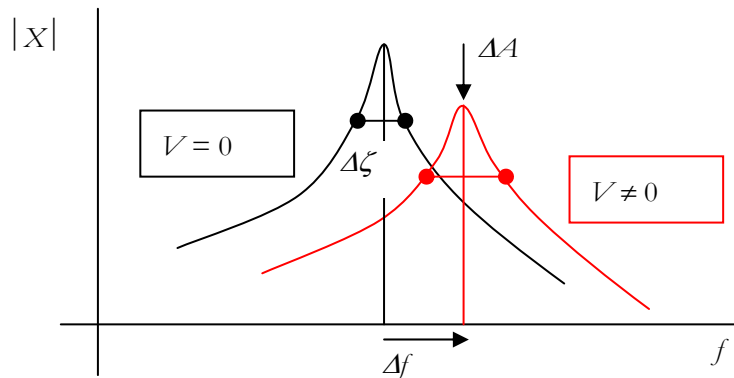


Figure 6-24: Effect of sweep rate on isolated peak

6.4.1 Sine sweep rate effect on modal parameters

The effects of the sine sweep rate V in octaves/minute on a given peak related to a mode with frequency f and amplification factor $Q = 1/(2\zeta)$ can be expressed as functions of the non-dimensional sweep parameter η :

Equation 16
$$\eta = \frac{Q^2 V \text{Ln } 2}{60 f}$$

The sweep rate of the form: $f = f_0 \exp(\beta t)$, with increasing frequencies ($\beta > 0$, hence $V > 0$, written V^+ with the superscript “+” to make the difference with decreasing frequencies), leads to analytical results dependent to the η parameter (cf. RD 6), as shown in following figures:

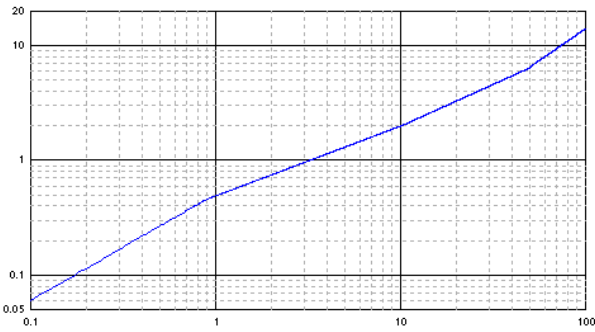


Figure 6-25: Variation $\frac{Q \Delta f^+}{f}(\eta)$

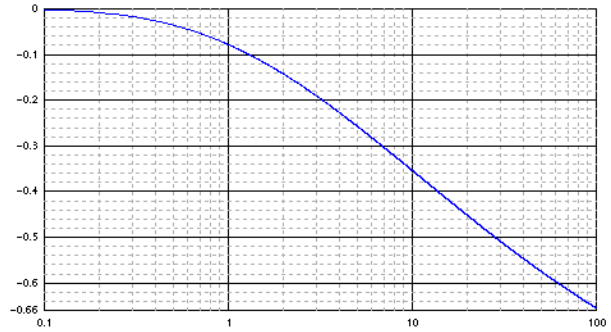


Figure 6-26: Variation $\frac{\Delta A^+}{A}(\eta)$

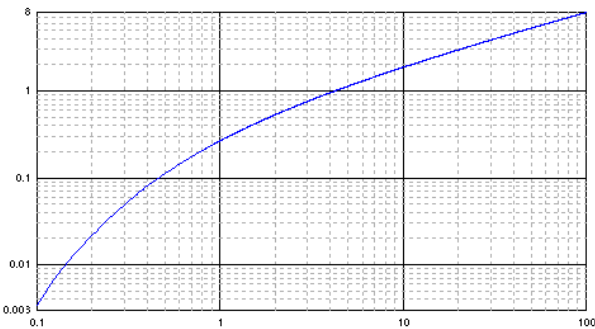


Figure 6-27: Variation $\frac{\Delta \zeta^+}{\zeta}(\eta)$

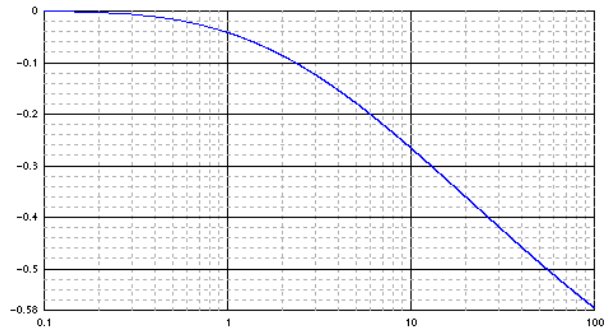


Figure 6-28: Variation $\frac{\Delta A^-}{A}(\eta)$

In case of decreasing frequencies sweep rate ($\beta < 0$, hence $V < 0$, written V^-), no information exists except for the variation of amplitude ΔA^- (cf. Figure 6-28). So, when comparing to $\frac{\Delta A^+}{A}$ variation, decreasing frequency has a lower effect on peak amplitude than increasing frequency. To extend rule for Δf^- and $\Delta \zeta^-$, it is proposed to take the variations Δf^+ and $\Delta \zeta^+$, and multiply them by the ratio $\alpha = \Delta A^- / \Delta A^+$, as illustrated by Figure 6-29. Complete formulation is presented in RD 6.

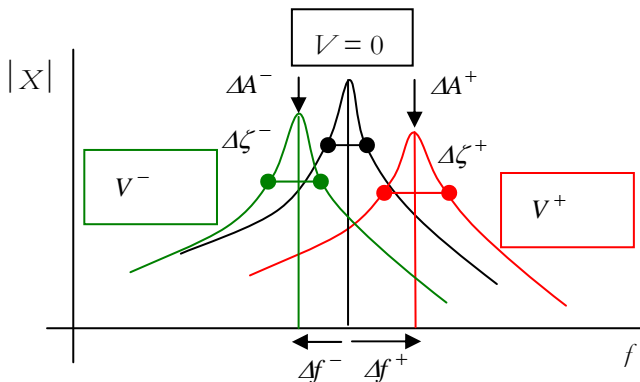


Figure 6-29: Increasing and decreasing frequencies

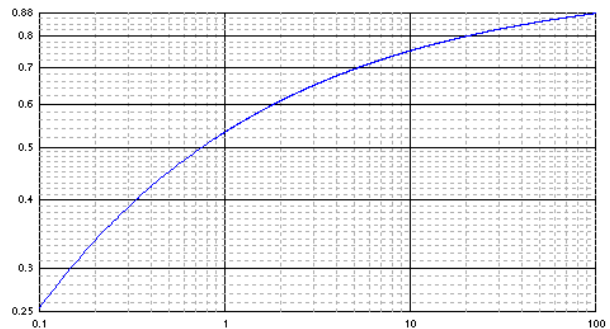
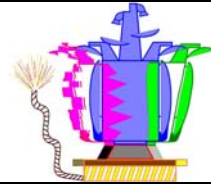


Figure 6-30: Ratio $\alpha = \Delta A^- / \Delta A^+(\eta)$



6.4.2 Sine sweep rate selection

During test it should be interesting to find the good compromise the sweep rate V as a function of the expected modes. The sweep rate has to be estimated from the frequency and the amplification factor $(f, Q)_k$ of each considered mode k for a given desired accuracy $(f, \zeta, \tilde{X}_{ir})_k$.

In RD 6, the detailed formulas express V versus $\Delta(f, A, \zeta)_k$, ΔA_k being related to $\Delta \tilde{X}_{ir,k}$, also depending of the sine sweep sense (positive or negative).

6.5 SENSOR LOCATION

Sensor location is of primary importance for test results since it defines the specimen dynamic behaviour by providing components of the deformed shapes but must allow making distinction between the shapes, which is conditioned by the number and the location of the sensors. So, it is worthwhile to improve it with respect to general criteria of mode distinction.

The structure mode shape components for a certain number of candidate DOFs should be available thanks to a mathematical model. Note that it is illusive to look for a high accuracy because the model is not perfect and the sensor location is only approximate in practice. The objective here is to give trends and avoid large errors.

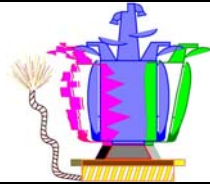
For a given number of sensors, a possible solution to optimize their location is to elaborate an indicator evaluating the performance of a given sensor configuration with respect to mode shape distinction, and use it as a cost function for an optimization process. Among possible criteria to distinguish between mode shapes, the MAC (Modal Assurance Criterion) is particularly interesting here. Between 2 mode shapes $\Phi_{i\underline{k}}$ and $\Phi_{i\underline{l}}$ (underlined subscript = fixed subscript), the MAC is given by:

Equation 17
$$\text{MAC}(\Phi_{i\underline{k}}, \Phi_{i\underline{l}}) = \frac{(\Phi_{i\underline{l}}^T \Phi_{i\underline{k}})^2}{(\Phi_{i\underline{k}}^T \Phi_{i\underline{k}})(\Phi_{i\underline{l}}^T \Phi_{i\underline{l}})}$$

It has values between 0 and 1, with 0 for two directly orthogonal shapes and 1 for two identical shapes. So, this criterion can quantify the distinction between two modes: 1 means no distinction and conversely 0 means max distinction. However, only two modes can be considered at the same time and it is necessary to extend this criterion to K mode shapes.

Let's consider I components i of K mode shapes k , hence the matrix $\Phi_{i\underline{k}}$ of size (I, K) . The determinant of the matrix $(\bar{\Phi}_{i\underline{k}}^T \bar{\Phi}_{i\underline{k}})$, where $\bar{\Phi}_{i\underline{k}}$ is the normalized shape of mode \underline{k} : $|\bar{\Phi}_{i\underline{k}}| = 1$, is related to the MACs as follows :

Equation 18
$$(\bar{\Phi}_{i\underline{k}}^T \bar{\Phi}_{i\underline{k}}) = \begin{bmatrix} 1 & & & \text{Symmetric} \\ & \ddots & & \\ \pm \sqrt{\text{MAC}(\Phi_{i\underline{k}}, \Phi_{i\underline{l}})} & & & \\ & & & 1 \end{bmatrix} \Rightarrow \det(\bar{\Phi}_{i\underline{k}}^T \bar{\Phi}_{i\underline{k}}) = 1 - \sum_{k,l} \text{MAC}(\Phi_{i\underline{k}}, \Phi_{i\underline{l}}) + \dots$$



The matrix $\overline{\Phi}_{ik}^T \overline{\Phi}_{ik}$ is diagonally dominant and its determinant, which has values between 0 and 1, corresponds to a combination of MACs which quantifies the distinction between the K modes: 0 means no distinction between 2 or more modes, and conversely 1 means max distinction between all the modes. So the indicator $\det(\overline{\Phi}_{ik}^T \overline{\Phi}_{ik})$ is well adapted to the present context. Some remarks:

- With the model, it could be possible to consider the true orthogonal properties of the modes, i.e. $(\Phi_{i_l}^T M_{ii} \Phi_{i_k}) = 0$, instead of $(\Phi_{i_l}^T \Phi_{i_k}) = 0$ but this is more complex to implement.
- Equation 18 is correct only if the number I of sensors is higher than or equal to the number K of modes. In practice, this is generally the case and if not, it is possible to adapt the indicator.

The problem is now to maximize $\det(\overline{\Phi}_{ik}^T \overline{\Phi}_{ik})$. Starting from a finite element model with N DOFs, the number of possible combinations is tremendously large and a drastic selection must be made for the i -set, $I \ll N$ to have a reasonable computer time. Thus the N initial DOFs are classified in 3 categories:

- 1) DOFs to be rejected: they cannot accommodate sensors (rotation DOFs, inaccessible zones ...) or have little interest for various reasons,
- 2) DOFs to be kept: obvious or imposed choice, critical location, DOF corresponding to a very local but important mode ...
- 3) DOFs possibly interesting: relatively high components on one or several modes, but avoiding redundancy ...

If the number of combinations is sufficiently limited, the categories 2 and 3 DOFs can be detected by a systematic approach, otherwise an univariate approach provides a satisfactory sub-optimum configuration.

The optimization is performed with a given number J of sensors. The optimization of this number can be made by trial and error, referencing to the optimum value obtained in each case for the cost function.

The proposed candidates $i(j)$ should provide a sufficient "observability" for each mode \underline{k} : even if the modes are well distinct. For a given j -set and a given mode \underline{k} : the observability $O(j, \underline{k})$ can be defined by:

$$\text{Equation 19} \quad O(j, \underline{k}) = \frac{\text{Max} |\Phi_{j\underline{k}}|}{\text{Max} |\Phi_{i\underline{k}}|}$$

i.e. the ratio between the max component of the i -set and the max component of the considered j -set. It has values between 0 and 1: 0 means no observability (all the components are null for this mode), and 1 means maximum observability (the max component is included). The optimization process with the proposed candidates $i(j)$ will provide an observability between:

$$\text{Equation 20} \quad \frac{\text{Max}_j \left(\text{Min}_i |\Phi_{i(j)\underline{k}}| \right)}{\text{Max} |\Phi_{i\underline{k}}|} \leq O(j, \underline{k}) \leq \frac{\text{Max} |\Phi_{i(j)\underline{k}}|}{\text{Max} |\Phi_{i\underline{k}}|}$$

These 2 extreme values should be appropriate: a value significantly lower than 1 for the maximum means that high components of mode \underline{k} are not candidates, and a low value for the minimum means that the optimization process can provide a low observability. If these values are not considered appropriate, the lists of candidates $i(j)$ should be modified.

7 DURING TEST AND POST TEST METHODOLOGIES

7.1 INTRODUCTION

The third phase focus on all activities related to test assessment and post processing in order to provide a better assessment of the raw test data, to calculate underlying properties to complete the calculated FRF and finally to provide new methodologies to deal with parasitic motion, to correct it effect and to deal with non linearities. Different methodologies have been developed to meet the multiple study objectives.

The methodologies studied concerns the following themes:

- **Test data validation** is important to provide a complete assessment.
The studied methodologies concern three main topics:
 - Use of low frequency data for check of sensor locations, orientations and scaling: the low frequency values which tend to the static transmissibilities are used.
 - Verification of FRF consistency: drive point FRF imaginary part must be positive, and other FRFs should build a symmetric FRF matrix through reciprocity principle.
 - Determination of static properties: they are derived from low frequency data (lower than the first eigenfrequencies). Two methods will be used: parabolic approach and residual mode approach, which consists in fitting the curve with a one-DOF system contribution.
- **Parasitic motion** is an important topic as it is currently neither evaluated nor corrected. First an estimation of parasitic motion is made at two levels defining adequate indicators: both global estimation and determination of rigid body components and deformation. Then a first estimation of parasitic motion effect on specimen dynamics is provided by a simple computation of the rigid body contribution of the base to the internal responses. However, the correct approach must take into account the shaker/specimen dynamic coupling. Thus the work concentrated on modal identification of the imperfectly guided specimen and adequate manipulation to recover the motion with perfectly guided specimen. This is possible with the force in the nominal direction in addition to the 6 components of the motion, the other ones being unnecessary but providing additional information and verification.
Unfortunately some limitations are met due to the numerical quality of the raw test data.
- **Non-linearities** are present in dynamic test data. They have been tackled in two domains:
 - A summary of methodology for detection, characterisation and quantification of non-linear structural behaviour: indicators permitting to characterize the different types of non-linearity. The use of classical indicators derived from the investigation of Nyquist plot distortions or coherence functions or those derived from extended techniques like the Hilbert transform have been addressed.
 - Improvement of modal parameters in presence of identified non-linearities: the approach is based on EMA method extended by terms permitting to describe the distortions of the response curves in order to increase the robustness of the modal identification process in the presence of non-linear structural behaviour.

- **Post-processing techniques** to improve efficiency and quality of test data exploitation:
 - Improved modal identification by determination of residual modes: they are based on 1-DOF system contributions and aim at avoiding modal truncation effect. They are derived from the difference between measured values and contribution of the identified modes.
 - Elaboration of reduced experimental models by modal or FRF coupling approaches.
 - Evaluation of correlation through a criterion based on FRF: the aim is to propose a new correlation method between two data sets (FEM and/or test) based on FRF peaks.

7.2 NEW CORRELATION CRITERIA BASED ON FRF

The actual “one axis-one day” test campaign context aims to validate the spacecraft structure mechanical qualification as fast as possible to reduce costs to deliver the spacecraft to the customer as fast as possible.

It is thus necessary to realize in test a correlation between FEM and real structure behaviour to validate the predictions for CLA or between two tests to follow behaviour evolution. Different powerful methods and tools exist to do such a modal identification and correlation, but these really efficient methods call for time to apply and are not automatized which is not compatible with the test time constraints.

The need is thus to extract modal behaviour and correlate quickly the FEM/hardware or test/another test (different input levels) by an automatized method allowing dealing with large amount of data.

The Fast Modal Extraction and Correlation method propose to provide an automatic FRF correlation by:

- Identifying automatically the peaks by a new method based on an exhaustive curve scanning to detect local and global maximums and a quick mode extraction by maximum number of curve peaks for a given thin frequency band
- Providing different visual indicators to assess quicker and efficiently the correlation.
- Keeping the same DynaWorks work environment to avoid time loss.

This method is an additional piece of information compared to standard modal approach.

7.2.1 Sensor global and local peak extraction

The principle is to scan the imaginary part of the curve by a threshold value to identify the global and local maximums. The threshold value is calculated as n subdivision **relatively** to the curve maximum value and **absolutely** as fixed threshold values.

For each different threshold values, the scan identifies local frequency bands and extracts the maximum value and associated frequency on the range, as shown in Figure 7-1.



Figure 7-1: Curve scanning principle with threshold values

A filter is applied to avoid detecting FRF local noisy maximums. For each local detected peak, it is necessary to verify if the curve threshold cut frequency band is:

- higher than $\alpha f \Rightarrow$ the cut band is high enough to consider it is not a noisy local maximum
- lower than $\alpha f \Rightarrow$ the detected peak could be a noisy maximum, it is thus necessary to verify there is no higher local maximum on a narrow frequency band in the peak vicinity on $[f(1 \mp \alpha/2)]$. If a higher maximum is found then this maximum is not selected. This allows identifying correctly noisy peaks.

α depend upon the spacecraft modal density and should be set to 4%.

The identified maximum values and frequencies can be displayed for each sensor or globally for the whole test at the end of the peak extraction process by the peak frequencies and the number of sensor for which one a local/global peaks has been detected, as shown in Figure 7-2.

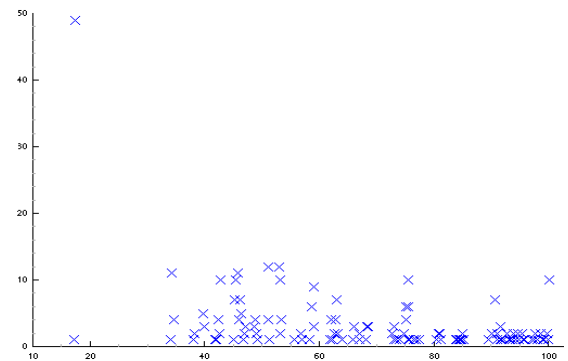


Figure 7-2: Number of sensor for which one a local/global maximum has been detected

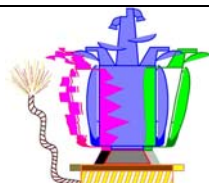
7.2.2 Mode extraction

Based on the previously identified peaks, the modes are extracted by:

- Frequency gathering. The principle is to analyse for each identified frequency, the number of other identified frequencies in its vicinity defined by the β parameter on the frequency band $[f(1 \mp \beta/2)]$ (β boundaries frequency band).
- Calculation of the peaks density. Modes are selected considering the gathering frequency band boundaries and the total number of mode selected on the gathered frequency band boundaries.

Such a process leads to consider three different cases (see Figure 7-3) completely detailed in RD 6:

1. **Case 1:** Fixed boundaries. For each peak frequencies, the β boundaries frequency band finds only one fixed band. The mode is extracted using, over the identified band, the frequency where the maximum numbers of sensor have a peak.
2. **Case 2:** Sliding boundaries but where it is possible to find a frequency including all the other ones. The mode is extracted using over the identified band, the frequency where the maximum number of sensor have a peak.
3. **Case 3:** Sliding boundaries but where it is not possible to find a frequency including all the other ones. The mode extraction considers the frequencies gathering the largest band and on this band the mode is extracted using the frequency where the maximum numbers of sensor have a peak. Once the first band has been treated, the higher and lower not selected bands are analysed to find the frequency where the maximum number of sensor have a peak.



	Frequency mode	Max mode	Number sensor	Number local sensors	Low index	High index	Line index	
1	17.1286	-1.80778	1	86	1	2	1	733X
2	17.3712	-30.2737	85	86	1	2	2	110X, 111X, 120X, 122X, 124X, 126X, 130X, 132CAX, 134X, 136CAX, 231CA
3	34.1	-2.73212	1	17	3	5	3	727X
4	34.1558	-13.6403	12	17	3	5	4	243CAX, 703X, 704X, 707X, 709X, 713X, 723X, 724X, 750X, 751X, 841X, 891:
5	34.7054	-8.56854	4	17	3	5	5	712X, 732X, 733X, 752X
6	38.1	-1.78754	1	5	6	7	6	743X
7	38.2931	-20.4692	4	5	6	7	7	651X, 891X, 900X, 907X
8	39.778	-2.10343	5	8	8	9	8	704X, 712X, 724X, 750X, 751X
9	39.9123	-1.89761	3	8	8	9	9	743X, 748X, 752X
10	41.7688	3.31118	1	6	10	12	10	707X
11	41.9947	-5.54426	1	36	10	14	11	744X
12	42.4016	-1.62271	4	36	10	14	12	090X, 713X, 733X, 740X
13	42.6361	-7.32379	7	35	11	14	13	243CAX, 300CAX, 300X, 407X, 703X, 723X, 915X
14	42.7471	-2.07203	23	35	11	14	14	081X, 200X, 201X, 202CAX, 202X, 204X, 211X, 280X, 311X, 313X, 404X, 630:
15	44.9753	2.13562	2	64	15	19	15	620X, 712X
16	45.1	3.44748	1	64	15	19	16	899X
17	45.219	-2.12967	8	77	15	21	17	702X, 723X, 732X, 750X, 751X, 752X, 759X, 813X
18	45.3652	-1.29551	27	77	15	21	18	060X, 063X, 080X, 081X, 091X, 130X, 134X, 136CAX, 200X, 201X, 202CAX, 2
19	45.723	-1.39207	26	87	15	22	19	064X, 066X, 090X, 132CAX, 300CAX, 300X, 301CAX, 301X, 304X, 311X, 312)
20	46.0378	-6.30066	5	90	17	24	20	050X, 707X, 721X, 748X, 863X
21	46.1	-7.01669	8	90	17	24	21	051X, 701X, 727X, 733X, 739X, 740X, 762X, 849X
22	46.3402	7.6308	10	59	19	25	22	713X, 742X, 901X, 904X, 907X, 915X, 925X, 954X, 965X, 975X
23	46.7785	2.78248	4	33	20	25	23	243CAX, 744X, 966X, 967X
24	46.8544	-3.50069	2	33	20	25	24	630X, 631X
25	47.1	-11.1279	4	20	22	25	25	750X, 751X, 752X, 759X

Figure 7-3: Peaks synthesis table

7.2.3 Mode building

Once the modes are extracted, it is possible to compare them to the peak frequencies and the number of sensor for which one a local/global maximum has been detected, as shown in Figure 7-4. The mode shapes are built using the sensors imaginary part.

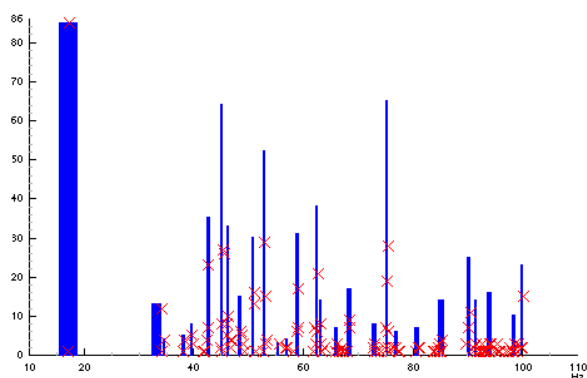


Figure 7-4: Comparison of the **extracted modes** with **the number of sensor where a maximum is detected**

7.2.4 Test correlation

The correlation between the two tests can be presented using two different types of indicator on the common filtered sensors, both based on the MAC formulation but using the mode shape imaginary part:

- **FrImAC** (Frequency Imaginary Assurance Criteria). The principle is to calculate the MAC matrix for all the test frequencies the two test correlation (as shown in Figure 7-5):

$$\text{Equation 21 } FrImAC(i) = \frac{\left(\sum_{k=1}^{\text{common sensors}} \varphi_k^{\text{test A}}(i) \cdot M \cdot \varphi_k^{\text{test B}}(i) \right)^2}{\left(\sum_{k=1}^{\text{common sensors}} \varphi_k^{\text{test A}}(i) \cdot M \cdot \varphi_k^{\text{test A}}(i) \right) \cdot \left(\sum_{k=1}^{\text{common sensors}} \varphi_k^{\text{test B}}(i) \cdot M \cdot \varphi_k^{\text{test B}}(i) \right)}$$

- **ImMAC** (Imaginary Modal Assurance Criteria). The principle is to calculate the MAC matrix for the modes extracted by the fast modal extraction methodology (as shown in Figure 7-6):

$$\text{Equation 22} \quad \text{ImMAC}(\varphi_i, \varphi_j) = \frac{\|\text{Im}(\varphi_i) \bullet M \bullet \text{Im}(\varphi_j)\|^2}{\|\text{Im}(\varphi_i) \bullet M \bullet \text{Im}(\varphi_i)\| \bullet \|\text{Im}(\varphi_j) \bullet M \bullet \text{Im}(\varphi_j)\|}$$

Where $\varphi_k^{\text{test } X}$ are the test X (test A or B) shape imaginary part at each frequency composed of the common sensors between test A and test B.

It can be note that the formulas are presented with M the mass matrix. Thus it is not mandatory but this could help to have better results thank to the mode orthogonality property.

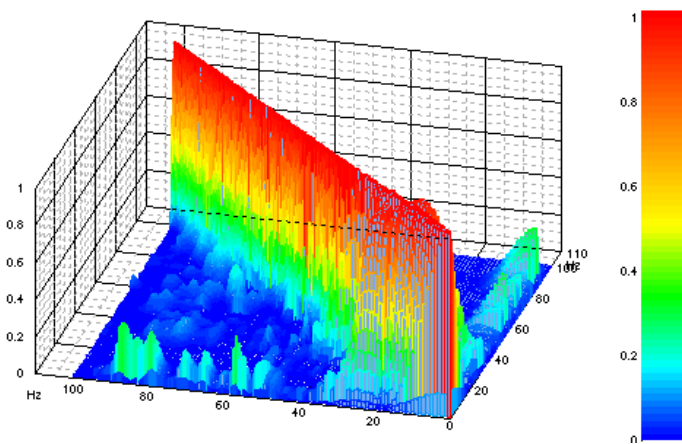


Figure 7-5: Frequency Imaginary Assurance Criteria

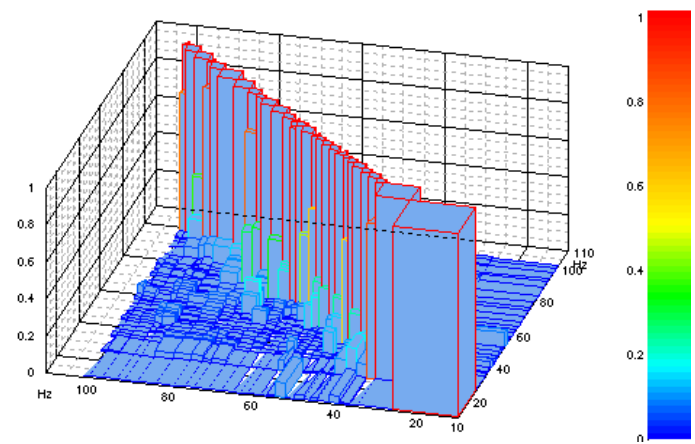


Figure 7-6: Imaginary Modal Assurance Criteria

7.3 TEST DATA QUALITY ASPECTS

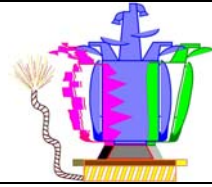
7.3.1 Parasitic motion

During base-drive vibration tests, the shaker table is not perfectly rigid or perfectly controlled and parasitic motions are observed superimposed to the nominal motion. They can be decomposed in two categories:

- A rigid body average motion with 5 components, the 2 non nominal translations and 3 rotations, which is due to the imperfections of the guidance system and the specimen mass dissymetries. It concerns relatively low frequencies, well below 100 Hz.
- A deformation round the previous motion due to the base flexibility. It depends to a certain extent on the interface dimensions and on the specimen stiffness. It concerns relatively high frequencies, *a priori* well above 100 Hz.

Significant parasitic motions may strongly perturb the dynamic responses and corresponding modes of the specimen. They have to be detected, measured and their effect on the specimen estimated if possible.

The study deals with the following points:



- A first estimation of parasitic motion based on the 6 rigid body components and the deformation around the rigid motion.
- A first estimation of the influence of parasitic motion on specimen dynamics can be calculated by a simple computation of the rigid body contribution of the base to the internal responses.
- This dynamic coupling can be estimated after test by modal identification of the imperfectly guided specimen and adequate manipulation can be envisaged to recover the motion with perfectly guided specimen. However, this operation remains delicate for different reasons.

7.3.1.1 First estimation of parasitic motions

The parasitic motions are defined as the difference between the motion specified at the base in a given direction, and the real motion generally measured by a set of n accelerometers b (base) of position $P_b (x, y, z)_b$ and orientation $(l, m, n)_b$, (direction cosines: $l_b^2 + m_b^2 + n_b^2 = 1$) as illustrated by Figure 7-7 with the typical case of 4 triaxes at 90° on a circle with radius R ($n = 12$).

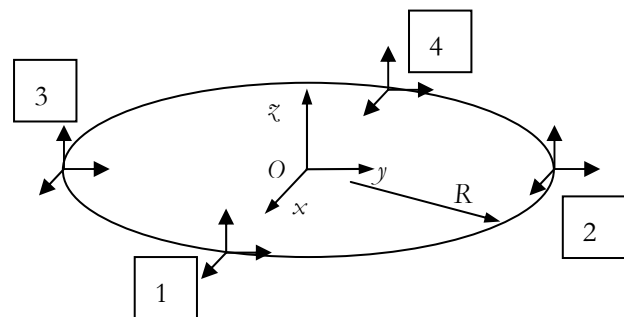


Figure 7-7: Measure of the base motion by 4 triaxes

At a first level, the parasitic motions can be estimated by direct difference between nominal and real amplitude of accelerations. Concerning the nominal amplitude, the situation is generally the following:

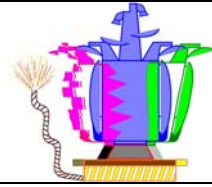
- Some accelerometers are in the nominal direction and must reflect the specified input level.
- The others are in a perpendicular direction and must theoretically have zero amplitude.

The following strategy can be used for an indicator at first level:

- Account for the mean value of the pilot amplitudes as reference amplitude.
- Computation versus frequency of the ratio:
 - $(\text{measure} - \text{reference}) / \text{reference}$ for the accelerometers in the nominal direction
 - $\text{measure} / \text{reference}$ for the accelerometers perpendicular to the nominal direction
 - general case of an accelerometer with α direction cosine in the nominal direction: $(\text{measure} - \text{reference} \times \alpha) / \text{reference}$
- Display of errors versus frequency by superposition of the n curves. Display of the envelope to have a unique indicator.

7.3.1.2 Parasitic motion components

At second level, the 5 components of the rigid body motion and the deformation around the previous motion can be determined using the amplitudes and the phases with respect to a reference pilot. The theory of the general case is recalled hereafter.



With a rigid body motion providing to the reference node (central node in practice) the accelerations $\ddot{u}_r = (\ddot{u}, \ddot{v}, \ddot{w}, \ddot{\theta}_x, \ddot{\theta}_y, \ddot{\theta}_z)_O$, the base acceleration \ddot{u}_b is given by:

Equation 23

$$\ddot{u}_b = \begin{bmatrix} l \\ m \\ n \end{bmatrix}_b \cdot \left(\begin{bmatrix} \ddot{u} \\ \ddot{v} \\ \ddot{w} \end{bmatrix}_O + \begin{bmatrix} \ddot{\theta}_x \\ \ddot{\theta}_y \\ \ddot{\theta}_z \end{bmatrix}_O \wedge \begin{bmatrix} x \\ y \\ z \end{bmatrix}_b \right)$$

So, for a set of n accelerometers b:

Equation 24 $\ddot{u}_b = T_{br} \ddot{u}_r$

T geometry matrix derived from the accelerometer positions/orientations, frequency independent, with size $n \times 6$.

Inversely, the rigid body motion at O can be derived from accelerometers b by pseudo-inverse:

Equation 25 $\ddot{u}_r = (T_{br})^+ \ddot{u}_b$ with $(T_{br})^+ = (T_{rb} T_{br})^{-1} T_{rb}$

If the motion of the base is not strictly rigid, Equation 25 gives the average motion at O . The difference between the accelerometers b and this average motion is (I : identity matrix):

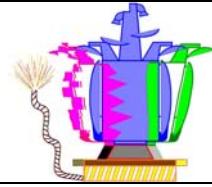
Equation 26 $\Delta \ddot{u}_b = (I_{bb} - T_{br} (T_{br})^+) \ddot{u}_b$

The component of \ddot{u}_r in the nominal direction represents the average nominal motion. The 5 other components of \ddot{u}_r (2 translations and 3 rotations) represent the average parasitic motions. The rotations can be written in terms of translations by multiplying them by the reference length: the radius R in the case of 4 triaxes at 90° (Figure 7-7). The components $\Delta \ddot{u}_b$ of Equation 26 represent the base deformation round the average motion. Hence the following strategy for the indicators:

- Computation of average nominal motion versus frequency from Equation 25
- Computation of the 5 average parasitic motions versus frequency from Equation 25 with transformation of rotations in translations and division of the amplitudes by those of the average nominal motion.
- Display of errors versus frequency by superposition of the 5 curves. Possible display of the envelope only to have a unique indicator.
- Computation of the n deformation motions versus frequency from Equation 26 and division of the amplitudes by those of the average nominal motion.
- Display of errors versus frequency by superposition of the n curves. Possible display of the envelope only to have a unique indicator.

7.3.1.3 Effect on the specimen

The parasitic motions indicate an interaction between the specimen and the shaker which modifies the specimen behavior. Its importance can be estimated by comparing the measures on the specimen and the rigid body motion due to the base.



Using the average motion \ddot{u}_r given by Equation 25, with 1 nominal component n and 5 parasitic components p , and considering the measures \ddot{u}_i of the accelerometers i on the specimen, the rigid body motion due to \ddot{u}_r is given as for Equation 24 by:

Equation 27
$$\ddot{u}_i = T_{ir} \ddot{u}_r$$

T geometry matrix derived from the accelerometer positions/orientations. This motion can be decomposed in a nominal contribution and a parasitic contribution:

Equation 28
$$\ddot{u}_{i,r} = \ddot{u}_{i,n} + \ddot{u}_{i,p} \quad \ddot{u}_{i,n} = T_{in} \ddot{u}_n \quad \ddot{u}_{i,p} = T_{ip} \ddot{u}_p$$

The vectors \ddot{u}_r , \ddot{u}_n and \ddot{u}_p can be used to elaborate indicators on the importance of the parasitic motions on \ddot{u}_i versus frequency, for example :

- The indicator $I_1 = \frac{|\ddot{u}_i - \ddot{u}_{i,r}|}{|\ddot{u}_i|}$ quantifies the importance of the relative motion $u_i - u_{i,r}$ with respect to the absolute motion u_i , but without distinguishing nominal and parasitic motion contribution.
- The indicator $I_2 = \frac{|\ddot{u}_{i,p}|}{|\ddot{u}_{i,n}|}$ quantifies the importance of the parasitic motion with respect to the nominal motion.

These two indicators can be used to estimate the importance of the parasitic motions on the measures, for example with the ratio I_2 / I_1 which, for a first bending mode of a beam-like structure means:

- $I_2 / I_1 \ll 1$: significant amplification with small parasitic contribution
- $I_2 / I_1 \gg 1$: small amplification with predominant parasitic contribution
- Between these extreme values: significant contribution.

However, a given value is not very easy to understand and more simple and interpretable indicators can be elaborated, as the following ones based on the imaginary parts, which has the advantage of being coherent with the RTMVI method used for modal identification:

Equation 29
$$I_3 = \frac{\max(\ddot{u}_b) - \min(\ddot{u}_b)}{\max(\ddot{u}_i) - \min(\ddot{u}_i)} \quad I'_3 = \frac{|\ddot{u}_b - \Delta \ddot{u}_b|}{|\ddot{u}_b|}$$

The indicator I_3 quantifies the contribution of the parasitic motions, and if this contribution is significant, the indicator I'_3 quantifies the contribution of the base rigid motion.

7.3.2 Motion of the specimen without parasitic motion

Flexibilities in the guidance system of a shaker may generate non negligible parasitic motions with large specimens. In this case, they significantly modify the dynamic responses of the specimen and distort the derived modal properties. These parasitic motions indicate an interaction between the specimen and the

shaker. They can be measured by a suitable set of accelerometers on the table. The question is then to remove them from the test results in order to find the dynamic behaviour of the specimen itself.

This problem can be theoretically solved with the following steps: first an identification of the modes of the imperfectly guided specimen, then reconstitution of missing FRF (Frequency Response Functions) to derive the FRF of the perfectly guided specimen. The reconstitution requires suitable modal identification and additional data such as static terms. The theoretical formulation is presented in the following.

7.3.2.1 Theoretical formulation

It is necessary to assume that the parasitic motions at shaker/specimen interface can be decomposed in two categories:

- a rigid body average motion with 5 components(2 non nominal translations and 3 rotations), which is linked to the imperfections of the guidance system combined with S/C dissymetries,
- a deformation around the previous motion due to the interface flexibility (test rig effect, concerning the shaker and the adapter).

In the frequency band generally considered, typically 5-100 Hz, the deformation is not very significant. In this case, only the 5 parasitic motion components have to be considered, as it will be assumed in the following (the theory could solve the general case, but would lead to major problems in practice).

In addition to the 6 acceleration components measured at interface (1 nominal + 5 parasitic), it is assumed that the 6 force components are also available, either from direct measurements with a force measurement device, or with a mass operator technique (combining S/C internal accelerations with mass coefficient).

The method proposed to remove the effect of the parasitic motions consists in manipulating the FRF $X(\omega)$ with $\omega=2\pi f$ circular frequency, derived from test results between possible excitations and responses.

So, let's consider the 6 force components F_r and the 6 acceleration components \ddot{u}_r at interface completed by internal acceleration components \ddot{u}_s , as shown in Figure 7-8. \ddot{u}_r is composed of the nominal acceleration \ddot{u}_n and the 5 parasitic accelerations \ddot{u}_p (2 translations and 3 rotations).

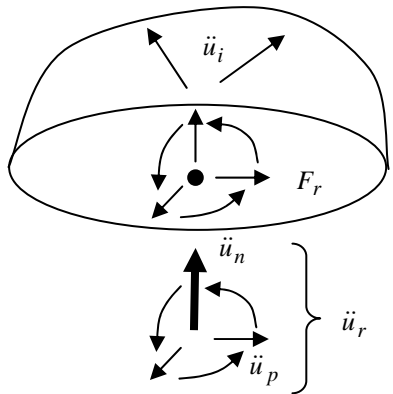
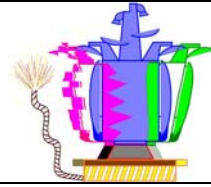


Figure 7-8: Measured forces and accelerations

The only excitation applied on the specimen is the nominal acceleration \ddot{u}_n , thus applied on the single DOF (Degree Of

Freedom) n . The other DOFs p have responses in acceleration \ddot{u}_p . On these DOFs p , excitations by external forces ϕ_p can be considered (don't confuse with the reaction forces F_p): they are null for an excitation by the shaker itself, but they could be generated by small external shakers for example.

In this case, the FRF of the imperfectly guided specimen between the possible excitations (\ddot{u}_n, ϕ_p) and the possible responses (F_n, \ddot{u}_{p+i}) are the following:



Equation 30

$$\begin{bmatrix} F_n \\ \ddot{u}_{p+i} \end{bmatrix} = \begin{bmatrix} M_{nn} & -T_{np} \\ T_{(p+i)n} & -\omega^2 G_{(p+i)p} \end{bmatrix} \begin{bmatrix} \ddot{u}_n \\ \varphi_p \end{bmatrix}$$

M_{nn} Dynamic mass of the imperfectly guided specimen in the nominal direction, given by the ratio F_n / \ddot{u}_n when $\varphi_p = 0$, thus available from measurements (or mass operator)

$T_{(p+i)n}$ Dynamic transmissibilities in accelerations of the imperfectly guided specimen between the nominal acceleration and the $(p+i)$ -set, given by the ratios $\ddot{u}_{p+i} / \ddot{u}_n$ when $\varphi_p = 0$, thus available from measurements

T_{np} Dynamic transmissibilities in forces of the imperfectly guided specimen between the p -set and the nominal acceleration, given by the ratios $-F_n / \varphi_p$ when $\ddot{u}_n = 0$, thus not available from measurements, but equal to T_{pn}^T from the reciprocal principle

$G_{(p+i)p}$ Dynamic flexibilities of the imperfectly guided specimen between the p -set and the $(p+i)$ -set, given by the ratios $\ddot{u}_{p+i} / \varphi_p$ when $\ddot{u}_n = 0$, thus not available from measurements

The dynamic flexibilities $G_{(p+i)p}$ can be reconstituted from the FRF M_{nn} and $T_{(p+i)n}$ by identification of the modal parameters of the imperfectly guided specimen, i.e.: L_{nk} modal participation factors, and mode components $\Phi_{(p+i)k}$, with the following reserves:

- these modal parameters must be completed by the static terms $G_{(p+i)p,stat} = G_{(p+i)p}(\omega = 0)$ in order to have a complete information for FRF reconstitution. In the process, $G_{(p+i)p,stat}$ can be replaced by the residual terms $G_{(p+i)p,res}$ representing the upper modes static contribution,
- all the important modes must be suitably identified: the final results depend closely on the quality of this static and modal identification.

Assuming that the FRF $M_{nn}(\omega)$, $T_{(p+i)n}(\omega)$ and $G_{(p+i)p}(\omega)$ of the imperfectly guided specimen are available, the perfectly guided specimen behavior is derived from Equation 30 by writing $\ddot{u}_p = 0$:

Equation 31 gives the external forces φ_p^* necessary to obtain $\ddot{u}_p = 0$, thus to suppress the parasitic motions.

Equation 31
$$\varphi_p^* = -[-\omega^2 G_{pp}]^{-1} T_{pn} \ddot{u}_n$$

Equation 32 and Equation 33 give the corresponding reaction force F_n^* in the nominal direction and the internal motion \ddot{u}_i^* , i.e. the dynamic responses of the perfectly guided specimen, and the problem is solved.

Equation 32
$$F_n^* = [M_{nn} + T_{np} [-\omega^2 G_{pp}]^{-1} T_{pn}] \ddot{u}_n$$

Equation 33
$$\ddot{u}_i^* = [T_{in} - G_{ip} [-\omega^2 G_{pp}]^{-1} T_{pn}] \ddot{u}_n$$

Note that only the force F_n in the nominal direction is directly involved in Equation 30 to Equation 33. However, the reaction F_p , measured or derived from mass operator, can be used at low frequencies to derive the static terms $G_{(p+i)p,stat}$, as it will be seen later.

7.3.2.2 Static terms

The static terms $G_{(p+i)p,stat} = G_{(p+i)p}(\omega=0)$ are given by the values of u_p and u_i for a static force $\varphi_p = 1$. For this static loading, u_i is related to u_p by $u_i = T_{ip,stat} u_p$, with $T_{ip,stat}$ expressing the rigid body motion directly related to the specimen geometry. So:

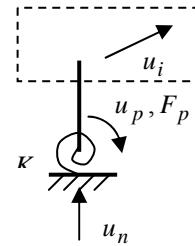
Equation 34
$$G_{ip,stat} = T_{ip,stat} G_{pp,stat}$$

and the only static term to get is $G_{pp,stat}$, which can be identified from T_{pn} and M_{pn} derived from test.

When p has only one component as for the academic case, M_{pn} is scalar and can be inverted to find $G_{pp,stat}$. When p has several components, 5 in the general case, this doesn't work: $G_{pp,stat}$ is a 5 x 5 matrix, a priori full, and M_{pn} is only a vector with 5 components which cannot be inverted. It would be necessary to have 5 independent load cases instead of 1. To overcome this problem, assumptions can be made, depending on the test configuration:

- **Lateral case:**

If we consider the case $u_n = u_x$ and 5 parasitic components: $u_p = (u_y, u_z, \theta_x, \theta_y, \theta_z)$. The static acceleration $\ddot{u}_n = \ddot{u}_x$ generates inertia forces $-F_p = -(F_y, F_z, M_x, M_y, M_z)$ which are measured (or derived from mass operator or from MCI properties).



The inertia forces depend on the specimen, but $G_{pp,stat}$ depends only on

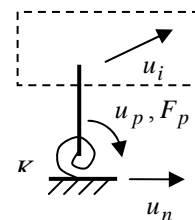
the sliding table flexibility on its bearings. If this flexibility is located near the interface, which has generally 2 planes of symmetry, the dof can be considered uncoupled and it comes:

Equation 35
$$\begin{bmatrix} u_y \\ u_z \\ \theta_x \\ \theta_y \\ \theta_z \end{bmatrix} = \begin{bmatrix} G_{u_y, u_y} & 0 & 0 & 0 & 0 \\ 0 & G_{u_z, u_z} & 0 & 0 & 0 \\ 0 & 0 & G_{\theta_x, \theta_x} & 0 & 0 \\ 0 & 0 & 0 & G_{\theta_y, \theta_y} & 0 \\ 0 & 0 & 0 & 0 & G_{\theta_z, \theta_z} \end{bmatrix} \begin{bmatrix} F_y \\ F_z \\ M_x \\ M_y \\ M_z \end{bmatrix}$$

In this case, the problem is solved: $G_{u_y, u_y} = u_y / F_y$, $G_{u_z, u_z} = u_z / F_z$.

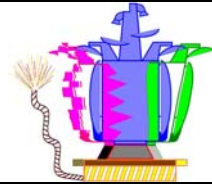
- **Vertical case:**

If we consider the excitation $u_n = u_z$, with 5 parasitic components: $u_p = (u_x, u_y, \theta_x, \theta_y, \theta_z)$. The static acceleration $\ddot{u}_n = \ddot{u}_z$ generates inertia forces $-F_p = -(F_x, F_y, M_x, M_y, M_z)$ which are measured or derived).



$G_{pp,stat}$ depends on the flexibility of the expansion head which differs

from the lateral case because of the guidance system which has also 2 planes of symmetry, but is located far from the interface: the bending motions couple translation and rotation degrees of freedom and it comes :



Equation 36

$$\begin{bmatrix} u_x \\ u_y \\ \theta_x \\ \theta_y \\ \theta_z \end{bmatrix} = \begin{bmatrix} G_{ux,ux} & 0 & 0 & G_{ux,\theta_y} & 0 \\ 0 & G_{uy,uy} & G_{uy,\theta_x} & 0 & 0 \\ 0 & G_{uy,\theta_x} & G_{\theta_x,\theta_x} & 0 & 0 \\ G_{ux,\theta_y} & 0 & 0 & G_{\theta_y,\theta_y} & 0 \\ 0 & 0 & 0 & 0 & G_{\theta_z,\theta_z} \end{bmatrix} \begin{bmatrix} F_x \\ F_{zy} \\ M_x \\ M_y \\ M_z \end{bmatrix}$$

The torsion case is solved, but the two bending ones require additional assumptions to determine all the terms. For each bending, there are 3 unknowns, for example for X (round the Y axis): $G_{ux,ux}$, G_{ux,θ_y} , G_{θ_y,θ_y} . The measure of F_x and M_y provides 2 equations. A third one must be found from math model or test results on the shaker.

7.3.2.3 Conclusions

In the general case, the process can be summarized as follows:

- classical modal identification, including static/residual terms, performed on the interface and internal accelerations and on the interface reaction force in the nominal direction,
- determination of static terms related to the interface parasitic components, which can be derived from the interface reaction forces at low frequencies and, for vertical runs, additional shaker data,
- reconstitution of a complete FRF set of the imperfectly guided specimen, using the previous data,
- manipulation of these FRF to derive the FRF of the perfectly guided specimen.

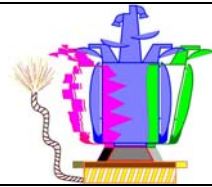
Its validity has been shown on an academic case with perfect data identification. So, the final results depend closely on the quality of the identification of all the static and modal terms involved.

7.3.2.4 Limitation of the parasitic motion removal methodology and tool

The methodology was validated on a simple academic case and the following conclusions can be made:

- The correction of the parasitic motion seems to be efficient but still with some limitations due to the data provided because:
 - The introduction of the perturbation does not seem to be mastered
 - The introduction of the modal damping ratio is questionable
- This correction is efficient but very sensitive to the quality of the modal identification and to the determination of the static term
- The modal damping ratio extraction is of poor accuracy and have an impact on the correction quality
- The determination of the static term is also of poor accuracy and jeopardizes the correction
- The creation of the parasitic flexibilities may be indicted for the computation of the static term

In conclusion to the parasitic motion removal, the academic case has validated the proposed approach. The simulation on an industrial case has shown encouraging results, but not completely satisfactory due to the quality of the data. Additional work is needed to understand all the reasons which can degrade the accuracy and to provide guidelines for such a process.



7.3.3 Static and residual terms for modal identification

To have a more accurate description of the specimen dynamic properties, the modal identification must be completed:

- **below the frequency band: by an accurate determination of the static terms**

They are derived from low frequency data where the specimen is quasi rigid.

Taking directly the asymptotic values X_0 to the FRF $X(\omega)$ given by the minimum frequencies measured can provide significant errors due to first mode amplifications. A better determination consists to use an approximation of $X(\omega)$ in an adequate low frequency band $[\omega_{\min}, \omega_{\max}]$, with ω_{\max} lower than the first eigenfrequency ω_1 ; the modal superposition approach can be written:

Equation 37
$$X(\omega) \approx X_0 + \sum_k \frac{(\omega / \omega_k)^2}{1 - (\omega / \omega_k)^2} \tilde{X}_k$$

X_0 static term, ω_k circular frequencies and \tilde{X}_k effective parameters of modes k , the effects of modal dampings ζ_k being neglected, with ω_{\max} not too close to ω_1 .

Among possible approaches to approximate the sum, the following ones have been selected:

- **Parabolic approach:** Only the first polynomial term of the development is kept:

Equation 38
$$\hat{X}(\omega) = X_0 + B \omega^2$$

This estimation requires the identification of the 2 parameters X_0 and B by least squares best fit. It is not very accurate because the higher order terms may be significant, but it is robust with respect to measurement noise.

- **Pseudo-mode approach:** The sum is approximated by the contribution of a unique “pseudo-mode” representing all the modes, which can also be interpreted as a residual mode to modal truncation with no mode kept:

Equation 39
$$\hat{X}(\omega) = X_0 + \tilde{X}_1 \frac{(\omega / \omega_1)^2}{1 - (\omega / \omega_1)^2}$$

This estimation requires the identification of 3 parameters X_0 , ω_1 and \tilde{X}_1 , instead of 2. It is more accurate than the parabolic one, but also more sensitive to measurement noise.

This is illustrated with the dynamic mass of the 2-DOF system of Figure 7-9. The results with various levels of measurement noise are given for the two approaches compared to a basic estimation of the average value \bar{X}_0 .

The pseudo-mode approach is much better without noise, but the errors are rapidly increasing with the noise level, contrary to the parabolic estimation which is not very sensitive

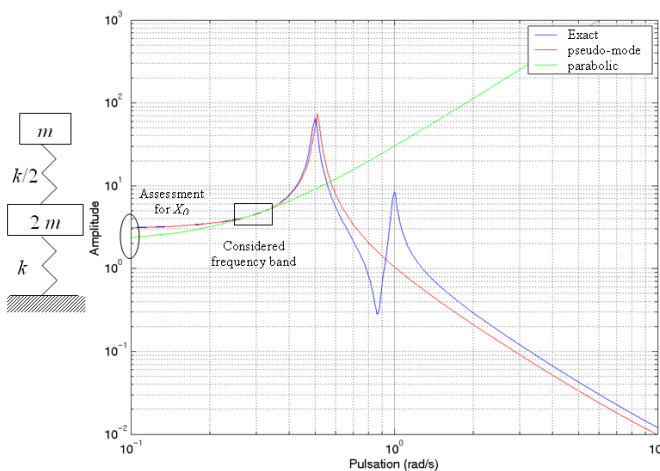
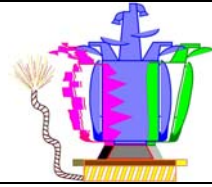


Figure 7-9: Errors on static term estimation with the dynamic mass of a 2-DOF system



By experience, it is worth to have the two approaches and select the one corresponding to the minimum variations between $X(\omega)$ and $\hat{X}(\omega)$.

- **beyond the frequency band: by an accurate determination of the residual terms**

A similar approach is used to determine a residual term representing the upper modes of the considered frequency band $[\omega_{\min}, \omega_{\max}]$, with now ω_{\max} higher than the last identified eigen frequency. The modal superposition approach for a given FRF $X(\omega)$ can be written:

Equation 40
$$X(\omega) \approx X_0 + \sum_{k \text{ kept}} \frac{(\omega / \omega_k)^2}{1 - (\omega / \omega_k)^2 + i 2 \zeta_k \omega / \omega_k} \tilde{X}_k + \sum_{k \text{ sup}} \frac{(\omega / \omega_k)^2}{1 - (\omega / \omega_k)^2} \tilde{X}_k$$

The static term X_0 comes from the previous section. The last sum can be approximated by the contribution of a unique mode, the “residual mode” representing all the upper modes after modal truncation (effect of its damping neglected):

Equation 41
$$\hat{X}_{res}(\omega) = \tilde{X}_{res} \frac{(\omega / \omega_{res})^2}{1 - (\omega / \omega_{res})^2} \approx X(\omega) - \left(X_0 + \sum_{k \text{ kept}} \frac{(\omega / \omega_k)^2}{1 - (\omega / \omega_k)^2} \tilde{X}_k \right)$$

For a given set of FRF $X_i(\omega)$, this requires the identification of the common parameter ω_{res} and the set of components $(\tilde{X}_{res})_i$, by least squares best fit.

This residual mode represents a second order correction to modal truncation effects and should provides a better fit for the measured FRF $X_i(\omega)$, more especially at the antiresonances and beyond the last identified eigen frequency.

7.3.4 Elaboration of reduced experimental model

Elaboration of experimental models consists in using directly experimental data without having resort to a finite element model. This can be performed by modal approach or by FRF coupling.

- Modal approach has been used in previous studies, leading to experimental modal reduced models in the case of excitation by forces. The theory shows that adequate experimental data can provide by itself the relevant mass, damping and stiffness matrices of a reduced model which can be directly connected to other models for subsequent coupled analysis.
- Experimental models can also be directly represented by FRF instead of eigenmodes, and combined to adjacent models by FRF coupling to derive the effect of parasitic motions. All the concerned FRFs must be available with sufficient quality to be conveniently manipulated.

7.3.4.1 Experimental modal reduced models

The basic idea, in a finite element context, is to project the structural properties on a reduced basis of mode shapes derived from static and/or eigenvalue analysis, as in modal synthesis, then to represent the modal DOF by adequate matrices, and recover the physical DOFs by suitable linear constraints.

In the case of excitation by forces, the formulation introduces static or residual flexibilities modifying the stiffness matrix of the modal model. In the case of a base excitation only, this comes to elaborate the equivalent effective mass model consisting of spring-mass systems in parallel, each one representing a mode with its effective mass, its stiffness given by the frequency, and its damper for damping

representation. The physical DOF i are recovered using the corresponding effective transmissibilities:

Equation 42
$$u_i = \sum_k \tilde{T}_{ir,k} \tilde{u}_{r,k}$$

with $\tilde{u}_{r,k}$ displacements of the effective mass of mode k excited by u_r , and $\tilde{T}_{ir,k}$ effective transmissibilities of mode k between i and r . Note that the residual mode of previous chapter provides naturally a second order correction to modal truncation.

In practice, the effective masses are derived from the dynamic masses in the 3 directions.

7.3.4.2 Experimental FRF models

For a given structure to be connected to the outer world by a set of connection DOF c , without excitation on its internal DOF, the required FRF for subsequent coupled analysis are:

- For solving the coupled problem at c -set DOF (first step): $X_{cc}(\omega)$
- For recovering the responses on a set of selected internal DOF s (second step): $X_{sc}(\omega)$

We consider a base excitation with a rigid base represented by DOF r and $X_{cc}(\omega) = M_{rr}(\omega)$ the dynamic mass of the structure. Thus we have to know all the terms of the transfer matrix $X_{cc}(\omega) = M_{rr}(\omega)$ which is a 6×6 matrix in the 3D general case with 3 translations and 3 rotations.

The tests provide data only for the 3 translations. The missing information is recovered by identification of modal terms (modal participation factors L_{rk}) and static terms (rigid body mass matrix \bar{M}_{rr}):

Equation 43
$$M_{rr}(\omega) \approx \bar{M}_{rr} + \sum_{k \text{ kept}} \frac{(\omega / \omega_k)^2}{1 - (\omega / \omega_k)^2 + i 2 \zeta_k \omega / \omega_k} \tilde{M}_{rr,k} \quad \text{with } \tilde{M}_{rr,k} = \frac{L_{rk} L_{kr}}{m_k}$$

The identification of Equation 43 limited to the terms $M_{rn}(\omega)$, n direction of excitation, provides the modal parameters $(\omega, \zeta, m, L_r)_k$ which is sufficient to reconstitute the other terms of $M_{rr}(\omega)$ if \bar{M}_{rr} is known and the important modes have been excited.

The problem is simplified if longitudinal and lateral behaviors can be uncoupled, giving independent FRF. The second step concerning recovery of selected internal responses with $X_{sr}(\omega)$ is straightforward: this comes to compute the responses of the structure to the base excitation found in the first step.

7.3.5 Measurement quality

Measured data provide FRF which must be coherent with respect to various properties, among which:

- Coherence of the low frequency data with the static properties of the specimen (dynamic transmissibilities and masses).
- Coherence of FRF with theoretical properties derived from basic mechanic considerations. For this subject, the drive point FRF must be distinguished from the other FRF.

Each coherence can be verified to have an assessment on the measurement quality.

		Ref : MTF.AIDT.TN.2168 Issue : 1 Rev. : 1 Date : 03/03/2010 Page : 59
--	--	---

7.3.5.1 Coherence of the low frequency data with the static properties

The static properties concern:

- The dynamic transmissibilities which must tend (at 0 Hz) to the static transmissibilities, directly related to the rigid body geometry in the case of a rigid body motion of the base. This allows checks of sensor locations, orientations and scaling factor.

The identified errors can easily be corrected.

In practice, as the parasitic motions are often small, providing quasi-pure translations on the specimen, the distances related to the sensors, which can be detected only by rotations, cannot be obtained. In this case, the sensor locations cannot be checked. On the contrary, the sensor orientation is directly concerned by the direction of the excitation and the detection of the axis error, including sign, is the main application of the low frequency transmissibilities.

- The dynamic masses (obtained from reaction forces measurement) which must tend (at 0 Hz) to the static masses, are directly related to the rigid body mass matrix, in the case of a rigid body motion of the base, i.e the MCI properties: mass, centre of gravity and inertia related to the base. In the usual case of excitation in translation only, inertia cannot be obtained, only mass and components of the centre of gravity:
 - from the force in the nominal direction : specimen mass M
 - from the 2 moments in the perpendicular directions: 2 components of centre of gravity (2 offsets in vertical, 1 offset and centre of gravity height in horizontal)
 - from the other components : effects of parasitic motions.

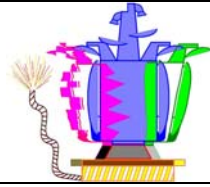
In practice, the reaction forces are not measured systematically and the mass properties cannot be checked with this approach. However, the mass can be derived from the coil current intensity but with poor accuracy, knowing the shaker moving mass involved or with the mass operator method with a good accuracy.

Both static properties can be estimated from the best curve fitting between parabolic and residual mode as described in §7.3.4.1. These errors give information on the quality of the considered measures.

7.3.5.2 Coherence with mechanical properties

Various properties related to FRF can be shown from theoretical considerations, and can be disturbed by test conditions. In this context, the drive point FRF, i.e. when the considered response is on the same DOF as the excitation, has an important role in the modal identification by providing the mode shape normalization and must be particularly checked.

As the contribution of each mode to the FRF is the product of the effective parameter by a dynamic amplification factor, the FRF imaginary part is always positive. For base driven test, the FRF is the dynamic mass in the direction of excitation: its imaginary part must be positive for all frequencies. If it is not the case in some frequency bands, various reasons can be found, such as problems related to the control of excitation or to the response measurement, parasitic motions or measurement noise.

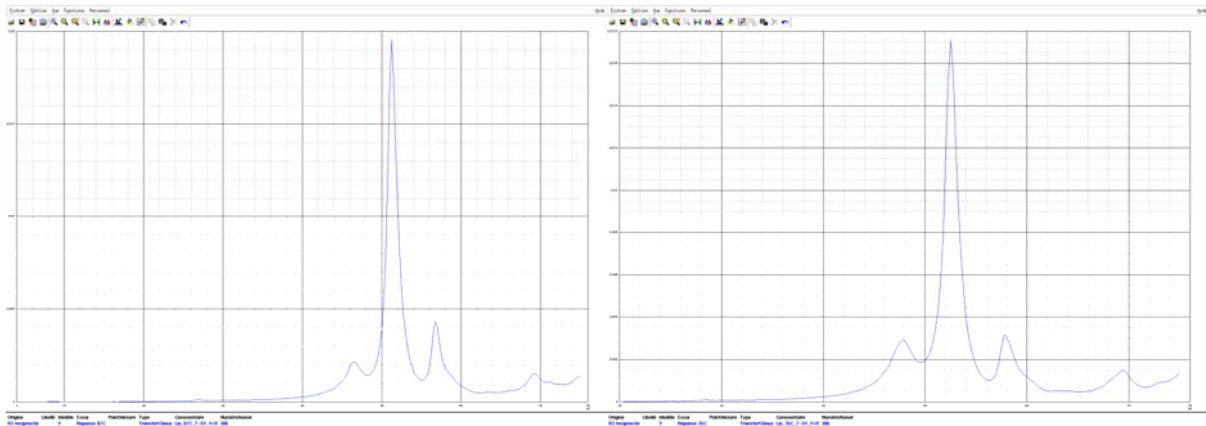


The other FRF have not this property: some effective parameters can be positive and others negative. In this case, the imaginary part can be negative in some frequency bands, providing various signs for the mode components.

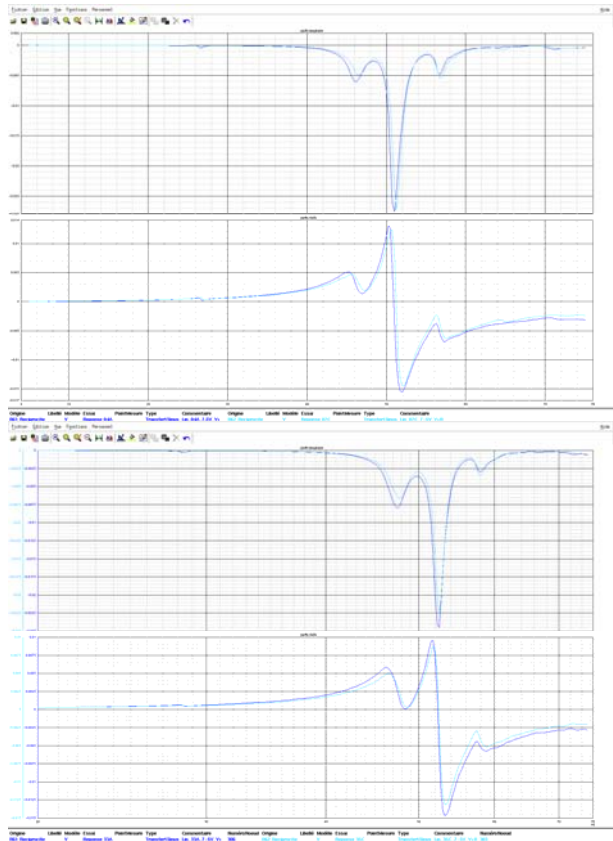
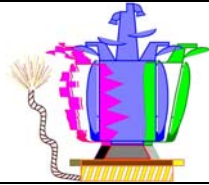
This is illustrated in Figure 7-10 gives the imaginary parts of two drive point FRF coming from a modal survey test. The values are always positive, thus acceptable.

The reciprocal principle states that the ratio between excitation and response remains the same when they permute thus the FRF matrix must be symmetric. This symmetry must be checked in modal survey test when using several excitation forces. For base driven test, this involves two runs in different directions and only the base motion limits the interest of this point since there is no other excitation on the S/C.

This is also illustrated in Figure 7-10 with the reciprocity results related to the same modal survey test. On these two examples, the curves have small but significant differences, showing that the reciprocity is not perfectly verified and giving an idea of the test discrepancies.



Drive point FRF imaginary parts



Other FRF real/imaginary parts for reciprocity

Figure 7-10: Modal survey test results on BIOLAB with 2 different input points

7.4 NON LINEAR ASPECTS

Even if test preparation are achieved with linear analysis, structural behaviour in test is most generally non linear. However the non linearity level could be more or less pronounced. In case of weak non linear behaviour the linear approach analysis is enough and justified. In the other case, a specific approach must be proposed to deal with the non linearities.

The approach proposed in the frame of the DYNAMITED study is first an overall introduction to non linear phenomena and secondly different methods for detection, characterisation and quantification of non-linearities in dynamic tests. Finally an approach for non-linear experimental modal analysis is proposed to interpolated or extrapolated non linear modal behaviour to not passed levels.

7.4.1 Detection, characterisation and quantification of non-linearities in dynamic tests

7.4.1.1 Introduction

Modal testing of complex assembled structures reveal different dynamic behaviour at different excitation levels which highlights the structures non-linear behaviour. As shown in the Figure 7-11, simulated FRF at different levels of constant excitation force amplitudes show non-linear behaviour on the first and the fifth resonance peak, whereas the other resonance peaks remain unaffected.

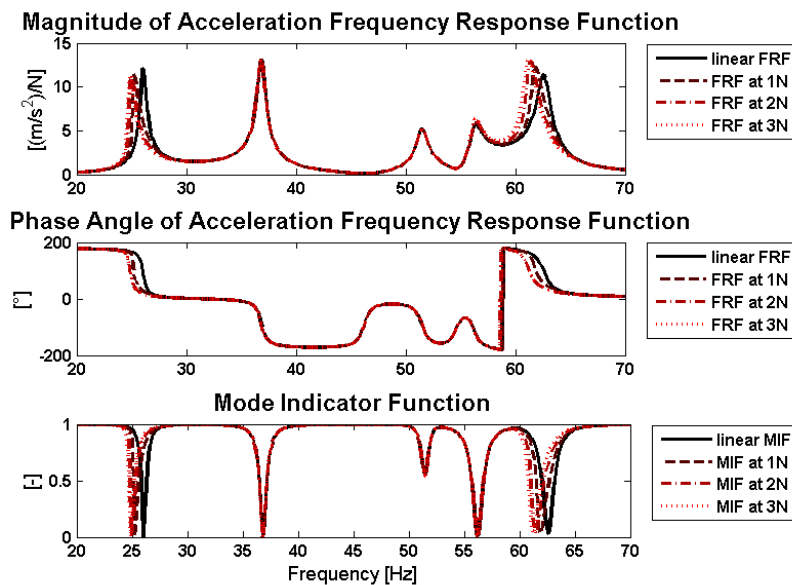


Figure 7-11: Non-linear acceleration FRF for different levels of constant excitation force

Applying experimental modal analysis to such non-linear FRFs highlights different difficulties: the modal parameters can no longer be considered as constant quantities and the underlying linear assumptions are no longer applicable.

Even if the structure is non-linear, not necessarily all modes are affected so conventional methods for experimental modal analysis can be applied to extract most of the modal parameters but poor accuracy should be expected for modes affected by non-linearities.

The detection and characterisation of non-linear structural behaviour is to support the non-linear experimental modal analysis. The basic non-linearity detection should be performed in any case to ensure the quality of experimental modal data. The characterization of non-linearities aims to categorize the non-linearity with respect to a suitable mathematical model to describe the non-linear effects.

The studied approach deals with some non-linearities of certain modes by applying individually amplitude dependent correction factors to the eigenfrequencies and to the damping ratios of the non-linear modes. The localization and FEM modelling of non-linearities is not required here. The characterization of non-linearities in this context is rather aimed at supporting test engineer in making the right choice for the *type* of correction factor applied to the eigenfrequencies and damping ratios of a few non-linear modes in experimental modal analysis. This also includes the trivial case that the methods should give an indication to which modes are non-linear and which modes remain linear when increasing the excitation force levels.

However, non-linear experimental modal analysis should always be considered as an extension of the conventional experimental modal analysis. Because of the significantly increased numerical effort involved in non-linear methods they should only be applied when the conventional (linear) methods yields unsatisfactory results which can be attributed to non-linear effects in the test data. In many practical cases non-linear effects can be small so that the effort involved in non-linear experimental modal analysis would not be justified when the increased effort is compared to the gain in information.

7.4.1.2 Sources and Consequences of Structural Non-Linearities

The sources of non-linearities can be manifold. It is widely accepted that the behaviour of non-linear structures in case of low excitation levels can be approximated with sufficient accuracy by a linear model.

A system is weakly non-linear when the displacement response in case of harmonic excitation is dominated by the fundamental harmonic (so that the response higher harmonics error is small) whereas it is strongly non-linear when the higher harmonics are a significant portion of the response.

When performing vibration measurements for modal identification it is recommended to check for possible deviations from linear behaviour which is essentially the detection of non-linearities. Once a non-linearity has been detected, the test engineer has to assess its influence on the global structural dynamics behaviour. The characterization of a non-linearity provides a means for the assessment, whether or not it is relevant to include the detected non-linearity in the FE model, or whether it is necessary to make special considerations in experimental modal analysis. This is helpful for finding a suitable model to describe the detected non-linear behaviour.

Even if the sources of non-linear behaviour are often locally concentrated, they nonetheless have an influence on the global dynamic behaviour, thus the consequences can be observed e.g. in:

- non-harmonic response portions due to purely harmonic excitation, as illustrated in Figure 7-12 showing the measured acceleration response of a base driven structure with local non-linearities at bolted flange joints. The higher harmonics become more and more important when the base acceleration level is increased and this effect is very pronounced in the acceleration response but can be much less significant in the displacement response

- distortion of frequency response functions when measured at different excitation force levels, as illustrated in Figure 7-13 showing frequency response functions of a non-linear structure simulated at different (constant) excitation force levels and plotted in the same Bode diagram. The FRFs show there are only fundamental harmonic and higher harmonics are filtered out. These FRFs are not “complete” as they only represent the stable response branches. Figure 7-14 illustrates the magnitude response of a system piece-wise linear stiffness where the non-linear response deviates from the linear one. The upper and lower stable branches of the non-linear response can be measured experimentally.

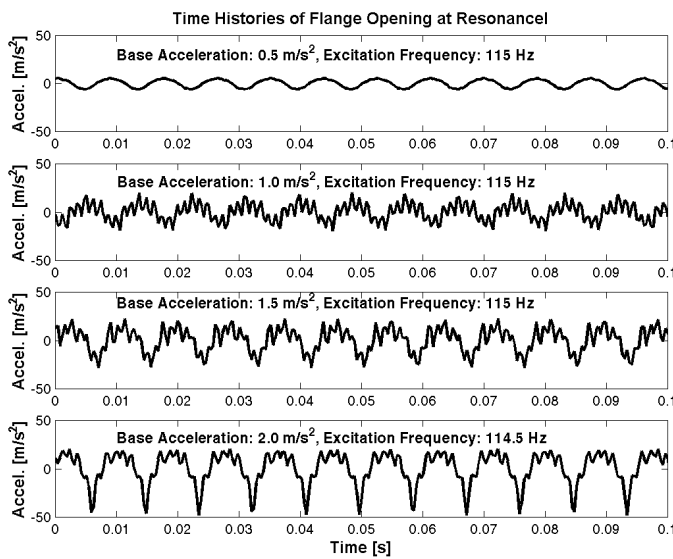


Figure 7-12: Higher harmonics in the acceleration time-domain response of a base driven structure with local non-linearities at bolted flange joints

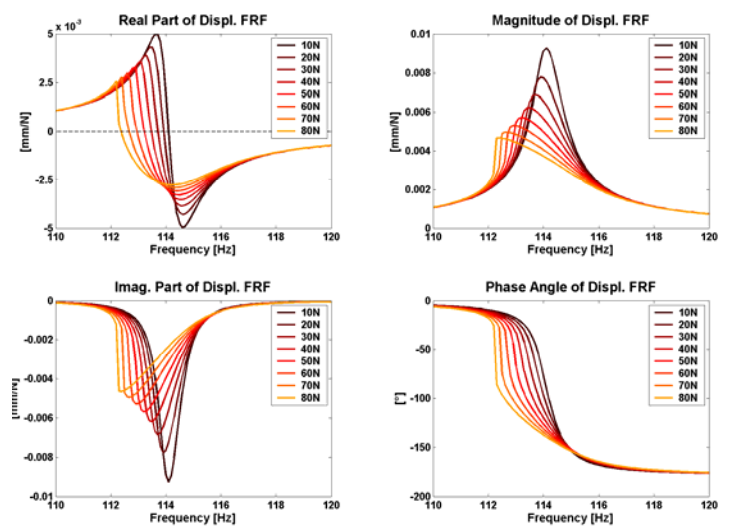


Figure 7-13: FRF of a structure with a softening stiffness and increasing damping non-linearity simulated for different excitation force levels

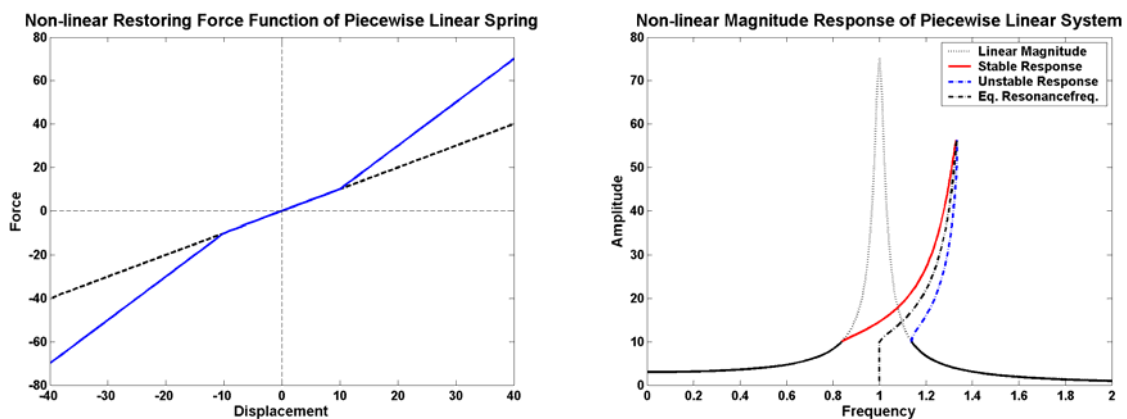


Figure 7-14: Restoring force function and non-linear magnitude response of a system with piece-wise linear stiffness

7.4.1.3 Different Methods for the Detection and Characterization of Non-Linearities

A huge number of methods exist for the detection and characterisation of non-linearities. Subsets of the most promising and practically relevant methods have been studied in the frame of the DYNAMITED study. As it is not possible to present all the methods in this final report, they are only shortly reminded in the next paragraphs whereas the complete methods descriptions are provided in RD 6.

The methods have been classified depending on the type of data to be used i.e. characterisation of non-linear structural behaviour by:

- analytical methods for the characterization of non-linearities
- methods based on frequency-domain response data
- methods based on time-domain response data
- methods based on dedicated excitation signals

Emphasis is given to methods which use frequency-domain response data, because this type of data is mostly used in engineering practice.

7.4.1.3.1 Analytical Methods for the Characterization of Non-Linearities

These methods are based on the idea to compare measured characteristic non-linear response features with a catalogue of basic analytical non-linear systems. The response features to be used can either be:

1. frequency domain response data measured at different excitation force levels or
2. modal features measured at different excitation force levels.

By experience, the mode shapes are less affected by non-linearities.

A simple approach for the detection and characterization of non-linearities is **the overlaid plot of transfer functions or FRFs measured at different levels of constant excitation force.**

The different FRF distortion characteristics are analysed on a single degree of freedom oscillator with a non-linear equation of motion in the frequency domain after applying the harmonic balance method:

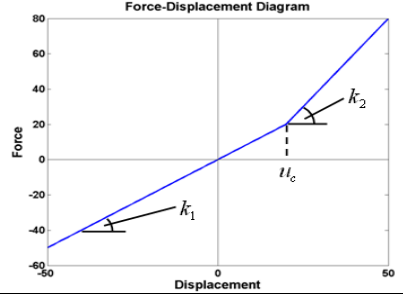
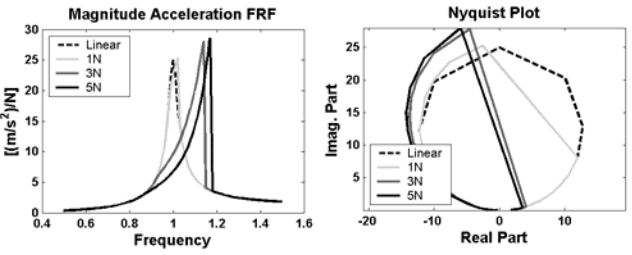
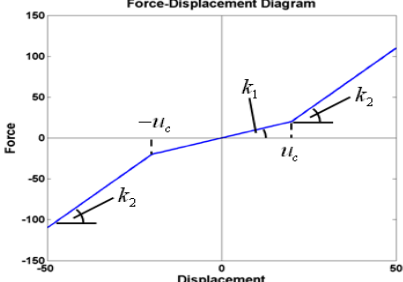
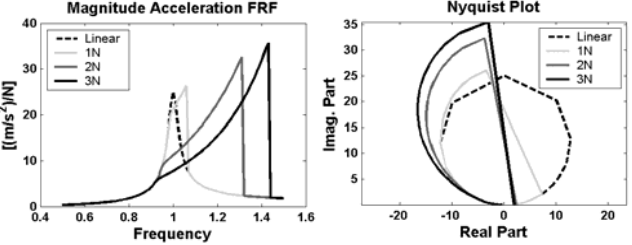
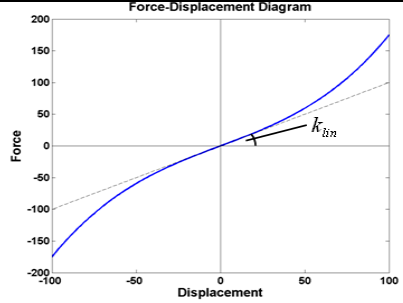
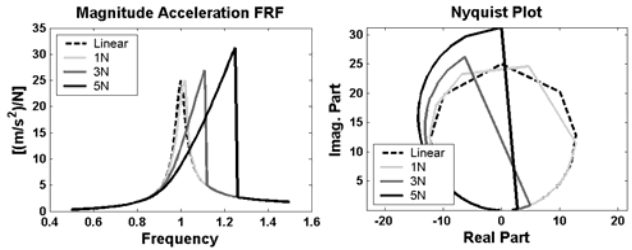
Equation 44
$$\left(-\Omega^2 m + j\Omega c_{eq}(\hat{u}) + k_{eq}(\hat{u})\right)\hat{u} = \hat{f}$$

In order to visualize the influence of amplitude dependent non-linear stiffness and damping on the resonance peak of the transfer function, the following “normalized” conditions are applied to this non-linear oscillator: constant unit mass $m = 1$, underlying linear stiffness is $k_{eq}(\hat{u} \approx 0) = 1$ and underlying linear damping is expressed by 2% modal damping ratio, i.e. $c_{eq}(\hat{u} \approx 0) = 0.04$.

Under these conditions, the angular eigenfrequency of the underlying linear system is $\omega = 1s^{-1}$ and the height of the resonance peak of the FRF is 25 (m/s²)/N at resonance.

Six types of non-linearities have been investigated and are briefly summed up in the Table 7-1. The non linear stiffness shape is given as well as its impact on a Nyquist diagram. Refer to RD 6 for more details.



Non linearity type	Equivalent non-linear stiffness	Characteristic FRF caused distortion
<p>a) Pre-loaded bilinear spring</p> <p>For low excitation force levels the non-linear FRF does not deviate much from the linear one. The distortions appear beyond the stiffness transition point where levels increase with increasing vibration amplitudes. The resonance frequency shift decreases at large vibration levels due to the convergence behaviour of the equivalent non-linear stiffness</p>		
<p>b) Clearance type non-linearity (piecewise linear spring)</p> <p>Due to the similarities in the describing functions of clearance type non-linearity and pre-loaded bilinear spring, there are also similarities in the FRF distortions.</p>		
<p>c) Cubic stiffness non-linearity</p> <p>This non-linearities type is widely used. It approximates the observed non-linear behaviour in a certain range of (low) vibration amplitudes but has a lack of physical reasoning and is therefore not always suited to extrapolate to larger vibration amplitude.</p> <p>The resonance peak shift increases with increasing vibration amplitudes and the equivalent non-linear stiffness does not converge towards a threshold value but diverges towards infinity for very large vibration amplitudes. This effect becomes even worse when using softening cubic springs (i.e. $k_{nl} < 0$). Models with polynomial type non-linearities can only be used as equivalent models to approximate the true non-linear behaviour of a structure within a limited range of vibration levels.</p>		



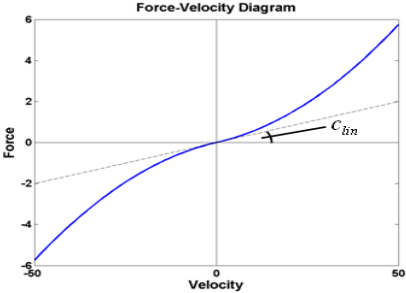
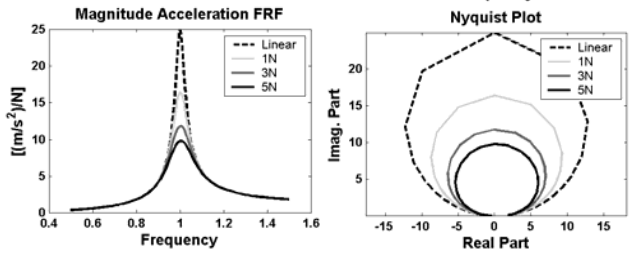
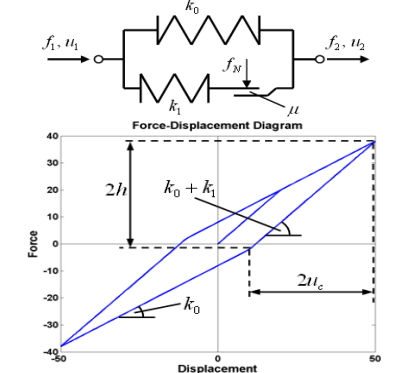
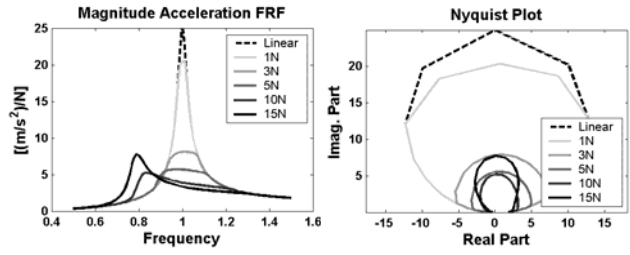
Non linearity type	Equivalent non-linear stiffness	Characteristic FRF caused distortion
<p>d) Quadratic damper</p> <p>Even if polynomial type non linearity doesn't represent physically the true non linear behaviour another type of used damping non-linearities is the quadratic damper.</p> <p>The influence of increasing damping is indicated by the reduction of the resonance peak magnitude, meaning that the level of damping increases with increasing response levels.</p>		
<p>e) Elasto-slip friction non-linearity</p> <p>This special type of friction non-linearity combines both, non-linear stiffness and non-linear damping effects. When the friction force limit is exceeded in the lower branch of the element, the stiffness k_l is no longer active, but instead the dry friction μf_N is used for force transmission and this will involve damping.</p> <p>The effect of increasing and decreasing damping can be observed together with a continuous shift of the resonance peak towards lower frequencies caused by the continuously decreasing equivalent stiffness.</p>		
<p>f) Combined stiffness and damping non-linearities</p> <p>For linear systems, the influence of stiffness and damping can be separated and investigated individually. A change of stiffness causes a resonance peak shift, whereas a change of damping causes attenuation of the peak magnitude. For non-linear systems, the influence of stiffness and damping non-linearities cannot be separated. The coupling between stiffness and damping non-linearities requires the simultaneous identification of these quantities. The Inverse FRF Method is able to distinguish between stiffness and damping non-linearities and thus detect whether or not a combined stiffness and damping non-linearity is present. The Restoring Force Method can identify combined non-linearity</p>		

Table 7-1: Non linearity type effects summary for analytical methods

On the other side, the **linearity plots** show the variation of eigenfrequencies and modal damping ratios of a single mode as a function of the vibration amplitude.

The linearity plots generation can be achieved by two ways:

- use the Phase Resonance Method (PRM) and measure the eigenfrequency and the damping ratio for each mode separately using a number of different excitation force levels
- use FRFs which have been measured at different (constant) force levels.

Eigenfrequency and modal damping ratio can be estimated from constant force level FRFs, based on the peak frequency and the resonance peak half power bandwidth extraction method.

Such linearity plots are shown in the Figure 7-15. For linear systems a straight line of constant value can be expected whereas here a drop of the eigenfrequency can be observed when increasing the vibration amplitudes.

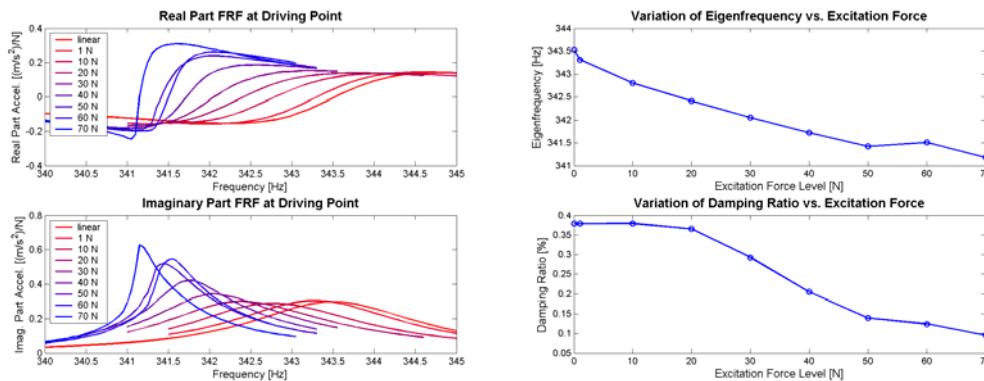


Figure 7-15: Non-linear FRFs and linearity plots

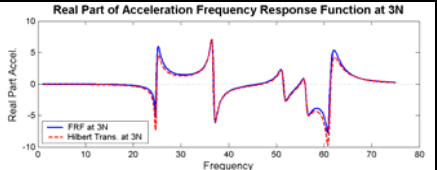
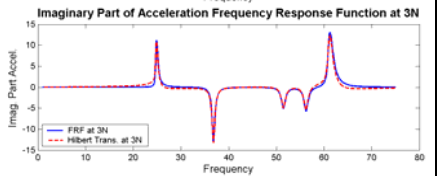
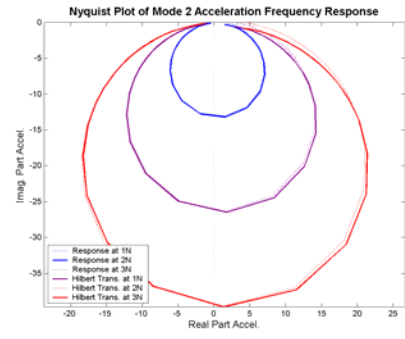
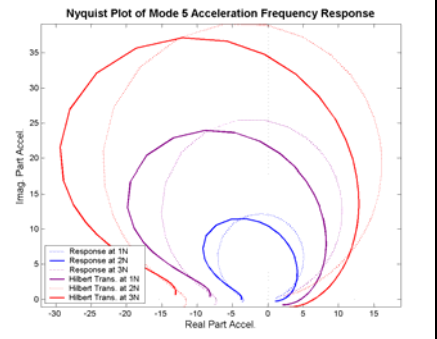
It can be mentioned the **modal characterization functions** (MoCF) which allow drawing the evolution of the eigenfrequency or modal excitation force amplitude as a function of the modal displacement amplitude. This is well suited to detect damping non-linearities since steady state harmonic responses are highly sensitive to damping.

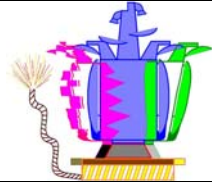
7.4.1.3.2 Methods based on Frequency Domain Response Data

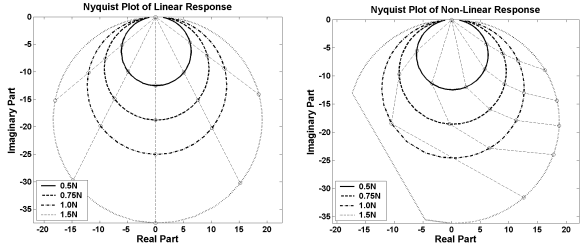
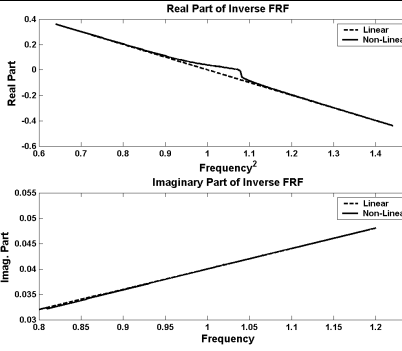
Structure non-linear behaviour may also be characterised by applying different kinds of signal processing and visualisation tools to the measured FRF and compare to a certain reference to highlight possible deviations from linear behaviour.

The techniques shortly described in the Table 7-2 only provide the detection of non-linear behaviour but not quantification. The non-linearity type to be used in non-linear modal analysis is thus largely dependent of the test engineer experience and feeling.



Method	Method description
Overlaid Bode Plots	<p>The simplest and straightforward method for the detection of non-linear behaviour based on overlaid Bode plots, i.e. the plot of magnitude and phase of a frequency response function versus excitation frequency.</p> <p>For a linear structure, the FRFs are invariant under different excitation force levels. The FRFs of non-linear structures are generally vibration amplitude dependent and, thus, are also dependent on the excitation force level.</p> <p>Nevertheless, the non-linearity of each resonance peak may be classified as softening or hardening stiffness, and increasing or decreasing damping with increasing vibration level.</p>
Hilbert Transformation of measured Transfer Functions	<p>The Hilbert transformation provides an estimate of the real part FRF from the corresponding imaginary part FRF and <i>vice versa</i>. It can thus detect non linearities by comparing each transformed part to the original FRF. Differences between the original FRF and its Hilbert transform indicate non-linear behaviour.</p> <p>Normally, Hilbert transformation can only be used to detect structures non-causality, and not to detect non-linearity. Nonetheless, it is widely accepted that non-causality detected by the Hilbert transform is also an indicator for non-linearity:</p> $G_{re}(\omega) = -\frac{2}{\pi} PV \int_{-\infty}^{+\infty} \frac{\Omega}{\Omega^2 - \omega^2} H_{im}(\Omega) d\Omega \quad G_{im}(\omega) = \frac{2\omega}{\pi} PV \int_{-\infty}^{+\infty} \frac{1}{\Omega^2 - \omega^2} H_{re}(\Omega) d\Omega$ <p>However, computation of the Hilbert transformation is not a trivial task as it requires the solution of a Cauchy-Principal-Value (PV) integral which extends from $-\infty$ to $+\infty$ in the frequency domain. Since FRFs can only be measured in a limited frequency band, the calculation of the Hilbert transform suffers from truncation errors. It might occur that differences between the original FRF and its Hilbert transform can appear which are the results of truncation errors and were not caused by non-linearity.</p> <div style="display: flex; justify-content: space-around;">   </div> <div style="display: flex; justify-content: space-around;">   </div>

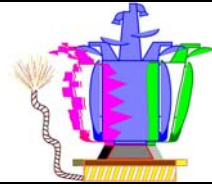


Method	Method description
Distortions of Frequency Isochrones in a Nyquist Plot	<p>The Nyquist plot can be used to detect non-linearities. Linear responses appear as (almost) circular curves in the Nyquist plot, whereas non-linearities cause distortions from the circular form. When the frequency responses (forced response, not FRF) obtained at different levels of excitation are plotted together in a single Nyquist plot, then the deviation of the frequency isochrones (lines which connect points of equal frequency among the different response curves) from straight lines indicate the presence of non-linearity.</p> 
Inverse FRF Plot	<p>The inverse FRF method seeks to separate the effects of non-linear stiffness and non-linear damping by using the inverse of an FRF:</p> $H(\Omega) = \frac{1}{-\Omega^2 m + j\Omega c + k} \rightarrow H^{-1}(\Omega) = (k - \Omega^2 m) + j(\Omega c)$ <p>For linear systems, the real part of the inverse FRF is linear when plotted over frequency squared. The imaginary part of the inverse FRF is directly proportional to the frequency in case of viscous damping, or constant in case of structural damping. If either stiffness or damping is amplitude dependent, then non-linearity is indicated by the inverse FRF plots deviating from the straight line characteristic. The inverse FRF method is essentially a single degree of freedom technique but can be applied to multi-DoF systems with well separated modes under certain conditions described in RD 6.</p> 
Coherence Function	<p>This spectral function that can provide a quick visual inspection of the quality of FRF measurement. It is defined between two spectrums $X(\Omega)$ and $Y(\Omega)$:</p> $\gamma^2(\Omega) = \frac{ S_{XY}(\Omega) ^2}{S_{XX}(\Omega)S_{YY}(\Omega)}$ <p>where $S_{XX}(\Omega) = X(\Omega) \cdot X^*(\Omega)$ is the auto-power spectrum of signal $x(t)$, $S_{YY}(\Omega) = Y(\Omega) \cdot Y^*(\Omega)$ is the auto-power spectrum of the signal $y(t)$, and $S_{XY}(\Omega) = X(\Omega) \cdot Y^*(\Omega)$ is the cross-power spectrum of the two signals. The coherence function γ^2 can only have values between 0 and 1, where a value close to 1 indicates good measurement conditions.</p> <p>The coherence is a rapid standard indicator of the presence of non-linearities in specific frequency bands or resonance regions. A low coherence may be a result of extraneous noise in the measurements due to signal treatment error or non-linear distortions. Unfortunately, non-linearities characterization is not possible and it is not possible to separate the influence of non-linear effects from poor measurement conditions.</p>



Method	Method description
Carpet Plots of Modal Damping	<p>Carpet plots are suited to detect damping non-linearities. They are generated thanks to Nyquist FRF plots. In fact, the modal damping ratio is given by the angles enclosing two points of a FRF resonance peak modal circle.</p> <p>The two response points must be located one before resonance, and the second one after resonance. The choice of the two points is arbitrary so that it can be performed for any pair of points available on the Nyquist plot. This can be observed in the figure where the response points before resonance are indicated in green and the response points after the resonance are indicated in red.</p> <p>Due to non-linearities, the Nyquist plots can deviate from the circular form and thus different damping ratios can be identified depending on the pair of response points used for damping identification. Damping non-linearities can be detected based on the surface plot generated by two pair response points as a function of the frequencies associated with these response points.</p> <p>A flat surface of constant value is linked to linear damping.</p> <p>If the carpet plot is not a planar surface of constant value, the mode under consideration has a non-linear damping. A characterization of the type of damping non-linearity is not trivial but also not impossible (see RD 6 for more details).</p> <div style="display: flex; justify-content: space-around; align-items: flex-start;"> <div style="text-align: center;"> $\xi_r = \frac{\Omega_a^2 - \Omega_b^2}{2\omega_r^2 \left(\tan\left(\frac{1}{2}\Theta_a\right) + \tan\left(\frac{1}{2}\Theta_b\right) \right)}$ $\approx \frac{\Omega_a - \Omega_b}{\omega_r \left(\tan\left(\frac{1}{2}\Theta_a\right) + \tan\left(\frac{1}{2}\Theta_b\right) \right)}$ </div> <div style="text-align: center;"> </div> <div style="text-align: center;"> </div> </div> <div style="display: flex; justify-content: space-around; align-items: center; margin-top: 20px;"> <div style="text-align: center;"> </div> <div style="text-align: center;"> </div> <div style="text-align: center;"> </div> </div>

Table 7-2: Method based on frequency domain



7.4.1.3.3 Methods based on Time Domain Response Data

Time domain methods for the detection and characterization of non-linearities are more advantaging over frequency-domain methods because more information is available from high frequency responses. These methods are based on the restoring force Surface and Force-State Mapping on one degree of freedom and their extension to multi degree of freedom and for base driven systems.

These methods are based on the restoring force Surface and Force-State Mapping, which is a good time-domain approach for the characterization of non-linearities. It is based on the non-linear equation of motion of a single degree of freedom system:

$$\text{Equation 45} \quad m\ddot{u}(t) + \underbrace{d(\dot{u})\dot{u}(t) + k(u)u(t)}_{f_R(u,\dot{u},t)} = f(t) \rightarrow m\ddot{u}(t) + f_R(u,\dot{u},t) = f(t)$$

$$\text{Equation 46} \quad f_R(u,\dot{u},t) = f(t) - m\ddot{u}(t)$$

Here, m is the mass of the system, $\ddot{u}(t)$ is the acceleration response, $f(t)$ is the time history of the excitation force. If these quantities are known by measurements, the restoring force $f_R(u,\dot{u},t)$ can be calculated as a function of time. It is obvious from the above equations, that in case of a linear system, the restoring force is a linear function of displacement $u(t)$ and also a linear function of velocity $\dot{u}(t)$:

$$\text{Equation 47} \quad f_R(u,\dot{u},t) = k u(t) + d \dot{u}(t)$$

The restoring force can be plotted as a 3D surface over displacement and velocity. The surface slope in the displacement direction gives the stiffness k and in the velocity direction gives the damping d .

In case of a linear system, the restoring force surface is a planar flat surface.

By curve-fitting of the 3D surface using a reasonable non-linearity model, it is possible to identify the model coefficients and thus completely describe mathematically the non-linearity.

As can be seen from Equation 47, the restoring force is indeed only a function of the state¹. The nature and shape of the surface will be independent of the time history of the applied force and requires a sufficiently large number of independent states in the test data. Moreover, this single degree of freedom technique requires the response of an isolated mode which call for very specific test configurations.

If the function is not of state (memory effect presence), this will not produce a repeatable 3D surface which will be difficult to interpret.

More discussions about this method are provided in RD 6.

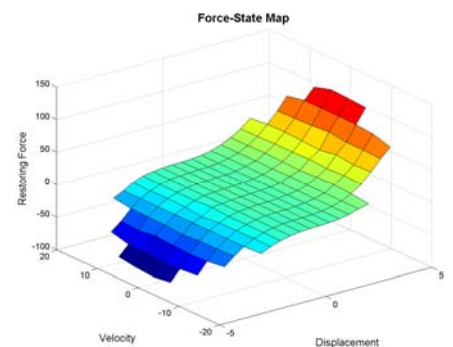
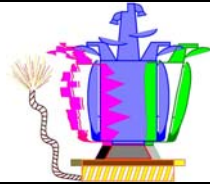


Figure 7-16: Restoring force surface generated from high level random excitation

¹ A state is a combination of displacement and velocity.



An extension of the force-state mapping to multi-degree of freedom systems is the INTL method (Identification of Non-linearities by Time series based Linearity plots). The main feature of this method is that the time domain representation of the restoring force is used in a curve fitting process to identify polynomial types of non-linearities. This is illustrated in the equation below, where the non-linear restoring force is expressed by a polynomial function of velocity and a polynomial function of displacement.

Equation 48

$$f_R(u, \dot{u}, t) = \delta_{d,1} \dot{u}(t) + \delta_{d,2} |\dot{u}(t)| \dot{u}(t) + \delta_{d,3} |\dot{u}^2(t)| \dot{u}(t) + \delta_{d,4} |\dot{u}^3(t)| \dot{u}(t) + \dots$$

$$+ \delta_{k,1} u(t) + \delta_{k,2} |u(t)| u(t) + \delta_{k,3} |u^2(t)| u(t) + \delta_{k,4} |u^3(t)| u(t) + \dots$$

Equation 49

$$f_R(u, \dot{u}, t) = \sum_{i=1}^s \delta_{d,i} |\dot{u}^{i-1}(t)| \dot{u}(t) + \sum_{j=1}^t \delta_{k,j} |u^{j-1}(t)| u(t)$$

Here, $\delta_{d,i}$ are the unknown polynomial coefficients for non-linear damping (linear damping included) and $\delta_{k,j}$ are the unknown polynomial coefficients for non-linear stiffness (linear stiffness included). Equation 49 can be formulated for each point t_l with $l = 1, \dots, n$ of the time history of the non-linear restoring force function. This yields the following equation system for the identification of the unknown polynomial coefficients:

Equation 50

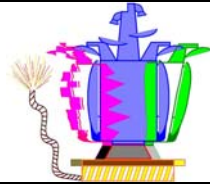
$$\underbrace{\begin{Bmatrix} f_R(u, \dot{u}, t_1) \\ f_R(u, \dot{u}, t_2) \\ \vdots \\ f_R(u, \dot{u}, t_n) \end{Bmatrix}}_{\{f_R\}} = \underbrace{\begin{bmatrix} \dot{u}(t_1) & \dots & |\dot{u}^{s-1}(t_1)| \dot{u}(t_1) & | & u(t_1) & \dots & |u^{t-1}(t_1)| u(t_1) \\ \dot{u}(t_2) & \dots & |\dot{u}^{s-1}(t_2)| \dot{u}(t_2) & | & u(t_2) & \dots & |u^{t-1}(t_2)| u(t_2) \\ \vdots & & \vdots & & \vdots & & \vdots \\ \dot{u}(t_n) & \dots & |\dot{u}^{s-1}(t_n)| \dot{u}(t_n) & | & u(t_n) & \dots & |u^{t-1}(t_n)| u(t_n) \end{bmatrix}}_{[A]} \underbrace{\begin{Bmatrix} \delta_{d,1} \\ \vdots \\ \delta_{d,s} \\ \delta_{k,1} \\ \vdots \\ \delta_{k,t} \end{Bmatrix}}_{\{\delta\}}$$

The unknown polynomial coefficients comprised in vector $\{\delta\}$ are then identified in a least squares sense by building the pseudo inverse of the coefficient matrix $[A]$:

Equation 51

$$\{\delta\} = [A]^+ \{f_R\} = \left[[A]^T [A] \right]^{-1} [A]^T \{f_R\}.$$

This curve fitting algorithm can only handle types of non-linearities, for which the coefficients are linear in the equations. This poses a limitation to this procedure, because if the true type of non-linearity is not contained in the coefficient matrix, only an equivalent model of polynomial type will be identified.



An extension of the Restoring Force Method for base driven Systems has been developed in the RD 6 and conclusions are briefly presented hereafter.

Based on the equation of motion of a conventional system, the derived equations lead to the Equation 52:

$$\text{Equation 52} \quad f_R(q_r, \dot{q}_r, t) = -\{\phi_r\}^T [M_{aa}] [T_G] \{\ddot{u}_b\} - m_r \frac{\{\phi_r\}^T}{\{\phi_r\}^T \{\phi_r\}} (\{\ddot{u}_a\} - [T_G] \{\ddot{u}_b\})$$

The determination of the non-linear modal restoring force f_R requires the modal mass m_r and the mode shape vector $\{\phi_r\}$ of the mode under consideration, which are identified for the underlying linear system from a modal survey test. The modal acceleration $\{\ddot{q}\}$ is determined from the physical accelerations $\{\ddot{u}\}$ by using the pseudo inverse of the mode shape matrix. The acceleration response of the unconstrained DoFs $\{\ddot{u}_a\}$ and the base acceleration $\{\ddot{u}_b\}$ are obtained from measurement. The partitions $[M_{aa}]$, $[K_{aa}]$, and $[K_{ab}]$ are obtained from the FE model of the structure. It should be mentioned, however, that the availability of the stiffness matrix is not a prerequisite, because the so-called geometry matrix $[T_G]$ can also be derived from geometrical considerations in case of statically determined boundary conditions.

The analytical system matrices must be compatible with the measured mode shape vector. This requires a reduction of the analytical system matrices to the measurement degrees of freedom which can be achieved by a FEM Guyan reduction.

It should be mentioned that, in principle, multi-point excitation with appropriated forces are required to apply the restoring force method to multi-DoF systems. When considering base driven systems, the excitation forces applied to different points of the structure is mainly determined by the mass distribution. This would prevent the successful application of the method to higher modes with complex deformation. Instead, it must be expected that the method can only be applied to some fundamental modes which can be excited with enforced motion at the base.

7.4.1.3.4 Methods based on dedicated Excitation Signals

Real structures are seldom completely linear. This can be proved by the violation of the principles of superposition and reciprocity. Nonetheless, many of them closely approximate linear behaviour so that most of the theory developed for modal analysis relies on linear behaviour.

The methods presented here are based on dedicated excitation force signals to detect non-linearities or to avoid the non-linearities directly in the experiment, which requires shaker excitation or base excitation on a shaking table.

Weak non-linearities in practical structures can be easily highlighted by developing on measurements different degree of amplitude control of the vibration levels. Non-linearities are characterised by FRF distortion increasing with increasing force level. But classical experimental modal analysis could not lie with such deformed FRFs because modal parameters extracted this way will suffer from inaccuracy, especially for the damping and the modal mass due to the distortion of the response curve.

The same kind of problem may occur for piloting with constant response amplitude measurements (notching). In such case, the response non-linearity is kept constant but the FRFs frequency peak of each level yield to slightly different results.

Each level considered separately lead to different linear FRF which are well suited for experimental modal analysis. The constant input level and constant output level testing is thus considered for:

- **Sinusoidal Excitation with constant Input Level**

Stepped-sine excitations are a standard for the investigation of non-linear behaviour of structures leading to clear distortion characteristic. The quite constant level sinusoidal excitation allows concentrating energy on a single spectral line to obtain large displacement amplitudes.

Constant output levels can only be obtained with feedback loop controller. Otherwise, the power amplifiers of electro-dynamic shakers are driven with voltage signals of constant amplitude which leads to force input level reduction around the resonance. This natural force level reduction is salutary to avoid risk of damaging the structure under test, especially in cases of lightly damped structures and powerful shakers.

Swept-sine test with a slow sweep rate is also appropriate for the characterization of non-linearities but care has to be taken by transforming the transient data into spectra to avoid averaging non-linear effects.

- **Sinusoidal Excitation with constant Response Level**

Steady-state non-linear response can express non-linear equivalent stiffness and damping properties as functions of the displacement amplitude. If the output is maintained at a constant level in a narrow frequency band around the mode of interest, the non-linearity will also be maintained at a constant level, at least approximately. In such a way non-linear FRF can be obtained which is closest to linear. Thus series of “linear” FRFs can be produced for different

constant output levels by means of stepped-sine testing of spanned amplitude range. Experimental modal analysis tools can be applied to extract the modal parameters and can be plotted as functions of the physical vibration amplitude of the measurement point. This is a so-called linearity plot which can be used to characterize the non-linearity.

Such linearity plot example is given in the Figure 7-17 showing modal stiffness and the modal damping over the modal vibration amplitude. A significant non-linear behaviour shows the modal stiffness reduction and the modal damping linear increasing.

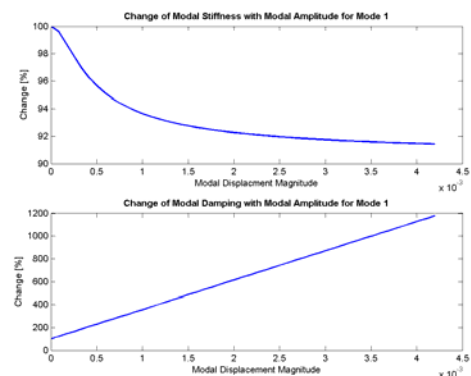
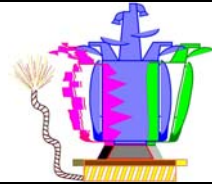


Figure 7-17: Change of modal stiffness and modal damping over modal displacement amplitude

The advantage of the constant response level testing is that the structure under test is prevented from being damaged. One of the drawbacks is that it is only applicable in a narrow frequency band around the resonance of an isolated non-linear mode.



- **Random Excitation**

The total energy introduced into the structure is spread over a broad frequency range. Consequently, the vibration amplitudes will be lower as with sinusoidal excitation and the non-linearities will be activated much less. Therefore, it is less well suited for generating distorted non-linear FRFs. Random excitation with constant power spectrum lead to rather linear FRFs, even in case of large power spectral densities, like for an averaging process which smooth the non-linear effects and makes them difficult to interpret for characterization of non-linearities.

Although the FRFs at different constant input force power spectral densities yields linear looking FRFs, a frequency shift of some resonance peaks may nonetheless be observed but is not adequate for the characterization of non-linearities. Nevertheless, FRFs can be produced quite fast using random excitation, since all frequencies in the frequency range of interest are excited simultaneously instead of exciting each frequency separately as it is done in a stepped-sine test.

- **Multi-Sine Excitation**

Such excitation, in contrast to the random excitation (which contains frequency components at all spectral lines), is designed to exclude particular frequencies from the excitation signal.

If the system excited by a multi-sine excitation force signal is linear, the response due to the excitation with a small number of discrete harmonic frequencies will also be a spectrum which is populated at exactly the same frequencies than the excitation spectrum. This can be concluded from the principle of superposition which is fulfilled in case of linear systems. If the system under test is non-linear, different frequency lines than those contained in the excitation signal will appear in the response and the non-linearity may be quantified by evaluating the amplitudes of the different spectral lines.

The multi-sine excitation is a fast non-linear detection technique particularly suited to characterise polynomial types of non-linearities. Special types of multi-sine excitation signals are defined to characterise odd order and even order non-linearities.

The disadvantage is that sophisticated equipment is required to produce the excitation signal.

7.4.2 An approach to non-linear experimental modal analysis

Present test and analysis methods are still based on the assumption of linear structural behaviour. The FRF resonance peak variations observed in the case of non-linear structural behaviour are not reflected by non-linear analytical modelling except using equivalent linear modelling adapted to a specific load level.

This approach can be tolerated since experience shows that in many cases the non-linear structural behaviour is not too strong so that the experimental modal data still lie within the natural scatter generated by other sources of test data variability like fabrication tolerances, multiple assembly or test reproducibility.

The studied approach aims to characterise the non-linear behaviour magnitude to determine if linear modelling is still applicable. If this is not the case, using linear code for experimental modal analysis will lead to important scatter. Thus extension of the UKL software ISSPA-FITKOR (called ISSPA_NL) have been developed to identify non-linear modal parameters in addition to the traditional modal parameters related to the underlying linear system.

The classical experimental modal analysis (EMA) are based on fitting an analytical modal model with eigenfrequencies, damping ratios, modal masses, and mode shape vectors to experimental response data.

The identification of the linear modal parameters in ISSPA_FITKOR is based on the equation for the linear frequency response:

$$\text{Equation 53} \quad \{u(\Omega)\} = \sum_r \frac{\{\phi_r\}\{\phi_r\}^T}{m_r} \frac{1}{\Omega^2 - \omega_r^2 + j2\xi_r\omega_r\Omega} \{f(\Omega)\} \quad (r = 1, \dots, nr = \text{no. of modes})$$

This equation describes the superposition of linear modal responses with $\{\phi\}$ being the mode shape vector, m is the modal mass, ω is the circular eigenfrequency, ξ is the damping ratio, and Ω is the excitation frequency. The extension to non-linear modal analysis in ISSPA_NL consists of two steps:

1. Amplitude dependent damping ratios and eigenfrequencies are introduced only for modes which exhibit non-linear behaviour. In this case the response equation is extended as follows:

$$\text{Equation 54} \quad \{u(\Omega)\} = \sum_r \frac{\{\phi_r\}\{\phi_r\}^T}{m_r} \frac{1}{\Omega^2 - \omega_r^2(\hat{u}_a) + j2\xi_r(\hat{u})\omega_r(\hat{u}_a)\Omega} \{f(\Omega)\} \quad \text{with}$$

$$\text{Equation 55} \quad \omega_r^2(\hat{u}) = \omega_{r,lin}^2 \left(1 + a_k \left(\frac{\hat{u}_a}{\hat{u}_{max}} \right)^{q_k} \right) \quad \text{and} \quad \text{Equation 56} \quad \xi_r(\hat{u}) = \xi_{r,lin} \left(1 + a_c \left(\frac{\hat{u}_a}{\hat{u}_{max}} \right)^{q_d} \left(\frac{\Omega}{\omega_r} \right)^{q_d p_d} \right)$$

$\omega_{r,lin}$, $\xi_{r,lin}$, m_r and $\{\phi_r\}$ represent the modal parameters extracted as usual from the measured response \hat{u} by classical EMA techniques. The Equation 54 exhibits more or less pronounced deviations from the measured response depending on the magnitude of the non-linearity.

The eigenfrequency and the damping ratio are functions of the measured amplitude \hat{u}_a which represents a RMS response calculated from the measured response vector $\{\hat{u}\}$:

$$\text{Equation 57} \quad \hat{u}_a = \left| \{\hat{u}(\Omega)\} \right| = \sqrt{\{\hat{u}(\Omega)\}^T \{\hat{u}(\Omega)\}}$$

The exponents q_k , q_d and p_d must be adjusted for different types of non-linearities. Some default values are given in RD 6 depending on the type of non-linearity.

The coefficients a_k and a_d govern respectively the magnitude of the frequency and the damping.

Even though the additional non-linear correction parameters do not have a direct physical interpretation, they can nonetheless be used to improve the identification process of the underlying linear system. These non-linear modal parameters should rather be considered as penalty parameters which shall account for non-linear distortions so that the traditional linear modal parameters can be identified with improved accuracy.

This non-linearity extension has been implemented in the software code ISSPA_NL based on ISSPA code, which is only suited to modify the synthesized response in close

vicinity of a non-linear response peak measured at a single load level. It does not permit to modify the underlying linear modal model if the non-linearity becomes too large.

2. At least three load levels have to be used for identifying equivalent linear modal data with classical EMA techniques. The non-linear correction can be applied at each load level. ISSPA_NL is used to interpolate or extrapolate the modal data to another not passed levels.

The interpolation starts from classical linear modal analysis data extracted by ISSPA_FITKOR from experimental FRF measured at three load levels.

Figure 7-18 shows the interpolation and extrapolation scheme where the three data points for the variable Z on the vertical axis stand for any of the extracted natural frequencies, modal displacements, modal damping values or modal masses.

The variable A stands for the load level used during the test. A distinction is made between:

- interpolation levels $A_{int,i}$ ($i=1, 2 \dots$) with the corresponding variable $Z_{int,i}$ located between levels A_1 and A_3 ($A_1 \leq A_{int,i} \leq A_3$) obtained by quadratic interpolation.
- extrapolation levels $A_{low,i}$ ($A_{up,i}$) with the corresponding variable $Z_{low,i}$ ($Z_{up,i}$) located below level A_1 (beyond level A_3) obtained by linear extrapolation wrt the tangents in A_1 (A_3)

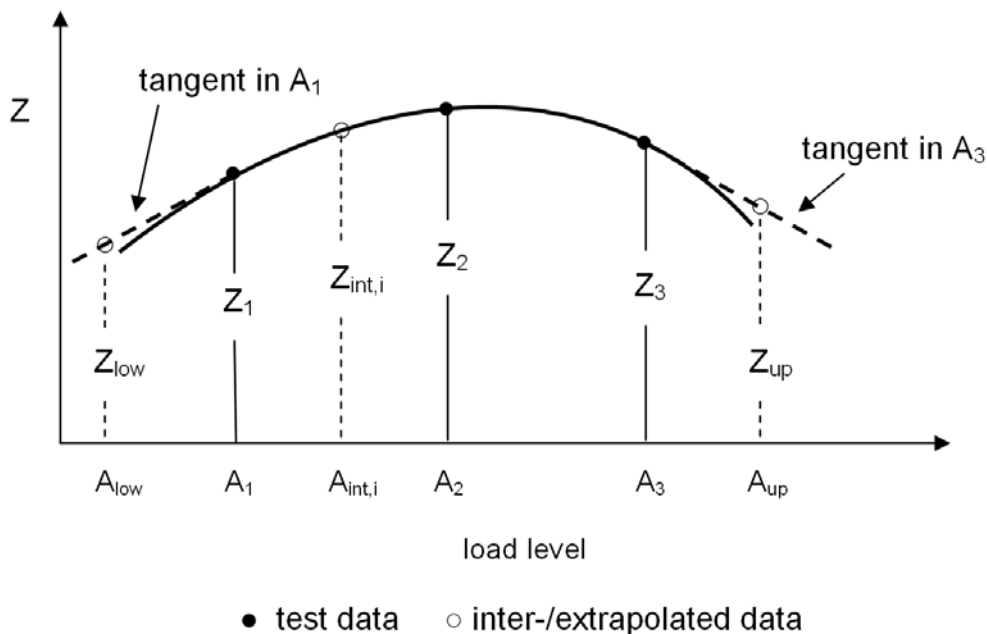


Figure 7-18: Interpolation scheme

The extrapolation must be bounded in a validity domain ($A_{low} \leq A_{low,i} \leq A_1$ and $A_3 \leq A_{up,i} \leq A_{up}$) where the bounds A_{low} and A_{up} are specified by the user, e.g. 10% of the measured levels.

See RD 6 for more details about the interpolation and extrapolation formulation.

8 IMPLEMENTATION IN TOOLS

To facilitate the test preparation and during test exploitations, the more mature methodologies have been implemented into tools in a DynaWorks environment. All the tools are directly accessible and executable from a Test view DynaWorks window in the “Dynamited” menu, as shown in the Figure 8-1.

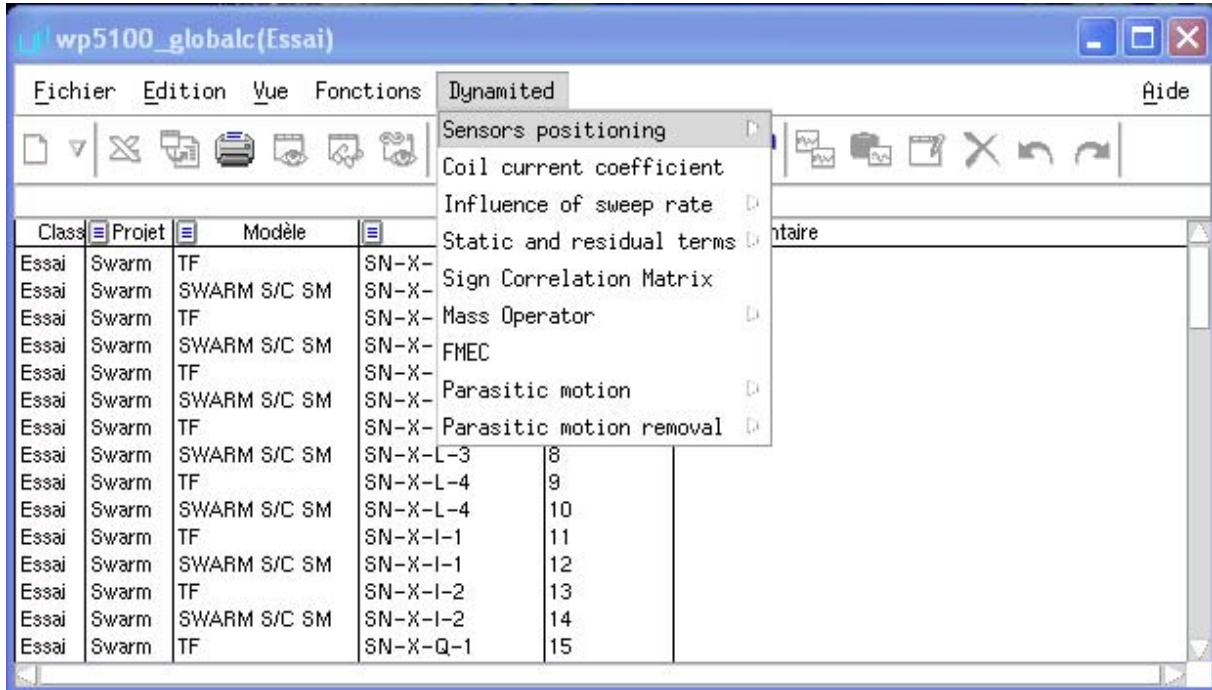


Figure 8-1: Overview of the “Dynamited” menu and functions

8.1 PRE TEST TOOLS

We present here the pre test methodologies implemented into tools and fully described in RD 11.

8.1.1 Coil current determination

The aim of this tool is to calculate before the test the right Newton per Ampere coefficient to use to recover the base load force with the coil current intensity.

The tool is executed on the blank tests and it is necessary to fulfil the three parameters: rigid mass in motion, number of pilot sensors to take into account and number of coil current measurements to take into account as shown in the Figure 8-2.

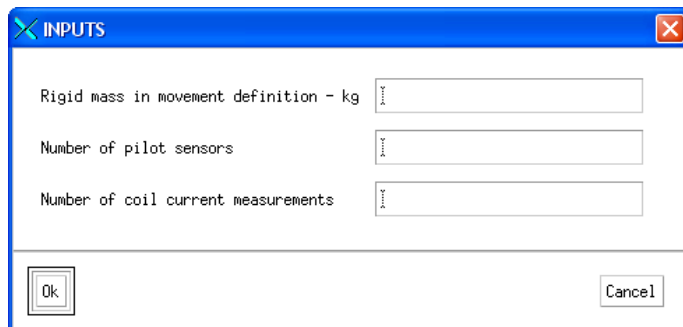


Figure 8-2: Overview of the coil current determination tool

After fulfilment of the pilot sensor names and coil current channel names, the tool outputs the frequency dependant coil current coefficient, as shown in Figure 8-3.

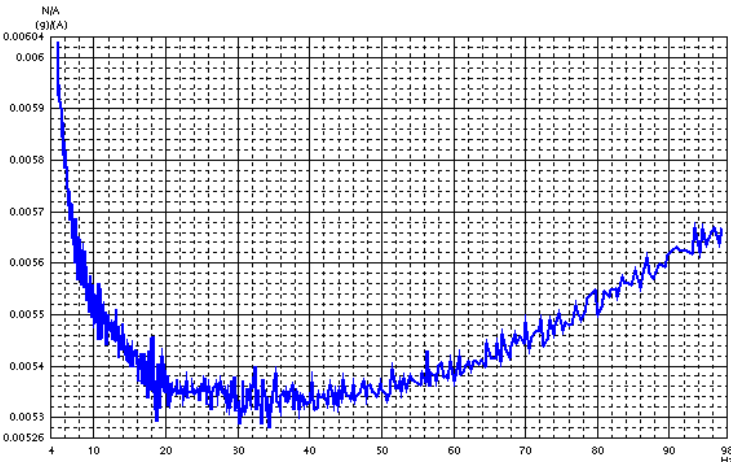


Figure 8-3: Coil current coefficient overview

8.1.2 Estimation of suitable sine sweep rate for test preparation on piloting aspects

The aim of this tool is to define, for an expected accuracy on Amplitude, Frequency and Damping, the suitable sine sweep rate for one mode or for the whole modes of a selected test.

The tool is executed on the test of interest and it is necessary to fulfil the piloting parameters (mode frequency, mode amplitude factor and sweep direction) and the desired accuracy for Amplitude, Frequency and Damping, as shown in Figure 8-4.

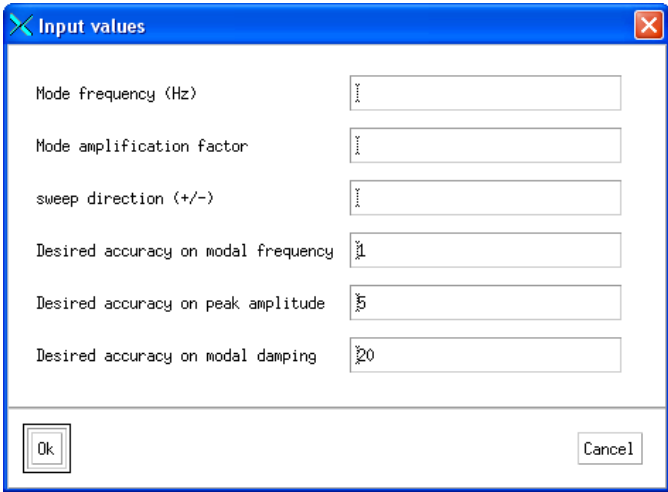


Figure 8-4: Overview of the sweep rate estimation tool

The tool outputs the maximum sweep rate for each accuracy goals, as shown in the Figure 8-5.

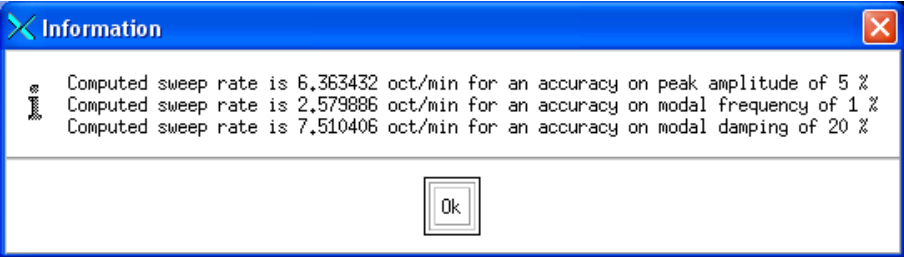
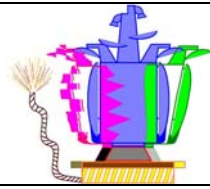


Figure 8-5: Maximum sweep rate for each accuracy goals



8.1.3 Sensor positioning for mode observability

The aim of this function is to determine the best sensor position wrt the mode distinguishability. This function allows also building an observability status of the modes.

It is necessary to import the candidates file (“don” format, see RD 11 for a detailed description), giving correspondence between NASTRAN dofs and measurement point names and the mode matrix in NASTRAN punch format

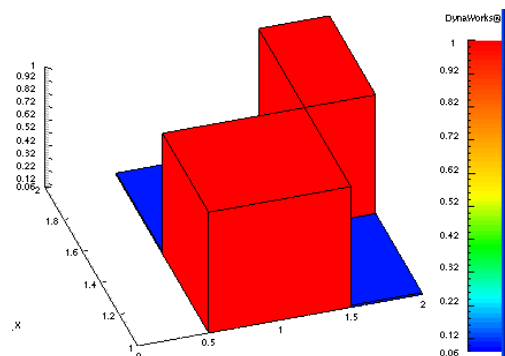
The tool is then executed. The user must choose the optimisation method between:

- Systematic (for a limited number of combination but leading to the best combination)
- Univariate (alternative approach for huge models, leading to a good combination but not necessarily the best) where it is necessary to define the maximum number of iteration and the convergence criterion

The tool calculates:

- the best dof for each sensor within the defined candidates
- the MAC matrix computed on the optimized DOFs

	Sensor	Grid-Dir
1	cap1	4-1
2	cap2	8-1



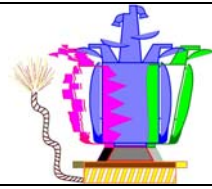
- the observability criterion (the ratio between the maximum component of the mode reduced to the optimized DOFs and the maximum component of the mode reduced to all the candidates DOFs, for each mode)

1	1	1
2	2	0.9

8.1.4 Sign correlation matrix


This tool aims at computing the estimation of sensor orientation for both prediction and test data; a correlation between both values is performed to check sensor orientation validity versus prediction. Three cases can occur for each sensor:

- difference between estimated angles is within a given tolerance: the coefficient associated to the sensor is 1
- difference between estimated angles is 180° (within tolerance): the coefficient affected is -1
- difference between estimated angles is out of tolerance: the associated coefficient is 0



The user must fulfil the input parameters including:

- the test predictions along the three axes,
- the available test data FRF,
- the type of data to consider
- the tolerance angle



The tool outputs are a synthesis table giving the correlation coefficient for each sensor.

PointMesure	prediction name	pred. static term	test name	test static term	pred. angle	test angle	coeff
64X	Sine X	0.999996	SN-Z-L-3	1.13793e-2	0.158259	89.348	1
92Z	Sine Z	0.980404	SN-Z-L-3	1.02503	11.3615	0	1
120Y	Sine Y	0.999891	SN-Z-L-3	0.135963	0.845573	82.1857	1
121X	Sine X	0.999996	SN-Z-L-3	-2.58461e-2	0.155766	91.481	1
121Y	Sine Y	0.999879	SN-Z-L-3	-0.145021	0.890434	98.3385	1
121Z	Sine Z	0.999647	SN-Z-L-3	-0.978539	1.52341	168.108	-1
123X	Sine X	0.999999	SN-Z-L-3	9.94412e-2	9.89117e-2	84.293	1
170X	Sine X	0.999991	SN-Z-L-3	-0.397252	0.242283	113.406	1
170Y	Sine Y	0.806992	SN-Z-L-3	-0.6033	36.0024	127.107	1
170Z	Sine Z	0.806898	SN-Z-L-3	-0.863314	36.0116	149.691	0

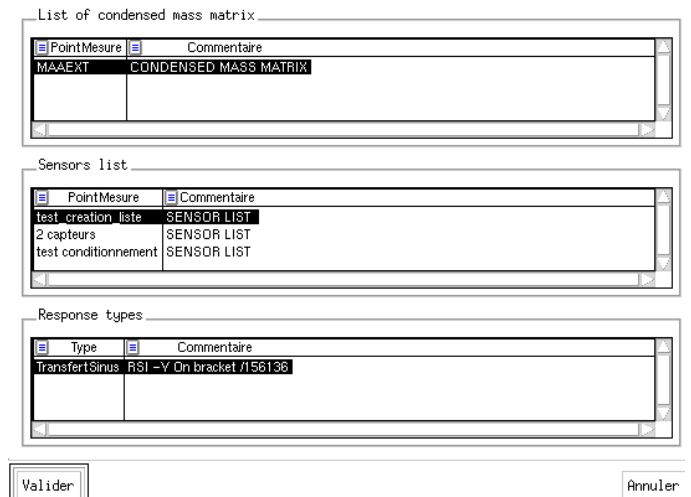
8.1.5 Mass operator tool

This mass operator tool aims at computing the condensed mass and stiffness matrices on a selected list of sensors and the load restitution.

It is necessary to import the data (sensor/GRID dofs correspondence as “.don” format, the condensed matrix partitioning vector as NASTRAN DMIG format and the condensed mass and stiffness matrices as OUTPUT4 format).

Once these operations are done, the user must define a set of valid sensor to calculate the load restitution.

Finally, the load restitution is calculated by selecting the mass matrix to consider, the set of valid sensor to consider and the type of data to be used.

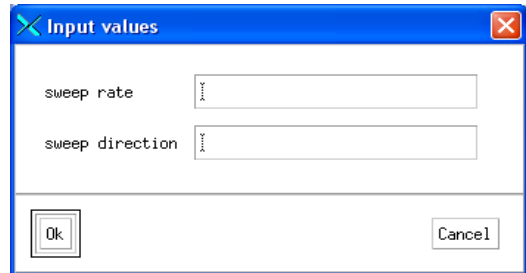


8.2 POST TEST TOOLS

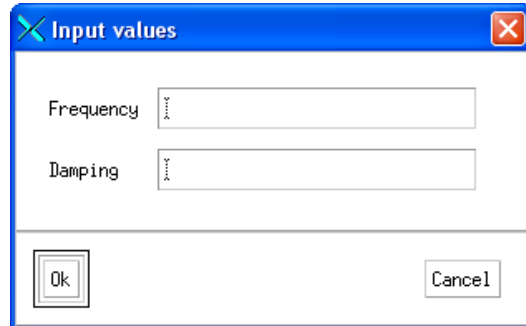
8.2.1 Estimation of sine sweep rate effects

The aim of this tool is to give for a given sine sweep rate the error introduced during the run on the modal parameters: Amplitude, Frequency and Damping.

It is just necessary to select a test and define the sweep rate and the sweep direction (increasing or decreasing).



The correction is calculated on the FRF. If no mode is linked to the test, the mode eigenfrequency and the damping ratio must be defined.

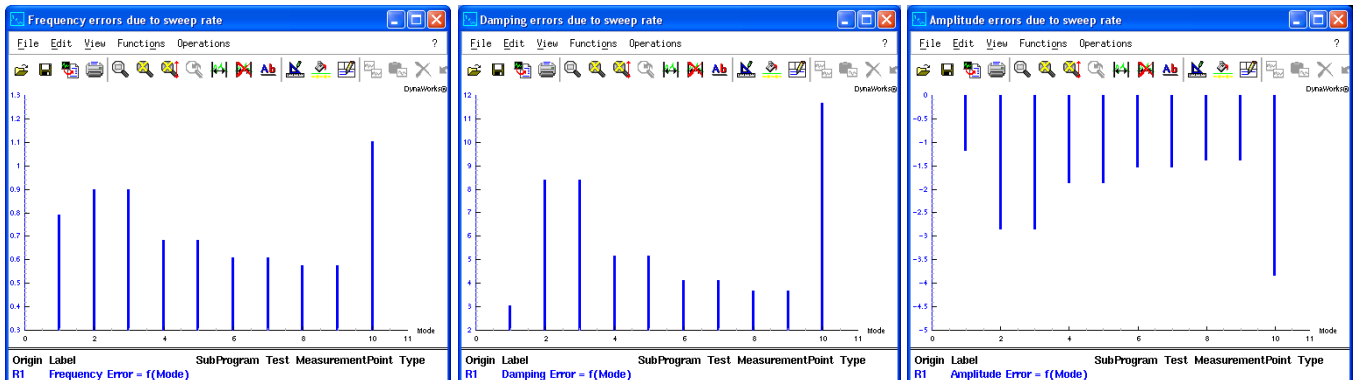


Finally the tool computes the errors and the corrected parameters:

	Mode	Frequency Error	Amplitude Error	Damping Error
1	1	1.42957	-8.60577	28.6395
2	2	0.897158	-2.86025	8.39375
3	3	0.897158	-2.86025	8.39375
4	4	0.681162	-1.85934	5.13162
5	5	0.681162	-1.85934	5.13162
6	6	0.607297	-1.53217	4.0935
7	7	0.607297	-1.53217	4.0935
8	8	0.574679	-1.39173	3.65389
9	9	0.574679	-1.39173	3.65389
10	10	1.10201	-3.83144	11.6469

	Title	1	2	3	4	5	6	7	8	9
1	Mode	1	2	3	4	5	6	7	8	9
2	Cor. freq	27.9438	35.2434	35.2434	47.2899	47.2899	53.4627	53.4627	56.7141	56.7141
3	Cor. damping	1.80095	2.16788	2.16788	2.10263	2.10263	2.08187	2.08187	2.07308	2.07308
4	IdResp 255	7.24578	13.4329	13.4329	11.5958	11.5958	7.69813	7.69813	3.56936	3.56936
5	IdResp 256	7.22548	9.69302	9.69302	3.21129	3.21129	10.4402	10.4402	5.2272	5.2272
6	IdResp 257	7.22192	0.743564	0.743564	11.7854	11.7854	1.72148	1.72148	4.23982	4.23982
7	IdResp 258	7.22513	9.67864	9.67864	2.78602	2.78602	10.2021	10.2021	5.40682	5.40682
8	IdResp 259	7.22686	13.4164	13.4164	11.5137	11.5137	7.34467	7.34467	2.18238	2.18238
9	IdResp 260	0.913942	0.971397	0.971397	0.981407	0.981407	0.984678	0.984678	0.986083	0.986083
10	IdResp 261	0.913942	0.971397	0.971397	0.981407	0.981407	0.984678	0.984678	0.986083	0.986083

This can be displayed as errors bars (Frequency, Damping, and Amplitude):



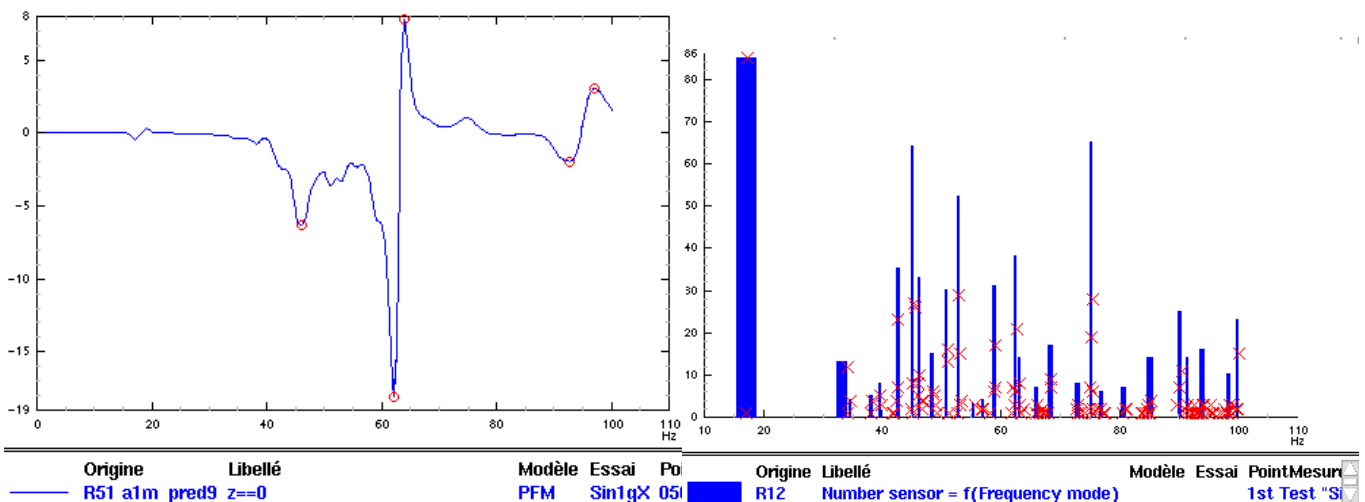
8.2.2 Fast modal extraction and correlation

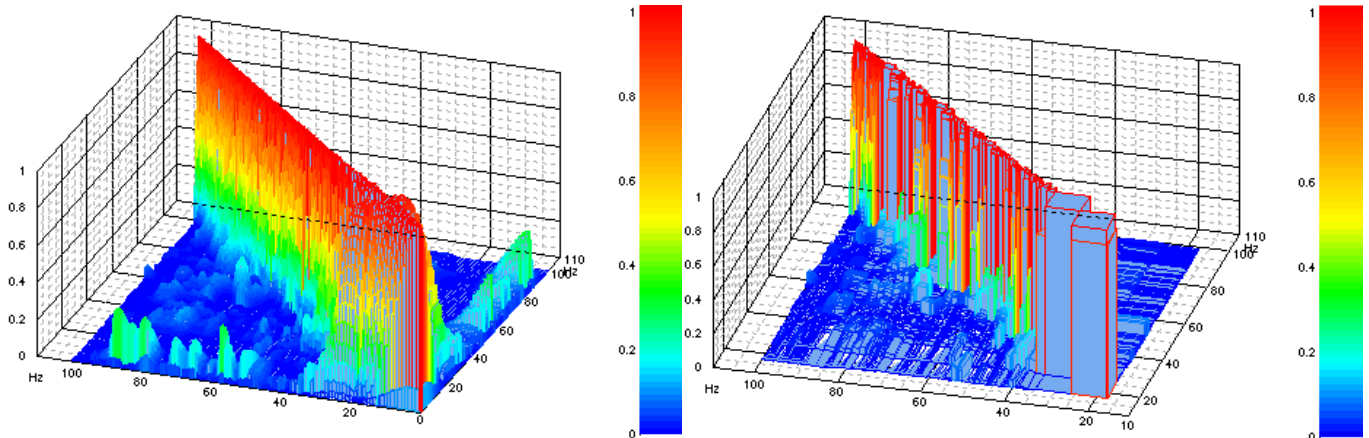
The Fast Modal Extraction and correlation tool aims to provide quick correlation between two tests.

The user must define the input parameters (including the definition of the two tests, the filters parameters, the definition of the data to save and the peaks and mode extraction parameters):

----> FIRST TEST PARAMETERS DEFINITION *		Analysis prediction		----> SECOND TEST PARAMETERS DEFINITION *		Test measurement	
1st test base type *		WORK base		2nd test base type *		WORK base	
1st test base name				2nd test base name			
1st test Program name				2nd test Program name			
1st test SubProgram name				2nd test SubProgram name			
1st Test name *				2nd Test name *			
1st test response class *				2nd test response class *			
1st test response type *				2nd test response type *			
----> FILTERS PARAMETERS DEFINITION		***** Write nothing here *****					
Use List for sensor selection *		Yes		Use Mass Matrix for Assurance Criterion calculation *		Yes	
Filter on mode selection *		X		Filter on mode shape building *		X	
----> SAVE DATA PARAMETERS DEFINITION		***** Write nothing here *****					
Save result data ? *		Yes		Test result save base type *		WORK base	
Test result save base name				Test Save IdTest number *		0	
----> FAST MODAL AND CORRELATION PARAMETERS		***** Write nothing here *****					
----> LOCAL AND GLOBAL CURVES PEAKS MAXIMUM EXTRACTION PARAMETERS		***** Write nothing here *****					
Minimum threshold considering a peak		1,000		Bandwidth percentage for local maximum determination - alpha		0,040	
Number of curve maximum RELATIVE threshold subdivision for maximum extraction		10		Number of curve ABSOLUTE threshold subdivision for maximum extraction >= 1		1	
----> MODE EXTRACTION		***** Write nothing here *****					
Mode extraction: frequency gathering percentage bandwidth - beta		0,020		Minimum number of sensor defining a mode		2	
<input type="button" value="Valider"/>		<input type="button" value="Annuler"/>					

The tool outputs the extracted peaks, their number, the mode extracted and the correlation between the two tests through the two indicators FrImAC and ImMAC:





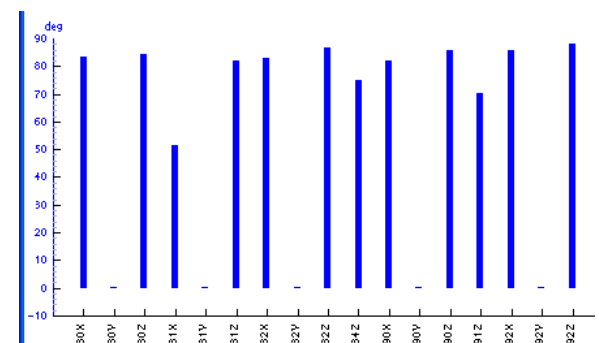
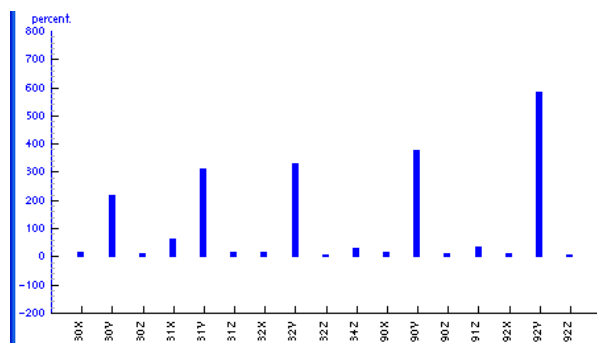
8.2.3 Static terms, residual modes and sensor orientation

This tool is composed of three functions allowing completing the transfer function database by:

- The “static term”
It is necessary to define the frequency range and the calculation is performed by a dual approach (parabolic or pseudo mode). The tool outputs the static term for each dof and the associated error.
- the “residual mode”
The tool outputs for each dof, the computed eigenfrequency and the residual mode component
- the “sensor orientation” estimation
The user must define the excitation axis and the static term tolerance. It outputs the orientation angle error (left) and estimation (right).

	id_resp	Meas. Pt	static term	error (%)
1	189	1X	-5.36902e-4	100000
2	190	1Y	1.00653	100000
3	191	1Z	-9.92918e-4	100000
4	192	2X	1.45738e-4	100000
5	193	2Y	1.00473	100000
6	194	2Z	-1.35435e-3	100000
7	195	3X	-5.56812e-4	100000
8	196	3Y	1.00719	100000
9	197	3Z	-5.35739e-3	100000
10	198	4Z	-8.78254e-3	100000
11	199	30X	-1.44015e-3	100000
12	200	30Y	1.00562	100000
13	201	30Z	1.3599e-2	100000
14	202	31X	-6.79039e-3	100000

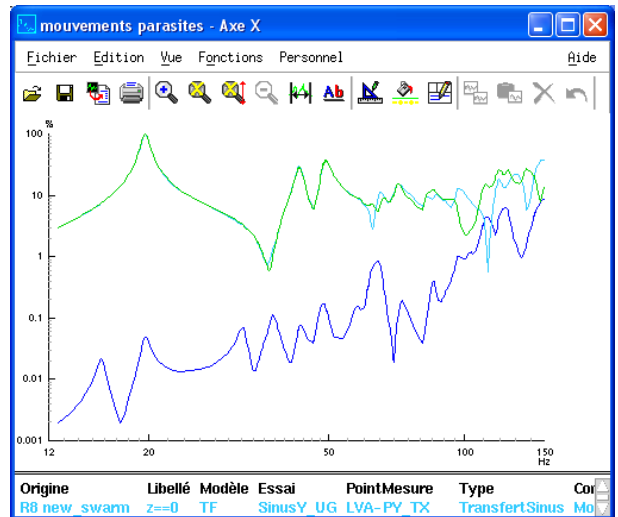
	Measurement Point	Freq.	Xk
1	1X	141.052	1.71404e-2
2	1Y	134.656	2.49424e-2
3	1Z	109.504	0.246781
4	2X	139.605	1.64456e-2
5	2Y	144.002	6.16643e-2
6	2Z	108.7	9.02163e-2
7	3X	138.38	1.82009e-2
8	3Y	134.719	2.69772e-2
9	3Z	89.239	-0.106495
10	4Z	114.475	-0.188441



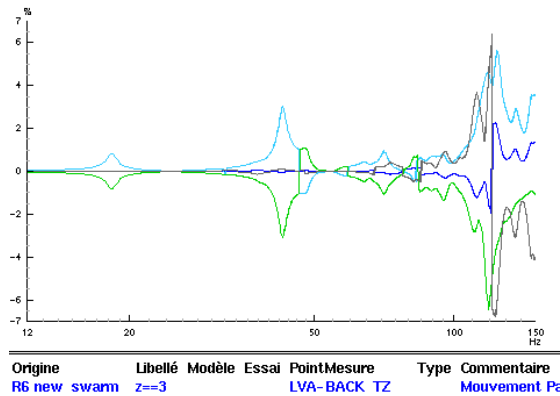
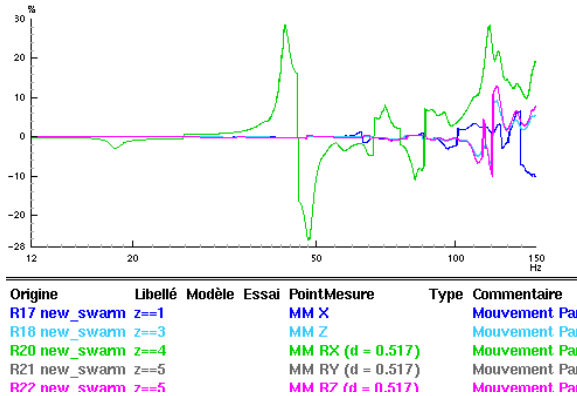
8.2.4 Parasitic motion

This tool is composed of three functions to estimate the parasitic motion:

- The “first estimation of parasitic motion”
The user must define the excitation axis, the accelerometers in the excitation direction and crossed directions. The tool outputs the parasitic motion error in each axis.

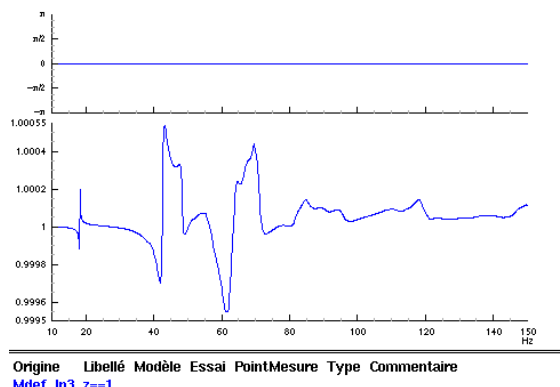
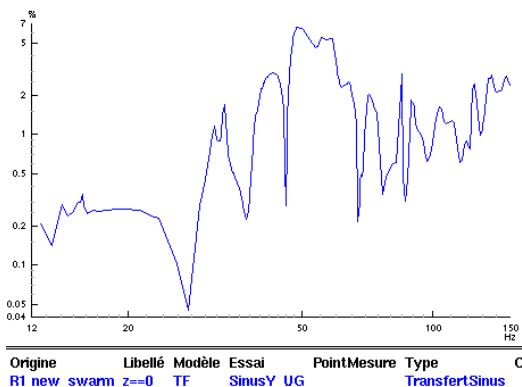


- the “parasitic motion component”
The user must define the excitation axis and for each pilot (in the excitation direction) and co-pilot (in the crossed direction) their exact position.
The tool outputs the rigid body parasitic motion (left) and the base deformation in each axis (right).



The “effect on the specimen”

The user must define the excitation axis, the pilots and their position and the dofs to estimate effect. The tool outputs the parasitic motion contribution (left) and the base deformation contribution (right).



8.2.5 Motion of the specimen without parasitic motion

The parasitic motion tool aims to correct calculated FRF to remove the parasitic motion effect and recover the perfectly guided specimen FRF.

As shown in §7.3.2.4, the application of the methodology shows limitations due to numerical precision and quality of the test data. Nevertheless, we present hereafter the main steps of the tools and refer to the RD 11 for a complete description.

This tool is composed of four parts that have to be performed successively:

- data preparation: this aims to prepare and check the test data before computation of the missing FRF.
- computation of missing FRF: this step aims to complete the data by the dynamic masses (ratio between effort in the nominal direction and the Pilot) and the FRF of the parasitic DOFs (ratio between the parasitic acceleration and the base effort in the relevant direction).
- RTMVI export for modal identification. This function aims at preparing the data in purpose of the modal identification task of the perturbed frfs.
- computation of corrected frfs. After modal identification of the imperfectly guided specimen, the final step is to compute the frfs of the perfectly guided specimen from these data.

8.2.6 ISSPA

The ISSPA tool is fully described in RD 4. The tool code application methodology is fully described in RD 11.

We mainly focus here on the new ISSPA_NL development and methodology.

The software ISSPA-nl is a postprocessor to the standard (linear) experimental modal analysis software ISSPA, which permits to extract modal data from experimental FRF measured during test. The tool allows applying two different methods in the case that the experimental response data reveal non-linear behaviour of the test structure:

- **Method A:** either to fit a non-linear analytical frequency response function to an experimental curve exhibiting non-linear distortions like that depicted in Figure 8-6 or

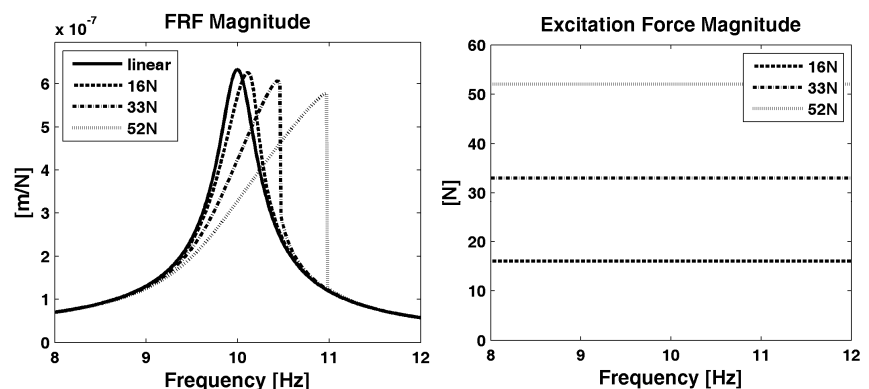
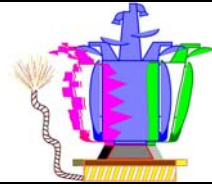


Figure 8-6 : FRF obtained from constant excitation force levels



- **Method B:** to extrapolate or interpolate modal data obtained from three different excitation force levels with notching like that depicted in Figure 8-7 to other than the measured load levels.

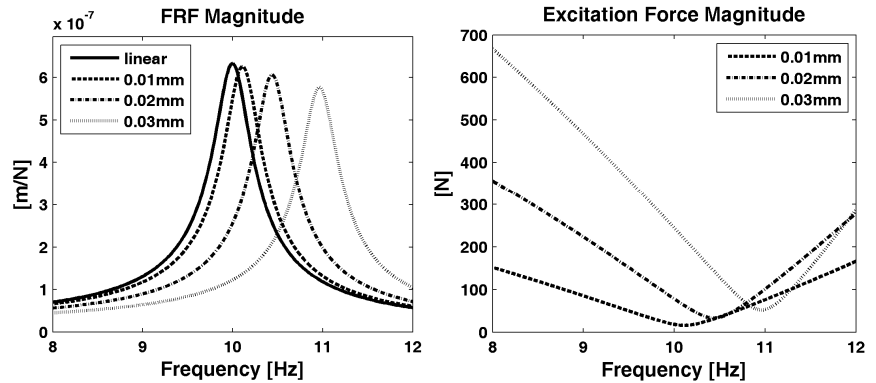


Figure 8-7 : FRF obtained from constant response levels

The process consists of the three following steps:

1. Detect any non linear behaviour by a visual analysis of the experimental FRF thank to the methods database presented in §7.4.1. In case of non-linear behaviour the user must determine the method to apply:
 - If the excitation forces were controlled to be constant at different levels the frequency responses exhibit non-linear distortions in which case method A may be applied.
 - If the absolute response in the range of selected resonance ranges was controlled to be constant (notching) the frequency responses do not exhibit significant non-linear distortions but a shift of the peaks and the magnitudes of the FRF depending on the absolute response levels. In this case method B may be applied.

This step is finalized by selecting the frequency ranges and load levels of each test run exhibiting non-linear structural behaviour.
2. Apply any standard linear EMA software (like ISSPA) to extract modal parameters (natural frequencies, mode shapes, modal damping and (pseudo) modal masses) from experimental FRF. The output consists of sets of modal data extracted from the frequency ranges and load levels selected in step 1. The modal data are visualized as a function of the load levels.
3. The last step consists of applying the postprocessor software ISSPA_nl.
 - **Method A:** the input consists of a modal data set extracted from a selected frequency range with some additional parameters characterizing the non-linearity type. The tool calculates non-linear analytical FRF fitted to the experimental curves exhibiting non-linear distortions.
 - **Method B:** the input consists of three modal data sets related to three different load levels extracted from a selected frequency range. The load levels are determined from the pilot notch depth. The tool calculates the three quasi linear analytical FRF fitted to the three experimental curves related to the measured response levels. ISSPA_NL calculates additional curves at any other load level within or outside the measured load level which are synthesized from interpolated or extrapolated modal data.

9 GUIDELINES

Following the developed methodologies and tools, general guidelines have been written to summarise all procedures and best practices that should be applied in order to have a satisfying preparation and securing of dynamic test.

Thus the guidelines have been split in two parts:

- Pre-test guidelines which aim to improve the test preparation and instrumentation.
The objectives are to anticipate possible difficulties during the test, secure the dynamic test progress and improve the performance during the test thanks to enhanced predictions.
- Post-test guidelines which aims to improve the test data assessment and exploitation.
The objectives are to provide during the test as quick as possible the test data assessment and to apply robust and efficient test data exploitation by completing the synthesised databases and providing a consolidated extrapolation for further level and a sharper understanding of unexpected behaviour.

9.1 PRE TEST GUIDELINES

9.1.1 Instrumentation guidelines

The spacecraft instrumentation may be improved by analysing and proposing the best sensor location and detecting possible difficulties due to a bad instrumentation.

Improving the test preparation consists to propose instrumentation in equation with the test objectives. The instrumentation improvement can be achieved by determining the best location for each sensor to better distinguish the mode shape of interest with a correct observability. Moreover, the measurement quality may be improved by determining error due to uncertainty parameters by a stochastic approach.

Improving the instrumentation location consists in considering the three following points:

- Determine sensors whose location may be changed from the other ones where location is fixed,
- Determine the test objective mode shapes to identify
- Improve the sensor location wrt the mode distinguishability and verify the observability of each mode of interest thanks to the sensor positioning tool.

But instrumentation may also be improved thanks to stochastic analysis as it is well fitted to determine on the whole sensors instrumentation the sensitivity wrt the different types of errors. The recommendation is thus to evaluate general test uncertainty impact on the FEM spacecraft and:

- determine the average error on amplitude and frequency due to test uncertainties
- identify sensors with high dispersion on their response.

Nowadays project time and cost budget doesn't allow to apply systematically stochastic analysis as it calls for time and a large amount of calculation runs. Thus it can be at least enough to consider the results and conclusions presented in §6.2 which are detailed in RD 6.

Finally, following the previous conclusions, some recommendations can be highlighted for instrumentation concerning special precautions to place some sensors at a precise location or highlight the possible difficulties that could appear in test due a bad instrumentation on some sensors.

9.1.2 Test preparation guidelines

Some activities can also be done before the test to improve the test preparation. They mainly concern the base load recovery, the Sine sweep rate and the Notching stochastic profile.

The base load recovery is an important topic in test if no dedicated device is available. This could be achieved by two different ways more or less precise.

The more accurate is the recovery with the condensed mass matrix. It is thus necessary to prepare before the test the input data (GRID dof/measurement point equivalence file in “.don” format, the matrix partitioning vector in “punch” format and the mass and stiffness static condensed matrices in “OUTPUT4” format). The six component loads recovery is achieved thanks to the mass operator tool.

The other method consists to use the coil current to extract the base load force in the excitation direction. This method is less accurate but gives the order of magnitude to correlate and give confidence with another method. Such method can be used thanks to the determination of the conversion coefficient (in Newton per Ampere) between the current and the force. This coefficient can be determined thanks to the coil current coefficient tool applied on the shaker calibration blank tests.

In order to prepare the test parameters it is also interesting to define the tests objectives and estimate (for information) the maximum associated sweep rate. It is consequently necessary to clearly define the modal parameters accuracy objectives (Amplitude, Damping and Frequency) to derive the maximum sweep rate for each one thanks to the sweep rate estimation tools.

Finally, important information is provided by the stochastic notching profile for test preparation. In fact this allows providing before the test three major advantages:

- **saving long negotiation time** in test by preparing the launcher authority as well as the customer to the eventuality that the real behaviour deviates slightly from the FEM behaviour (due to the different uncertainties presented in §6.2.6) and anticipate the reflexion of what is acceptable or not in term of input spectrum levels. If the worst input spectrum is agreed before the test, this can save important time and stress in test.
- **Giving confidence** in the notching prediction robustness thank to the probability associated to each mode.
- **Improving efficiency and spacecraft knowledge** as this highlights before the test the system level causes of problem and their reasons which can be easier to analyse than during test.

		Ref : MTF.AIDT.TN.2168 Issue : 1 Rev. : 1 Date : 03/03/2010 Page : 91
--	--	---

9.2 POST TEST GUIDELINES

The objectives of the during-test and post-test procedures are to provide some general guidelines summarising all procedures and best practices to apply during and after a test:

- to provide as quick as possible the test data assessment,
- to apply a robust and efficient test data exploitation,
- to calculate correct transfer functions to provide a robust exploitation for further level,
- To extract modal parameters and correct the FRF to recover the perfectly guided behaviour.

Post test guidelines are base on the pre-existing ASTRIUM test process which has been which has been reconsidered to complete missing points and reconsider non justified steps and to complete the process including the new DYNAMITED methodologies and tools.

Theses guidelines are split into six mains categories (and steps) presented hereafter:

0. Tools preparation guidelines
1. Test data assessment guidelines
2. Test data and Transfer Function exploitation guidelines
3. Test extrapolation to higher level guidelines
4. Run sheet consolidation guidelines
5. Modal extraction & correction and non linear exploitation guidelines

The complete Dynamic Test Check List process is provided in annex in §13. The detailed description of the test process is provided in RD 8. We introduce hereafter the main steps of the process by highlighting particular new points wrt the previous process.

9.2.1 Step 0: Tools preparation guidelines

This first guideline aims to prepare the tools by preparing input files and calculating preliminary data. It is split into 5 tasks (only steps 1, 4 and 5 present news from the pre-existing ASTRIUM process):

1. Update macros input files (Sine, Acoustic, Random). This allows loading of data, parameters and variables necessary for the macros. Nevertheless a particular attention will have to be paid to the definition of the pilot sensor in a **positive normal order** (see RD 8 for more details).
2. Implement run sheet (Sine, Random). This aims to prepare the parameters for data assessment.
3. Frequency band definition (Sine, Acoustic, Random). This aims to define some frequency bands to verify the mode correlation, the evolution from a previous one and the CLA coverage.
4. Coil current coefficient calculation (Sine, Random). This aims to provide the Newton per Ampere coefficient for base load recovery based on coil current thanks to the developed tool.
5. Prepare additional sensors (Sine, Acoustic, Random). This aims to prepare input file for additional sensor calculation by considering new mass operator sensors to recover QSL.

9.2.2 Step 1: Test data assessment guidelines

This second guideline aims to begin the raw test treatment by providing assessment upon the data validity before the data exploitation. It could be split into 9 tasks (only steps 3 to 9 present news from the pre-existing ASTRIUM process):

1. Transfer function calculation (Sine, Acoustic, Random). This aims to calculate the test transfer function for further exploitation and extrapolation to higher level.
2. Global/Fundamental comparison (Sine). This steps aims to identify problem by Global/Fundamental signal comparison.
3. Estimation of static term (Sine, Random). This aims to complete the transfer function database with the FRF extrapolation to the very low frequencies. The output of the “Estimation of static term” tool is a table giving the static term for each measurement point.
4. Sensor orientation estimation (Sine, Random). This aims to estimate the sensors orientation and error.
5. Sign correlation matrix (Sine, Random). The “Sign Correlation” tool aims to validate the instrumentation correlation between the FEM and the specimen for every dof.
6. 1st estimation of parasitic motion (Sine, Random). This aims to provide a first estimation of the parasitic motion thanks to the developed tool.
7. Build condensation set (Sine, Random). This aims to build the largest set of valid sensors which will be used for mass operator condensation and correlation.
8. Parasitic motion component (Sine, Random). This aims to provide a second order estimation of the parasitic motion components thanks to the developed tool.
9. Sweep rate effect (Sine). This aims to estimate the sine sweep rate effect on the frequency, damping and amplitude error of the transfer functions thanks to the developed tool.

Once test data have been assessed, if no problem has been detected, then the post processing can continue in step 2, otherwise, if some real problems are highlighted, it is necessary to do a deep investigation to understand the problem before continuing exploitation which can be achieved in step 5.

9.2.3 Step 2: Test data and transfer function exploitation guidelines

This third guideline aims to exploit the assessed test data and transfer function for further extrapolation by completing the databases. It could be split into 13 tasks (only steps 1, 2, 8 and 9 present news from the pre-existing ASTRIUM process):

1. Mass operator on Test Data (Sine, Random). This aims to calculate the raw base load thanks to the new mass operator tool.
2. Mass operator on Transfer Functions. Identical from (1) but applied on transfer functions.
3. Additional sensor on Test Data (Sine, Acoustic, Random). This aims to exploit the raw test data by adding in the base additional information.

4. Additional sensor on Transfer Functions. Identical from (3) but applied on transfer functions.
5. Max band per frequency range on Test Data (Sine, Acoustic, Random). This aims to calculate the maximum per frequency range of each sensor on the raw test data.
6. Max band per frequency range on Transfer Function Identical from (5) but applied on transfer functions.
7. g_{RMS} calculation (Acoustic, Random). This aims to calculate the achieved RMS levels on all the measurements and compare it to the allowable.
8. Test correlation with FEM (Sine, Random). This aims to provide a correlation between the FEM and the tested specimen to verify the correlation quality which depends directly the base limitation validity as well as the coupled load analysis results.
9. Test correlation with previous run (Sine, Acoustic, Random). This aims to provide a correlation between the previous run and the actual run to verify the tested specimen evolution between the two runs and check that no major problem is met.
10. Extrapolation Sine to Random (Random). This aims to multiply the calculated transfer functions by an input random spectrum to calculate the sensor responses under this spectrum.
11. Comparison Test Data / Limitation (Sine, Acoustic, Random). This aims to valuate the achieved test responses wrt the corresponding allowables by curve comparison.
12. Comparison Test Transfer functions / FEM (Sine, Random). This aims to provide an exhaustive correlation between the FEM and the tested specimen thank to the transfer function comparison.
13. Comparison Test Transfer functions / Previous run TF (Sine, Acoustic, Random). This aims to provide an exhaustive comparison between the actual test and the previous test.

Once the raw test data and transfer functions have been exploited, if it is not necessary to extrapolate to higher level then the post-processing can continue in step 5, otherwise it continues by steps 3, 4 and 5.

9.2.4 Step 3: Test extrapolation to higher level guidelines

This fourth guideline aims to provide a general path to extrapolate to higher level run. None step of this guideline present news from the pre-existing ASTRIUM process. However, it is composed of the 4 following tasks:

1. Notching prediction on Limitation data (Sine, Acoustic, Random)
2. Iterative notching on value (Sine, Acoustic, Random)
3. Sensor Response (Random)
4. g_{RMS} calculation (Acoustic, Random)

Once the final notched spectrum is correct and lower or equals than the final notched spectrum obtained from limitation data base, it can be proceed to the run sheet consolidation (step 4) or if this is not verified continue the iterative notching on value process.

9.2.5 Step 4: Run sheet consolidation guidelines

This fifth guideline aims to consolidate the run sheet to higher level. It could be split into 8 tasks (only step 8 presents news from the pre-existing ASTRIUM process):

1. Verification of abort margins (Sine, Acoustic, Random). It aims to calculate the abort margin with the good notched input profile.
2. Check abort margins with Pilot Inaccuracy (Sine, Random). It aims to check the abort margins when taking into account the Pilot Inaccuracy effect.
3. Sensor Response (Sine, Random). It aims to calculate the expected response level under the last final notched spectrum taking into account the pilot inaccuracy.
4. Comparison Extrapolation / Limitation (Sine, Acoustic, Random). It aims to compare the expected extrapolated levels with the limitation database to verify if none exceedance has been forgotten in the run sheet preparation process.
5. g_{RMS} calculation (Acoustic, Random). It aims to calculate the expected RMS levels on all the measurements and compare it to the allowable.
6. Max band per frequency range on Extrapolated Data (Sine, Acoustic, Random). It aims to calculate for the extrapolated levels, the maximum per frequency range of each sensor.
7. Final verification (Sine, Acoustic, Random). It aims to proceed to a final run sheet verification.
8. Maximum sweep rate estimation. It aims to estimate the maximum sweep rate to avoid exceeding the defined accuracy on modal frequency, peak amplitude and modal damping thanks to the developed tool

Once the run sheet parameters have been verified and the maximum sweep rate has been estimated, the user continues the final test investigation by the last step 5.

9.2.6 Step 5: Modal extraction & correction and non linear exploitation guidelines

This last guideline aims to go beyond the usual exploitation in test to extract modes and correct the imperfectly guided specimen to recover the behaviour under a perfect guidance and to extract non linear parameter to predict non linear behaviour at other levels. It could be split into 8 tasks:

1. Estimation of residual mode (Sine, Random). It aims to complete the transfer function database with the FRF extrapolation to the high frequencies by calculating the behaviour of a residual mode thanks to the developed tool.
2. Effect on the specimen (Sine, Random). It aims to compute the effect of the parasitic motions on the specimen thanks to the developed tool.

3. Data preparation (Sine, Random). In order to remove the parasitic motion from the transfer functions to recover the perfectly guided spacecraft behaviour, this task aims to prepare data for the application.
4. Computation of missing FRF (Sine, Random). It aims to complete the calculated transfer function database with the missing FRF to recover the perfectly guided motion thanks to the developed tool.
5. RTMVI export (Sine, Random). It aims to prepare the data in purpose of the modal identification task of the perturbed FRFs.
6. Computation of corrected FRF (Sine, Random). It aims to calculate the FRFs of the perfectly guided specimen thanks to the developed tool.
7. Identification of non linearity (Sine, Random). It aims to detect, characterize and quantify non-linearities thanks to the developed methodologies.
8. Non linear extrapolation to higher level (Sine, Random). It aims to interpolate or extrapolate the non linear behaviour to other not passed levels thanks to the developed tool.

Such guidelines allows a better test preparation and assessment of the test data and also improves the preparation quality and the during test and post test data processing.

10 REAL LIFE APPLICATION CASE

The fourth study phase consist in testing all developed methodologies, tools and procedures to demonstrate the tools functionality in a real scale test and especially to demonstrate their efficiency and their added value, in test preparation and securing, test progress and final test assessment.

The chosen application is the SWARM spacecraft (an ESA programme under the responsibility of Astrium GmbH) whose sine tests occurred in IABG test facility centre in June/July 2009.

The application of the pre test methodologies and tools highlight:

- a better definition of the sensors locations wrt the modes of interest even if the tool powerful is most applicable for modal survey test than for system level qualification test where instrumentation location is often dictated by specific equipment foot measurement or co location wrt sub system test levels for comparison. Nevertheless, the new methodology and tools highlight a save of time and additional valuable information to optimize sensor location in case of modal survey test of about at least 1 week.
- An important additional valuable information thanks to stochastic analysis application leading to highlight sensors with high dispersion and make special recommendation for instrumentation accuracy even if it could not have been directly applied on the SWARM sine test preparation due to time constraints (about 1 month effort). The stochastic notching profile is a new output piece of information allowing a far better robustness confidence detailing the different uncertainty impact for negotiation with the customer and launcher authority.

The application of the post test methodologies, guidelines and tools on the SWARM sine test data provides:

- New powerful guidelines well adapted for application in a real test context. These guidelines give a test post processing process to provide quickly and rationally new additional information for raw data synthesis, extraction of additional data and preparation for higher level test. Moreover, these guidelines allow data post processing for two analysts in parallel.
- Important time can be saved thanks to theses new approaches which are roughly estimated around 4 hours per test.
- New powerful methodologies and tools are also available for specific deeper investigation in case of problem met in test (investigation for detection, characterisation and quantification of non linear behaviour, interpolation or extrapolation of non linear behaviour to not pass level) as well as the recovery of the perfectly guided motion. Even if this last tools is not fully operational due to limitations on the numerical accuracy of the test data, the tool basis exists and may be improved to reach the goal.

The methodologies, tools and guidelines developed in the frame of the DYNAMITED study have consequently demonstrated their efficiency to improve the test preparation and in test to save time, provide a better and faster assessment of test data and improve data processing and data synthesis.

		Ref : MTF.AIDT.TN.2168 Issue : 1 Rev. : 1 Date : 03/03/2010 Page : 97
--	--	---

11 ATV TEST DATA

ESA encountered some problems during the ATV qualification tests for which the agency required an additional expertise to understand and highlight the unexpected phenomenon encountered thanks to the INTESPACE test facility centre deep experience and expertise tools.

The context is that while performing a sine vibration test, the amplification factors were incorrectly determined resulting to notch levels significantly below the minimum excitation levels required by the launcher authority for successful spacecraft qualification. Early conclusions were raising potential disturbances of the time signals and possible inappropriate application of post-test data processing methods as a reason for over estimation of dynamic amplification factors. In order to further investigate on these issues, ESA have been provided different data:

- Time history of COLA signal
- Time histories of the four pilots at the spacecraft base (excitation signals)
- Time history at the interface between the spacecraft structure and a sensitive spacecraft component (response signal)

On conclusion, the study of these signals has raised many questions without answers and a few remarks:

- the sampling frequency was too low to hope for a good analysis (see RD 10 recommendations).
- the signals showed high disturbance around 40 Hz which may be due to some coupling between the specimen and the excitation, or to some problems in the excitation control (servo control) which is quite tricky in this case because the excitation is provided from hydraulic shakers that are known for non linearities and high level harmonics that could not have been recovered here.
- the beating phenomenon may be due to 2 closed modes which induce an envelope frequency $f_2 - f_1$
- the pilot sensor 02L may be questionable since the levels observed are far from the levels of other pilots
- signal processing was not able to remove noise and improve signal quality, even if the signal is not so distorted regarding the acquisition method;
- the computation of the transfer function directly influences the extraction of the Q factor, but the Q factor calculated from simulation data was not recovered. However, we do not know either the strategy used to recover this Q factor, but we find a quite different value than the one calculated during the ATV test campaign.

Moreover other post processing methods have not been applied because they were estimated not more efficient as the ones implemented in DynaWorks.

Finally, piloting problems and sampling frequencies may be the reasons for the poor quality of these test data leading to inject level below the minimum required by the launcher authorities.

12 CONCLUSIONS

12.1 STUDY CONCLUSIONS

The DYNAMITED study allowed providing very fruitful improvements in a wide variety of mechanical testing domains served by a great competent specialist team in their domain of interest.

The state of the art allowed highlighting the actual test process, methodologies, tools and uncertainties to server as entry in the following study steps.

The pre-test activities investigated new approaches based on uncertainty derivation to uncertainty on modal parameters which revealed interesting results. Theses data could then be derived as stochastic notching profile which is of great importance in test preparation to save precious time in test in terms of efficiency, robustness and confidence. New base load recovery techniques were discussed and implemented in tools. The sine sweep rate effect have been fully discussed and two methods were proposed to estimate the maximum sweep rate wrt some predefined accuracies on modal parameters and to correct the modal parameters for a given sweep rate. Finally an original method and tool were proposed for sensor positioning in order to improve some sensors location wrt some mode of interest to maximize the distinguishability with and observability status.

The post test studies have also investigated a wide variety of domains. First a new fast modal extraction and correlation methodology has been proposed. This allows providing a quick correlation between FEM and test as well as to follow the specimen behavior evolution between two different tests. A second major milestone has also been achieved thanks to a sharper synthesis of the parasitic motion and an approach to remove its effect to recover the perfectly guided specimen behavior. Unless it is limited to numerical problems linked to test data quality, theses method are very ambitious and are a first step for a further realization by slight different approaches. Moreover, some methods to elaborate reduced experimental model were proposed. The study summarized the basic verification to do in order to assess the measurement quality. Finally an important effort has been done to propose a complete catalogue of powerful and applicable method to detect, characterize and quantify non linear phenomenon. This has been extened by a method and a tool to interpolate and/or extrapolate the non linear behaviour to other not passed levels.

The most promising and useful methods in test have been implemented in 14 new tools in DynaWorks environment and one as an ISSPA extension to ensure an efficient industrial use of all the developments.

Based on the development and fruitful technical discussions, a new consideration of the best practice in test has been recorded, leading to propose a new process to improve test preparation, assessment and exploitation.

The methodologies, tools and guidelines developed in the frame of this study have been deployed on the SWARM STM qualification test at a real scale to demonstrate their efficiency, robustness and reliability. The methods allow saving about 4 hours per test thanks to the enhanced process ands tools.

However, all these developments have proposed new original and ambitious methods which bring an important improvement in the test preparation, assessment and exploitation.

12.2 THE STEP BEYOND DYNAMITED ...

The DYNAMITED study provided an important improvement in the assessment and exploitation of the mechanical test data.

Nevertheless, all the domains tackled could not solve all the problems. We consequently propose hereafter different ways of interest to carry on the important work achieved thanks to this study. They are presented by activity domains:

- **Stochastic analysis**

They have revealed to be of great interest in the frame of this study. The output results of this approach lead to an important knowledge and understanding of the mechanical behaviour, physical phenomena and uncertainty expression on the modal parameters. Moreover the stochastic notching profile leads to surround of the true mechanical behaviour allowing saving time and giving an important confidence and robustness to the prediction. It would thus be important to apply systematically such process in test preparation. A way of improvement would consist in providing simplified stochastic analysis to integrate this approach in the standard process.

The study of other probabilistic approaches by FEM or test can lead to improve hardware and prediction reliability.

Finally the integration of other kind of parameters (risk, cost and performance) can help to manage differently programs in order to improve cost and schedule.

- **Extrapolation of the measured dof to all the FEM dof**

The test sensors allow providing displacement on the instrumented dof only. The next milestone would consist in extending for each point location the recovery of the three directions components. The final step will consist into the extrapolation of these measurements to the not measured dof to provide a complete FEM mode shape display.

- **FEM error localization for a quicker model correction**

Based on the previous extrapolation, a more complete correlation can be achieved to localize errors between the model and the true specimen behaviour and thus provide a quicker and more efficient correction of the model.

- **Hardware knowledge**

The actual amplification used for test prediction are most generally based on a standard damping factor applied to the whole frequency range. In case of important deviation from this behaviour on specific mode a damping melting law could be applied to correct such imperfection. Nevertheless, by experience it is known that every mode are not equally damped.

It is thus proposed here to capitalise on a damping behaviour and use error localisation to derivate typical material or subsystem error range.

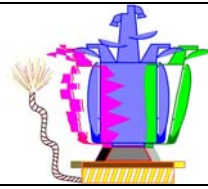
- **Methodologies for test prediction modelling coupled with shaker model**

As shown in this study, the parasitic motion is linked to the shaker imperfection and the mechanical coupling with the specimen behaviour.

The proposed approach would consist here to improve the coupling knowledge and expected

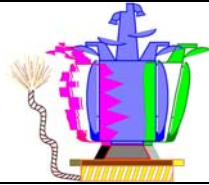
transverse coupling, pilotability, frequency, damping and amplification shift thanks to the study of the coupled system specimen + representative model of the shaker. From such a study some recommendation or improvement could be drawn concerning the test fixture impact and quality.

- **Non linearities** remains an important domain to work with many aspects not yet investigated:
 - **Extend non linear detection, characterisation and quantification by an automatic application of the non linear tool package**
As shown in this study an important catalogue of methods and tools allow detecting, identifying and characterising non linear behaviour. However, they call for time and a good knowledge of the methods which could miss in test to mechanical analyst. It is thus proposed to provide a general tool to apply on the FRF to turn toward a type of method than another one. This participates in test to improve efficiency and expertise and to save time.
 - **Investigate other way to deal with non linearities**
The way proposed in this study to deal with non linearities is ambitious and covers an important range of data and non linearities. Nevertheless other types of test data could be used to detect, characterize and quantify non linearities and have not been investigated in the frame of DYNAMITED. It is thus proposed to study different treatments which are also importantly used by the mechanical testing community to extract more information (SRS, difference filtered/RMS signals, different type of waterfall, ...)
 - **Derivation of Non-linear Finite Element Models by Sequential Linear Model Updating**
The idea consists to build a NASTRAN non linear linked FEM using non linear parameters. Linearly updated models utilizing computational parameter updating tool and modal data from low level runs can be generated. Then it is possible to generate a sequence of linear updated models utilizing the modal data interpolated at an arbitrary number of load levels between low and qualification level and evaluate the evolution of the non-linear model parameters over the load levels. Then the discrete non-linear parameter values can be introduced into NASTRAN non-linear elements. The non-linear model can be then validated using shaking table test data.
- **Parasitic motion removal**
This study proposed a very original and ambitious method to remove parasitic motion in order to recover the perfectly guided specimen behaviour. This method revealed some limitations in the $G_{pp, stat}$ term calculation due to imperfect numerical data quality. However it is a first step to reach the goal. Different other approaches can be proposed to achieve a correct identification of the term.



13 ANNEXES: NEW TEST PROCESS

Step 0 - Macros tools preparation		Step 2 - Test data and Transfer Function exploitation		Step 3 - Test extrapolation to higher level		Step 4 - Run sheet consolidation		Step 5 - Modal extraction & correction and non linear exploitation					
0.1 - S A R Update macros input file For every run (if changes) <input type="checkbox"/> macros_data.mac (A1) <input type="checkbox"/> Update macros data file <input type="checkbox"/> run name (test_name) <input type="checkbox"/> define list (list_name) <input type="checkbox"/> default Project name (program_name) <input type="checkbox"/> default SubProgram name (subprogram_name) <input type="checkbox"/> Plot directory name (plot_directory) <input type="checkbox"/> caption name (caption_name) <input type="checkbox"/> comments (use_comment & comment_file) <input type="checkbox"/> default class (class_choice) <input type="checkbox"/> default type (type_choice) <input type="checkbox"/> Additional filter (other_choice) <input type="checkbox"/> default language (conf_choice) <input type="checkbox"/> pilot names and number (nbr_pilot_sensor & register_number) <input type="checkbox"/> Co-pilot names <input type="checkbox"/> For Acoustic no Co-pilot <input type="checkbox"/> Define Pilot & Co-pilots in positive normal order <input type="checkbox"/> DW8 macros - Load macros data <input type="checkbox"/> Load the macros variables		0.2 - S R Implement run sheet For every run <input type="checkbox"/> test_run_name.don <input type="checkbox"/> Option A5 <input type="checkbox"/> macros_data.mac <input type="checkbox"/> Caution if file is still opened in task 0.1 <input type="checkbox"/> Update the .mac file in the notching run sheet section <input type="checkbox"/> Update notch file menu (notch_file)		2.1 - S R Mass Operator on Test Data For every run <input type="checkbox"/> DYNAMITED - Mass Operator <input type="checkbox"/> Work base test data (phased) <input type="checkbox"/> Calculate the load force and moment for the system and each sub-systems <input type="checkbox"/> Define the largest set of valid sensors (if necessary) <input type="checkbox"/> Calculate the Si/C base load force and moment <input type="checkbox"/> Calculate for each sub system the base load force and moment <input type="checkbox"/> Print Si/C loads <input type="checkbox"/> Print Sub System loads		2.2 - S R Mass Operator on TF For every run <input type="checkbox"/> DYNAMITED - Mass Operator <input type="checkbox"/> Calculated Transfer Function <input type="checkbox"/> Calculate the load force and moment for the system and each sub-systems <input type="checkbox"/> Define the largest set of valid sensors (if necessary) <input type="checkbox"/> Calculate the Si/C base load force and moment <input type="checkbox"/> Calculate for each sub system the base load force and moment <input type="checkbox"/> Print Si/C loads <input type="checkbox"/> Print Sub System loads		3.1 - S A R Notching pred. on Limitation data For every run <input type="checkbox"/> prediction_don = <input type="checkbox"/> Option A5 <input type="checkbox"/> DW8 macros - Prediction <input type="checkbox"/> Transfer Function <input type="checkbox"/> (S) Sine Limitations / (A) Acoustic / (R) Random <input type="checkbox"/> Without Pilot Inaccuracy <input type="checkbox"/> Prediction ID number = <input type="checkbox"/> Verify Limitation/TF & TFLimitation equiv. <input type="checkbox"/> Calculate the notching spectrum based on the Limitation database <input type="checkbox"/> Identify the deepest notch sensors: <input type="checkbox"/> Plot the deepest notch <input type="checkbox"/> Plot the contribution of each sensor <input type="checkbox"/> Plot the notching summary table (R9 or _notching_summary_test_PredID_type.asc from the plot directory)		4.1 - S A R Verification of abort margins For every run <input type="checkbox"/> prediction_don = <input type="checkbox"/> Option A5 <input type="checkbox"/> DW8 macros - Prediction <input type="checkbox"/> Transfer Function <input type="checkbox"/> (S) Sine on Values / (A) Acoustic / (R) Random <input type="checkbox"/> Without Pilot Inaccuracy <input type="checkbox"/> Prediction ID number = <input type="checkbox"/> Verify abort margins (R14) <input type="checkbox"/> Print final notched spectrum		5.1 - S R Estimation of residual mode For every run <input type="checkbox"/> DYNAMITED - Estimation of residual mode <input type="checkbox"/> Transfer Function <input type="checkbox"/> Calculation of the FRF residual mode for parasitic motion removal	
0.3 - S A R Frequency band definition Once per axis (first low level run) <input type="checkbox"/> macros_data.mac <input type="checkbox"/> Define the freq. boundaries for the max band per freq. range and the octave band <input type="checkbox"/> nbr_oct <input type="checkbox"/> Band boundaries		2.3 - S A R Additional sensors on TD For every run <input type="checkbox"/> DW8 macros - Additional sensors <input type="checkbox"/> Work base test data <input type="checkbox"/> Calculation of Lateral and Resultant sensors, QSL, Coil Current and Bisenor <input type="checkbox"/> QSL <input type="checkbox"/> Lateral and Resultant sensors <input type="checkbox"/> Coil current base load <input type="checkbox"/> Bisenor		2.4 - S A R Additional sensors on TF For every run <input type="checkbox"/> DW8 macros - Additional sensors <input type="checkbox"/> Calculated Transfer Function <input type="checkbox"/> Calculation of Lateral and Resultant sensors, QSL, Coil Current and Bisenor <input type="checkbox"/> QSL <input type="checkbox"/> Lateral and Resultant sensors <input type="checkbox"/> Coil current base load <input type="checkbox"/> Bisenor		3.2 - S A R Iterative notching on value For every prediction <input type="checkbox"/> prediction_don = <input type="checkbox"/> Option A5 <input type="checkbox"/> DW8 macros - Prediction <input type="checkbox"/> Calculated Transfer Function <input type="checkbox"/> (S) Sine on Values / (A) Acoustic / (R) Random <input type="checkbox"/> Without Pilot Inaccuracy <input type="checkbox"/> Calculate the notching spectrum based on the defined values <input type="checkbox"/> Plot the deepest notch <input type="checkbox"/> Compare the deepest notch to the deepest notch calculated with Limitation database <input type="checkbox"/> Identify the differences: <input type="checkbox"/> Iterate to find the set of sensor and right criteria to cover the deepest notch from Limitation database		4.2 - S R Check abort margins with PI For every prediction <input type="checkbox"/> prediction_don = <input type="checkbox"/> Option A5 <input type="checkbox"/> DW8 macros - Prediction <input type="checkbox"/> Transfer Function <input type="checkbox"/> (S) Sine on Values / (A) Acoustic / (R) Random <input type="checkbox"/> Without Pilot Inaccuracy <input type="checkbox"/> Prediction ID number = <input type="checkbox"/> Verify abort margins (R14)		5.2 - S R Effect on the specimen For every run <input type="checkbox"/> DYNAMITED - Parasitic motion components <input type="checkbox"/> Raw test data <input type="checkbox"/> Determine the contributions of the parasitic motion and of the base rigid motion on the specimen			
0.4 - S R Coil Current coefficient calcul. Once per axis (first low level run) <input type="checkbox"/> DYNAMITED - Coil Current <input type="checkbox"/> Blank test <input type="checkbox"/> Determine the shaker coil current coefficient to estimate force load from coil current <input type="checkbox"/> Moving mass = <input type="checkbox"/> Chosen coefficient = <input type="checkbox"/> Print different data		0.5 - S A R Prepare additional sensors For every run (if changes) <input type="checkbox"/> lateral_res resultant.don <input type="checkbox"/> Option A3 <input type="checkbox"/> Bisenor.don <input type="checkbox"/> Option A4 <input type="checkbox"/> mazzor.don <input type="checkbox"/> Option A5 <input type="checkbox"/> Prepare additional sensors (lateral & resultant, Bisenor and Coil current base load) for further calculation		2.5 - S A R Max band per freq. range on TD For every run <input type="checkbox"/> DW8 macros - Max band per frequency range <input type="checkbox"/> Work base test data <input type="checkbox"/> Calculation of the test maximum per frequency ranges to check max levels <input type="checkbox"/> Give the maxB_test_type.asc to the architecte		2.6 - S R Max band per freq. range on TF For every run <input type="checkbox"/> DW8 macros - Max band per frequency range <input type="checkbox"/> Calculated Transfer Function <input type="checkbox"/> Calculation of the TF maximum per frequency ranges to check max levels <input type="checkbox"/> Give the maxB_test_TF.asc to the architecte		4.3 - S R Sensor Response For every prediction <input type="checkbox"/> DW8 macros - Sensor Response <input type="checkbox"/> Calculated Transfer Function <input type="checkbox"/> Calculate the achieved levels with PI <input type="checkbox"/> Is there exceedance? YES/NO		5.3 - S R Data preparation For every run <input type="checkbox"/> Load Macro Data (cf. §1.1) <input type="checkbox"/> Check TF has been calculated (cf. §1.3) <input type="checkbox"/> Check Si/C loads are calculated (cf. §2.1) <input type="checkbox"/> Verification that mandatory data are present in the work base			
1.1 - S A R Transfer Function Calculation For every run <input type="checkbox"/> DW8 macros - Pilot and Transfer function calculation <input type="checkbox"/> Global/Fundamental Test <input type="checkbox"/> Raw test data <input type="checkbox"/> Calculate Pilot (depending upon the strategy), Transfer Function and Phase <input type="checkbox"/> Response type: Fundamental <input type="checkbox"/> OR Global OR Other: <input type="checkbox"/> Plotting strategy: Max QSL Average <input type="checkbox"/> Phase: Automatic Phase Calculation (APC) <input type="checkbox"/> If APC, reference phase sensor: <input type="checkbox"/> Other: <input type="checkbox"/> Pilot Inaccuracy calculation <input type="checkbox"/> Print Pilot <input type="checkbox"/> Print Pilot Inaccuracy <input type="checkbox"/> For Acoustic no Pilot Inaccuracy		1.2 - S Global/Fundamental compar. For every run <input type="checkbox"/> DW8 macros - Display responses <input type="checkbox"/> Global/Fundamental Test <input type="checkbox"/> Raw test data <input type="checkbox"/> Compare the Global and Fundamental of every raw data to detect different kind of problem <input type="checkbox"/> Note in the lower box: Dead sensors <input type="checkbox"/> Suspicious sensors <input type="checkbox"/> Difference G/F <input type="checkbox"/> Print different data		2.7 - A R gRMS calculation For every run <input type="checkbox"/> DW8 macros - gRMS calculation <input type="checkbox"/> Work base test data <input type="checkbox"/> Calculate the gRMS levels to determine the achieved levels <input type="checkbox"/> Calculate cumulated RMS levels <input type="checkbox"/> Print gRMS synthesis (R11)		2.8 - S R Test correlation with FEM For every run <input type="checkbox"/> Not necessary for control low level <input type="checkbox"/> DYNAMITED - FMCC <input type="checkbox"/> Calculated Transfer Function <input type="checkbox"/> Estimate correlation between the FEM and the test specimen <input type="checkbox"/> Save correlation matrices (FrimAC and imMAC) <input type="checkbox"/> Print different data		4.4 - S A R Comp. Extrapolation/Limitation For every prediction <input type="checkbox"/> DW8 macros - Display responses <input type="checkbox"/> Note in the lower box exceedances <input type="checkbox"/> Print different data <input type="checkbox"/> Is there exceedance? YES/NO		5.4 - S R Computation of missing FRF For every run <input type="checkbox"/> DYNAMITED - Missing FRF computation <input type="checkbox"/> Calculate the missing FRF for parasitic motion removal			
1.3 - S R Estimation of static term For every run <input type="checkbox"/> DYNAMITED - Estimation of static term <input type="checkbox"/> Transfer Function <input type="checkbox"/> Calculation of the FRF static terms for residual mode calculation and parasitic motion removal <input type="checkbox"/> Frequency band int = <input type="checkbox"/> Frequency band end = <input type="checkbox"/> Save manually the output register in the WORK base		1.4 - S R Sensor orientation estim. Once per axis (first low level run) <input type="checkbox"/> DYNAMITED - Estimation of sensor orientation <input type="checkbox"/> Transfer Function <input type="checkbox"/> Estimation of the sensor orientation error and the equivalent error angle <input type="checkbox"/> Apply verification for in axis sensors <input type="checkbox"/> Apply verification for out of excitation axis sensors <input type="checkbox"/> Note in the lower box: Dead sensors <input type="checkbox"/> Suspicious sensors		2.9 - S A R Test correlation with previous run For every run <input type="checkbox"/> DYNAMITED - FMCC <input type="checkbox"/> For control low level run correlation is verified with the first low level run <input type="checkbox"/> Calculated Transfer Function <input type="checkbox"/> Estimate correlation between the actual run and the previous run to detect mode evolution <input type="checkbox"/> Save correlation matrices (FrimAC and imMAC) <input type="checkbox"/> Print different data		3.3 - R Sensor Response For every prediction <input type="checkbox"/> DW8 macros - Sensor Response <input type="checkbox"/> Calculated Transfer Function <input type="checkbox"/> Calculate the gRMS levels to determine the achieved levels <input type="checkbox"/> Calculate Cumulated RMS levels <input type="checkbox"/> Print gRMS synthesis (R11)		4.5 - A R gRMS calculation For every prediction <input type="checkbox"/> DW8 macros - gRMS calculation <input type="checkbox"/> (A) Pred_acou / (R) Notched Response <input type="checkbox"/> Calculate the gRMS levels to determine the achieved levels <input type="checkbox"/> Calculate cumulated RMS levels <input type="checkbox"/> Print gRMS synthesis (R11)		5.5 - S R RTMVI export For every run <input type="checkbox"/> DYNAMITED - RTMVI export <input type="checkbox"/> Extract mode with RTMVI in DW8 5.2 <input type="checkbox"/> Extract test mode with the RTMVI method and prepare the test to save results			
1.5 - S R 1st estimation of parasitic motion For every run <input type="checkbox"/> DYNAMITED - First estimation <input type="checkbox"/> Raw test data <input type="checkbox"/> Calculation of the first rough estimation of the parasitic motion in the excitation and crossed directions <input type="checkbox"/> Save manually the output register in the WORK base		1.5 - S R Sign Correlation Matrix For every run (if changes) <input type="checkbox"/> DYNAMITED - Sign Correlation <input type="checkbox"/> Transfer Function <input type="checkbox"/> Assess the sensor sign correlation between FEM and Test specimen instrumentation for MANSOP and FMCC <input type="checkbox"/> Select the three axis sine predictions (1 per axis) <input type="checkbox"/> Set the correlation matrix: <input type="checkbox"/> Verify real part coherence <input type="checkbox"/> Set to ±1 correct data <input type="checkbox"/> Set to 0 not correct data from real part = dead and suspicious sensors		2.10 - R Extrapolation Sine to Random For Sine (low level) to Random <input type="checkbox"/> DW8 macros - Sine to Random <input type="checkbox"/> Calculated Transfer Function <input type="checkbox"/> Extrapolate Sine levels to a random specified spectrum <input type="checkbox"/> Define random input spectrum in RS		3.4 - A R gRMS calculation For every prediction <input type="checkbox"/> DW8 macros - gRMS calculation <input type="checkbox"/> (A) Pred_acou / (R) Notched Response <input type="checkbox"/> Calculate the gRMS levels to determine the achieved levels <input type="checkbox"/> Calculate Cumulated RMS levels <input type="checkbox"/> Print gRMS synthesis (R11)		4.6 - S A R Max band per freq. range on Extrap. For every run <input type="checkbox"/> DW8 macros - Max band per frequency range <input type="checkbox"/> Notched Responses <input type="checkbox"/> Calculation of the test maximum per frequency ranges to check max levels <input type="checkbox"/> Give the maxB_test_type.asc to the architecte		5.6 - S R Computation of corrected FRF For every run <input type="checkbox"/> DYNAMITED - Corrected FRF computation <input type="checkbox"/> Enter the longitudinal shaker characteristics <input type="checkbox"/> Calculation of the corrected FRF without the parasitic motion effect			
1.6 - S R 1st estimation of parasitic motion For every run <input type="checkbox"/> DYNAMITED - First estimation <input type="checkbox"/> Raw test data <input type="checkbox"/> Calculation of the first rough estimation of the parasitic motion in the excitation and crossed directions <input type="checkbox"/> Save manually the output register in the WORK base		1.7 - S R Build condensation set For every run <input type="checkbox"/> DYNAMITED - Mass Operator <input type="checkbox"/> Define the largest set of valid sensors <input type="checkbox"/> Set name: <input type="checkbox"/> opt.don <input type="checkbox"/> Option A3		2.11 - S A R Comparison Test Data / Limitation For every run <input type="checkbox"/> Not necessary for control low level <input type="checkbox"/> DW8 macros - Display responses <input type="checkbox"/> Kind of display: Test - Limitation <input type="checkbox"/> Work base test data <input type="checkbox"/> Evaluate the test response wrt the allowables and check low margins <input type="checkbox"/> Note in the lower box: Dead sensors <input type="checkbox"/> Suspicious sensors <input type="checkbox"/> Exceedances <input type="checkbox"/> Print different data		3.4 - A R gRMS calculation For every prediction <input type="checkbox"/> DW8 macros - gRMS calculation <input type="checkbox"/> (A) Pred_acou / (R) Notched Response <input type="checkbox"/> Calculate the gRMS levels to determine the achieved levels <input type="checkbox"/> Calculate Cumulated RMS levels <input type="checkbox"/> Print gRMS synthesis (R11)		4.7 - S A R Final verification For every run <input type="checkbox"/> Verify that the prediction_don content is equal to the run sheet parameters		5.7 - S R Detect. & charact. non-linear behav. For every run if problem <input type="checkbox"/> ISBPA - Non linear identification <input type="checkbox"/> The objective is to identify the non linearities and the parameters for extrapolation to higher level			
1.8 - S R Parasitic motion component For every run <input type="checkbox"/> DYNAMITED - Parasitic motion components <input type="checkbox"/> Raw test data <input type="checkbox"/> Estimation of the errors due to the parasitic motion in directions different from the excitation one and the parasitic motion deformation		2.12 - S R Comparison Test TF / FEM For every run <input type="checkbox"/> Not necessary for control low level <input type="checkbox"/> DW8 macros - Display responses → Load macros data: Class="Response" & Type="All" <input type="checkbox"/> Calculated Transfer Function <input type="checkbox"/> Comparison of the test TF with the FEM predictions <input type="checkbox"/> Note in the lower box: Important differences sensors <input type="checkbox"/> Suspicious points <input type="checkbox"/> Print different data		2.13 - S A R Compar. Test TF / Previous run TF For every run <input type="checkbox"/> DYNAMITED - Display responses <input type="checkbox"/> Calculated Transfer Function <input type="checkbox"/> For control low level run comparison is performed with the first low level and on TF and/or test data <input type="checkbox"/> For acoustic runs, it is advised to apply this function on raw test data <input type="checkbox"/> Comparison of the test TF with the previous test TF to detect evolutions <input type="checkbox"/> Note in the lower box: Important differences sensors <input type="checkbox"/> Suspicious points <input type="checkbox"/> Print different data		4.8 - S Maximum sweep rate estimation For every run <input type="checkbox"/> DYNAMITED - Sweep rate prediction <input type="checkbox"/> Calculated Transfer Function <input type="checkbox"/> Estimate maximum sweep rate wrt accuracy <input type="checkbox"/> Accuracy: Modal frequency= <input type="checkbox"/> Peak amplitude= Modal damping= <input type="checkbox"/> Minimum sweep rate =		5.8 - S R Non-linear experim. modal analysis For every run if problem <input type="checkbox"/> ISBPA - Non linear extrapolation <input type="checkbox"/> The objective is to extrapolate the non linear behaviour to higher level					
1.9 - S Sweep rate effect For every run <input type="checkbox"/> DYNAMITED - Sweep rate effect <input type="checkbox"/> Calculated Transfer Function <input type="checkbox"/> Estimate the frequency, damping and amplitude error due to sweep rate		2.19 - S A R Comparison Test TF / Limitation For every run <input type="checkbox"/> Not necessary for control low level <input type="checkbox"/> DW8 macros - Display responses <input type="checkbox"/> Kind of display: Test - Limitation <input type="checkbox"/> Work base test data <input type="checkbox"/> Evaluate the test response wrt the allowables and check low margins <input type="checkbox"/> Note in the lower box: Dead sensors <input type="checkbox"/> Suspicious sensors <input type="checkbox"/> Exceedances <input type="checkbox"/> Print different data		3.5 - S A R Acoustic & Random: Deepest notch ≥ Limitation Deepest notch and RMS levels ≥ allowables? <input type="checkbox"/> YES <input type="checkbox"/> NO		4.9 - S A R Final verification For every run <input type="checkbox"/> Verify that the prediction_don content is equal to the run sheet parameters		REMARK BOX Dead sensors Suspicious sensors / Important differences G/F					



DISTRIBUTION LIST

	Overall document		Summary
	Action	Information	
<u>ASTRIUM :</u>			
A. CAPITAINE		X	
S. LABORDE	X		
J.-B. VERGNIAUD		X	
Doc ASG24 (L. MONGET)	X		
<u>ESA :</u>			
A. CALVI		X	
<u>INTESPACE :</u>			
E. CAVRO	X		
A. GIRARD	X		
<u>UNIVERSITY OF KÄSSEL :</u>			
M. LINK		X	
<u>DLR :</u>			
M. BOSWALD		X	